A case study of the distribution of high wind speeds in the Greater Victoria area using wind data from the School-Based Weather Station Network.

by

Miho Matsuda
B.Sc., University of Victoria, 2005

A Thesis Submitted in Partial Fulfillment
of the Requirement for the Degree of

MASTER OF SCIENCE

in the Department of Geography

A case study of the distribution of high wind speeds in the Greater Victoria area using wind data from the School-Based Weather Station Network.

by

Miho Matsuda
B.Sc., University of Victoria, 2005

Supervisory Committee

Dr. Stanton E. Tuller, Supervisor
(Department of Geography)

Dr. Ian J. Walker, Department Member
(Department of Geography)

Dr. Andrew J. Weaver, Outside Member
(School of Earth and Ocean Science)

Supervisory Committee

Dr. Stanton E. Tuller, Supervisor
(Department of Geography)

Dr. Ian J. Walker, Department Member
(Department of Geography)

Dr. Andrew J. Weaver, Outside Member
(School of Earth and Ocean Science)

ABSTRACT

This thesis presents the distribution of strong wind and wind pressure in the Greater Victoria area associated with winter mid-latitude cyclones based on climate data from the School-Based Weather Station Network during 6 selected days in the winters of 2006, 2007 and 2008. The objectives of this study are i) to test whether synoptic conditions favourable to severe mid-latitude cyclonic storms that are well described in the literature were associated with the selected storms, ii) to determine the time patterns of high wind speed and its direction and maximum gusts, iii) to test necessity of considering the spatial variation in air density and its controls in general assessments of the spatial variation in wind pressure and wind damage potential in the local area, iv) to identify potential areas susceptible to wind damage. Observations taken every second were from Davis Vantage Pro2 ™ Plus weather stations located on the southern edge of school building roofs. Thirty-minute means and gust wind speeds were used. All six storms went north of Victoria. The synoptic conditions associated with the selected mid-latitude cyclones agreed with the ones described in literature. Strongest winds at most stations were generally from the southwest, and multiple wind speed peaks were found. The daily maximum gust wind speeds were found before and/or after the highest mean wind speed peak. The spatial variation in air density and its controls were found to be negligible. Although there are a number of interacting causes of the distribution, strongest winds were at stations with smooth surrounding surfaces, close to the southern shoreline, on exposed slopes and/or near relief constrictions. The area with greatest wind speeds and damage potential was found from the east of downtown extending to Lansdowne Middle School. This study provides new knowledge of winds in the Greater Victoria area and contributes to people's better response to wind storms, land use planning and forecasting severe windstorms.

Table of Contents

List of Tables

List of Figures

List of Equations

List of Acronyms

BC – British Columbia

CIPM – Comité International des Poids et Mesures

E – east

ENE – east-northeast

ESE – east-southeast

ESRL – Earth System Research Laboratory

ID – identification

MB – millibar

N – north

NCEP – National Centers for Environmental Prediction

NE- northeast

NNE – north-northeast

NNW – north-northwest

NW – northwest

S – south

SD – school district

SE – southeast

SSE – south-southeast

SSW – south-southwest

Stn. – station

SW – southwest

W – west

WMO – World Meteorological Organization

WNW – west-northwest

WSW – west-southwest

UV – ultraviolet

Acknowledgements

I have had many people who helped me complete this thesis. First, I would like to thank my supervisor, Dr. Stanton E. Tuller. He showed me the way, but allowed me to choose the path. This thesis would not have been possible without his extraordinary patience, kind instruction and unchangeable support. I would also like to thank my supervisory committee members Drs. Ian Walker and Andrew Weaver and former supervisory committee member Dr. Barrie Bonsal for their advice and feedback. I would also like to thank Dr. Andrew Weaver and Edward Wiebe for their climate data and technical support, Daniel Brendle-Moczuk for the beautiful map of the study area and Darlene Li for her trustful secretarial work for the graduate students. The fieldwork for this study would not have been possible without the support of the school districts 61, 62 and 63 and principals of the schools. Many thanks also to Dr. Sookuk Park for always providing me with warm friendship and support. Finally, I would like to thank my parents, Yayoi and Miyo, and my brother, Takashi, for their unwavering support and encouragement. I really appreciate you always being there for me.

Chapter 1

Introduction

Victoria has had frequent visits of winter mid-latitude cyclones. A few of these are accompanied by very high wind speeds and resulting damage. It is common that strong winds blow down branches of trees as well as whole trees to cause power outage, road closure and partial destruction of buildings and other property. Objects displaced by strong winds can destroy other objects and/or themselves. Damage is caused by high wind pressure, which is a function of air density and the square of the wind speed acting on the objects. A number of studies have addressed wind associated with winter mid-latitude cyclones in northwest Washington and southwest British Columbia. These include modification of winds by local topography, such as the Olympic Mountains (Ferber and Mass 1990; Mass and Ferber 1990; Colle and Mass 1996; Steenburgh and Mass 1996; Colle *et al*. 1999; Chien *et al*. 2001), the Strait of Juan de Fuca (Overland and Walter 1981; Colle and Mass 2000), coastal mountains of Vancouver Island and Washington state (Overland and Bond 1995; Doyle and Bond 2001; Yu and Bond 2002), and the Fraser River valley (Mass *et al*. 1995). Mass and Dotson (2010) reviewed some strong winter mid-latitude cyclones which struck the Pacific Northwest in the past century.

In contrast to the number of wind studies around Greater Victoria, studies done on winds within Greater Victoria are limited. Topics include analysis and forecasting of wind direction (McIntyre 1952), air pollution (Chilton 1973), wind comparison between downtown and a residential area (Tuller 1974), summer daytime onshore flow (Tuller 1995), and the 1953-95 trends in measured wind speed at Victoria International Airport (Tuller 2004). Little work has been done on the distribution of wind speed, wind pressure and its climate variables over Greater Victoria under the influence of winter mid-latitude cyclones. The main reason is a lack of weather stations.

Fortunately, the School-Based Weather Station Network, which started operating in Victoria in March 2002, now allows us to investigate the distribution of various climate elements over Greater Victoria. The School-Based Weather Station Network was implemented by Dr. Andrew Weaver of the University of Victoria and has been developed mainly by him and Ed Wiebe. It has been a partnership with British Columbia school districts and funded by the BC Year of Science, the NSERC PromoScience program, NEC Corporation, CTV Vancouver Island and many individuals (School-Based Weather Station Network 2012a). Saenko (2008) utilized wind data from 32 weather stations in the Network located in Victoria, Saanich, Oak Bay, Esquimalt and View Royal. She reported that Lansdowne Middle School (Stn. ID 25), Victoria High School (Stn. ID 8) and South Park Elementary School (Stn. ID 23) had the highest cold season wind power potential (Figure. 1.1; Table A1).

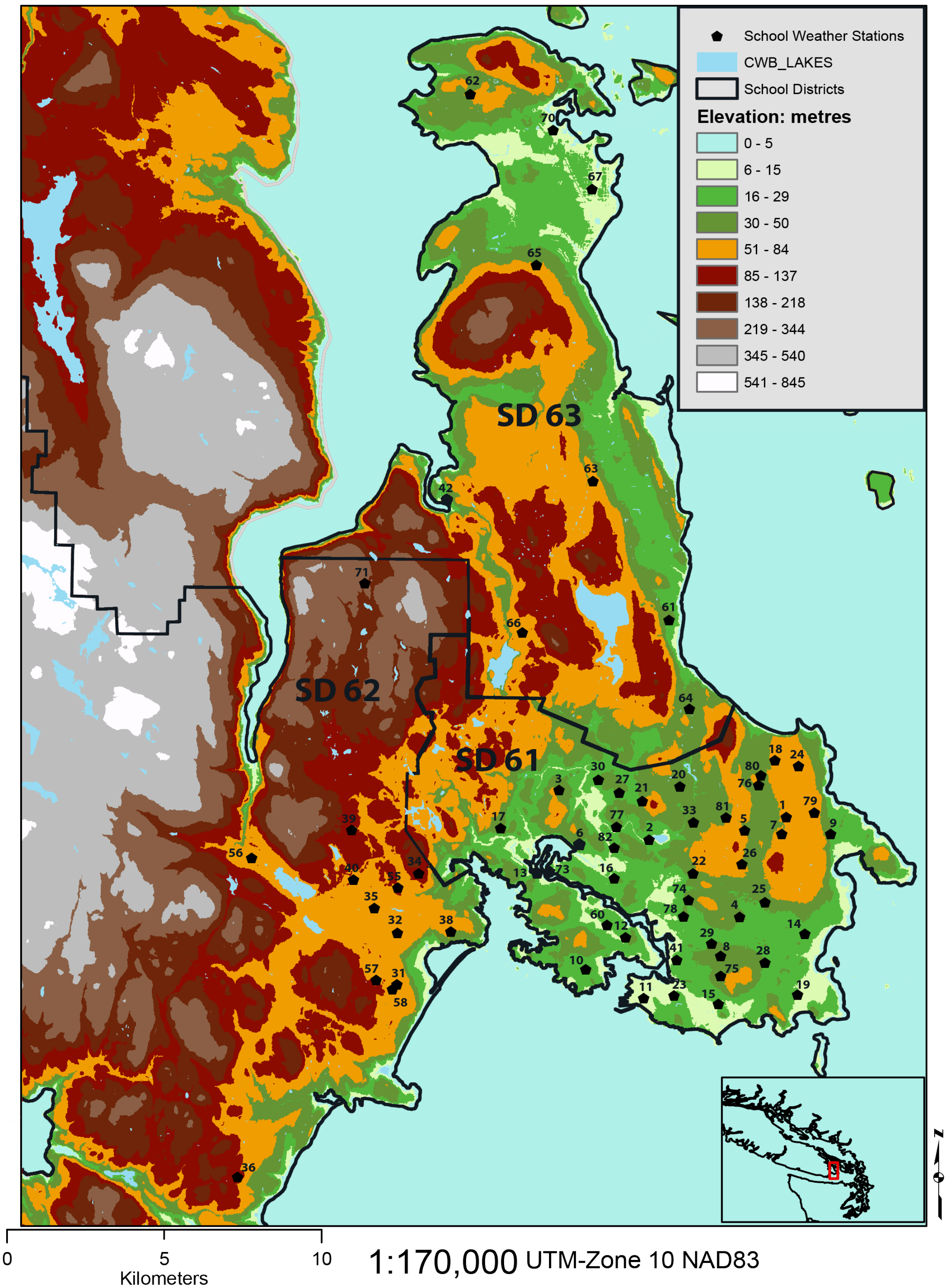

Figure 1.1: Study area and weather stations (Brendle-Moczuk 2010). School districts 61, 62 and 63 are located in the southeast, southwest and north parts of the study area, respectively. The original map was partially modified, and the numbers of the station identifications (Stn. ID) were added by the author of this study.

The purpose of this study is to describe the spatial and time patterns of wind speed, wind direction, wind pressure, and air density and its variables in the Greater Victoria area associated with winter mid-latitude cyclones. The following structure and objectives were set to achieve the goal.

i. To test whether synoptic conditions favourable for severe mid-latitude cyclonic storms that are well described in the literature were associated with the selected storms. This may enable forecasters to better predict the severity of storms in the local area.
ii. To determine the time patterns of high wind speed and its direction and maximum gusts which would help people, repair personnel, emergency responders and so on plan their responses to severe storms.
iii. To test whether or not the spatial variation in air density and its controls play only a minor role in the variations of wind pressure and therefore might not need to be considered in general assessments of the spatial variation in wind pressure and wind damage potential in the local area.
iv. To identify areas most susceptible to high wind speed and wind damage to allow better preparation for severe storms and land use planning.

In order to carry out these objectives, climate data from the School-Based Weather Station Network during a total of 6 selected days in the winters of 2006, 2007 and 2008 were utilized. The number of stations which recorded wind speed data varied from a minimum of 40 on Dec. 15, 2006 to a maximum of 65 (Table A2) and the regional coverage included the entire Saanich Peninsula and some of the western communities. This is the first time that wind speed, gust wind speed, wind pressure and air density variations in Greater Victoria under the influence of winter mid-latitude cyclones are addressed. Although this is a preliminary study with a small sample size, it contributes to new knowledge on the strong wind distribution in most of the populated areas of Greater Victoria.

Chapter 2

Theory

2.1 Formation and development of winter mid-latitude cyclones affecting the North American west coast

Winter mid-latitude cyclones which affect the study area mainly form over the Pacific Ocean (Moran and Morgan 1994). In order for them to form and develop, the right surface and upper level atmosphere conditions are necessary (Ahrens 1988; Lutgens and Tarbuck 1989; Moran and Morgan 1994; Aguado and Burt 2004). Life of a mid-latitude cyclone in the northern hemisphere usually starts along the polar front, which separates cold polar northeasterlies north of the front and warm subtropical southwesterlies south of the front. The convergence of these flows creates cyclonic wind shear to produce a net counterclockwise rotation. If conditions are favourable, the front assumes a wavelike shape. The cold air begins to push southward and form a cold front. The warm air begins to push northward and form a warm front. The lowest pressure region is found at the apex of the wave, which also becomes the centre of the counterclockwise circulation. This converging air circulation is associated with vertical lifting of air, particularly when the warm air pushing northward moves over the cold air. Isobars around the low pressure centre have abrupt changes in direction across cold and warm fronts because of different properties of air masses in front of and behind each front. A cold front generally moves forward faster than a warm front, so that the warm sector between these fronts starts being displaced aloft and closing to form an occluded front. The cyclones reach their maturity at this occlusion stage. Movement of the occluded front is often slower than that of the other fronts, and the so-called bent-back occlusion can be formed around the low pressure centre because of the circulation of the cyclones. Mass (2008) analyzed a highly realistic simulation of the Dec. 15, 2006 cyclone with a bent-back occlusion which struck Greater Victoria. He stated that a region of large pressure gradient south of the low pressure centre is related to the strongest winds and is a fairly common feature of mid-latitude cyclones. This configuration of an occluded front tends to stay longer over an area under the cyclones' influence than do the other fronts (Lutgens and Tarbuck 1989; Moran and Morgan 1994). Once the warm sector is completely displaced aloft, and cold air fills the cyclone at low levels, the pressure gradient decreases, and the cyclones gradually disappear.

For the cyclones to form and develop, the most crucial upper atmosphere condition is divergence (Ahrens 1988; Lutgens and Tarbuck 1989; Moran and Morgan 1994; Aguado and Burt 2004). Because surface winds around the cyclones are converging, accumulating air at the centre of the cyclones has to go somewhere in order for the pressure gradient around the cyclones to exist. The fast-moving jet stream is most often above the middle atmosphere position of the sloping polar front. When a path of the jet stream has north-south oriented high-amplitude waves with troughs and ridges, changes of airflow speed and direction cause horizontal convergence and divergence in the upper atmosphere (Moran and Morgan 1994). The strongest divergence occurs just downwind of trough axes where vorticity decreases. There, a lifting mechanism is created, and surface air is drawn upward to the jet stream. The jet stream can swiftly carry the surface air downstream, and surface air pressure decreases rapidly and low level convergence into the low centre increases until the convergence equals the upper air divergence (Ahrens 1988). An increased surface air pressure gradient, in turn, contributes to generating, developing and intensifying the cyclones. Therefore, cyclones are usually found under the region of upper level divergence and move toward the northeast, being steered by the westerlies at the 500 hPa level directly above them. Both the jet stream and the polar front strengthen in winter because of the large latitudinal temperature gradient. In addition, their locations shift further south (Ahrens 1988). As a result, more cyclones form and approach Greater Victoria in winter.

Other features in the upper level atmosphere that can develop and intensify cyclones are air temperature advections and shortwaves. The cold air temperature advection occurs when the wind blows from colder to warmer regions across the isotherms. The warm air temperature advection occurs when the wind blows from warmer to colder regions across the isotherms. If cold air advection occurs upstream of a longwave trough axis, the trough can deepen because of lowered pressure by dense and sinking cold air. If warm air advection occurs downstream of a trough axis, the ridge of a longwave strengthens because of raised pressure by lighter rising warm air. As a result, the longwaves are intensified to produce greater divergence and convergence (Ahrens 1988). Although the major sources of energy for mid-latitude cyclones are the potential energy at the meeting zone of the cold and warmer air masses along the front and the latent heat of condensation, the vertical motions of sinking cold air and rising warm air caused by air temperature advection also provide energy which helps the cyclones develop and intensify (Ahrens 1988; Aguado and Burt 2004). Shortwaves are small ripples superimposed on longwaves and move eastward faster than the longwaves. They are caused by air temperature advections. The vertically moving air undergoes a slight turning to the right in regions of cold air temperature advection and to the left in areas of warm air temperature advection, forming ripples. The shortwaves located downwind of a longwave trough axis can increase the divergence and strengthen surface cyclones (Aguado and Burt 2004).

Passage of cyclones' fronts causes noticeable change in some climate elements recorded at weather stations because of different airflow and properties of air masses before and behind the fronts. For example, when a warm front passes, wind generally shifts from southeasterly to southwesterly, and air temperature rises. Passage of a cold front is accompanied by wind shift from southwesterly to northwesterly, an increase in air pressure and a sudden drop of air temperature. A passing occluded front causes wind shift from southeasterly or southerly to westerly or northwesterly, and change in air pressure from falling to rising (Ahrens 1988; Moran and Morgan 1994; Aguado and Burt 2004). In terms of air temperature, we often get cooler maritime polar air over us after an occluded front passes.

The cyclones generally move northeastward. Therefore, the first signs of a storm's approach should be observed in the westernmost part of an area (Lutgens and Tarbuck 1989).

2.2 Topographic effects on winds

Two kinds of influences that local topography exerts on wind are thermal and physical (ASHRAE 1989). Physical influences are more powerful when wind is strong.

However, flow dynamics over complex topography are complicated, so only wind speed effects of isolated features common in the study area are discussed in this section.

One of the topographic factors which affect wind speed is surface roughness. Greater surface roughness causes greater surface drag. As the surface drag increases, the surface shear stress increases and wind speed decreases (Oke 1987; Walker and Hesp 2013). The influence of surface roughness on boundary layer wind speed has been studied extensively. Surface roughness length (z_0) is the measure of surface roughness used when estimating wind speed variation with height in the neutrally stable boundary layer using a logarithmic decay curve (Oke 1987; Laporte 2010). Although there are many roughness length classification systems and debate on their accuracy, the Davenport classification (Table 2.1) is most widely used in North America (Laporte 2010).

Table 2.1: Davenport classification of effective terrain roughness (Wieringa *et al.* 2001). Zero plane displacement (d) is a vertical length of the displaced height (usually above the roughness length) where wind speed reaches zero in the logarithmic wind speed profile for rough surfaces (Sellers 1965).

z_0 (m)	Landscape Description
1: Sea (0.0002)	Open sea or lake (irrespective of wave size), tidal flat, snow covered flat plain, featureless desert, tarmac and concrete with a free fetch of several kilometers.
2: Smooth (0.005)	Featureless land surface without any noticeable obstacles and with negligible vegetation: e.g. beaches, pack ice without large ridges, marsh and snow-covered or fallow open country.
3: Open (0.03)	Level country with low vegetation (e.g. grass) and isolated obstacles with separations of at least 50 obstacle heights; e.g. grazing land without windbreaks, heather, moor and tundra, runway area of airports. Ice with ridges across-wind.
4: Roughly Open (0.10)	Cultivated or natural areas with low crops or plant covers, or moderately open country with occasional obstacles (e.g. low hedges, isolated low buildings or trees) at relative horizontal distances of at least 20 obstacle heights.
5: Rough (0.25)	Cultivated or natural area with high crops or crops of varying height, and scattered obstacles at relative distances of 12 to 15 obstacle heights for porous objects (e.g. shelterbelts) or 8 to 12 obstacle heights for low solid objects (e.g. buildings). Analysis may need d.
6: Very Rough (0.5)	Intensively cultivated landscape with many rather large obstacle groups (large farms, clumps of forest) separated by open spaces of about 8 obstacle heights. Low densely-planted major vegetation like bushland, orchards, young forest. Also, area moderately covered by low buildings with interspaces of 3 to 7 building heights and no high trees. Analysis requires d.
7: Skimming (1.0)	Landscape regularly covered with similar-size large obstacles, with open spaces of the same order of magnitude as obstacle heights; e.g. mature regular forests, densely built-up area without much building height variation. Analysis requires d.
8: Chaotic (≥ 2.0)	City centers with mixture of low-rise and high-rise buildings, or large forests of irregular height with many clearings. Analysis by windtunnel advised.

The sea, vegetation and buildings are major topographic features creating surface roughness around and in the study area. Among these, the sea has the least surface roughness (Table 2.1). This indicates that when wind blows from the sea to the land, the area facing the sea receives stronger wind than the area inland. Surface roughness created by vegetation differs depending mainly on its height and density. Taller vegetation increases surface roughness and reduces wind speed (Walker and Hesp 2013). Density of vegetation affects the extent of downwind flow retardation. In the case of shelterbelts, high density vegetation is effective in lowering wind speed immediately to the lee, but a cavity created in the lee draws the faster moving air down from above so that the wind can regain its speed fairly quickly. On the other hand, medium density vegetation causes less downwind flow retardation immediately to the lee, but airflow passing through the vegetation mitigates the cavity formation. As a result, medium density vegetation can provide farther downwind flow retardation than low or high density vegetation (Nägeli 1946 in Oke 1987; van Eimern *et al*. 1964; Watts 1965). If height of the shelterbelt is h, it is reported that the point of 100% speed recovery for low, medium and high density vegetation at the lee could occur about 25 h, 30 h and 20 h from the shelterbelt, respectively (Nägeli 1946 in Oke 1987).

Tall buildings can create much greater surface roughness than vegetation due to their height, sharp edges and rigidity. The building materials are generally impermeable and far denser than vegetation, so wind speed significantly decreases at the lee edge, but an intense low pressure cavity created by the buildings draws faster moving air down from above. Buildings can also deflect strong wind down to the ground on the windward side and increase surface level wind speeds here and around the sides of buildings (Oke 1987; Wieringa *et al.* 2001).

The main features in rural and urban surface roughness are vegetation and buildings, respectively. Therefore, different influence of the vegetation and buildings on wind speed also affects wind speed in urban and rural areas. In general, surface roughness of urban areas is greater than rural areas, and wind speed in rural areas is usually higher. However, wind speed within the urban area might significantly increase in the situations when faster moving air above is deflected downwards by the tall buildings or is channeled into streets parallel to the regional airflow though the Network's anemometers mounted on the roof of school buildings will not catch such street level wind speed increase (Oke 1987).

Another topographic factor which affects wind speed is relief which includes hills, valleys, constrictions, slopes and escarpments. If relief is too significant for approaching airflow to fully adjust, a low pressure area is produced at the base or the lowest point of the features, and airflow is stagnated. As a result, wind speed decreases. On the windward slopes, vertical constriction of airflow occurs because of the protruding topographic features from a flat surface, and airflow accelerates to increase wind speed with a maximum at the crest of the features. Wind speed also increases at the narrowest point of constrictions such as a valley neck or mountain pass and around the sides of the hill where horizontal constriction of airflow occurs (Oke 1987; Walker and Hesp 2013). If the topographic features are steep, flow separation eventuates, and bolster and lee eddies which have an opposite wind direction to the regional wind form in the low pressure areas. The effects of those topographic features on change in wind speed and direction are strongest when the approaching wind has high speed and a right angle to the longer axis of the hills, valleys and escarpments or the shorter axis across the constrictions (Oke 1987).

2.3 Effects of an anemometer on a building on wind data

Different anemometer heights and locations influence the wind speed. Horizontal speed of wind in the boundary layer increases with height because frictional drag caused by the surface decreases with height (Oke 1987). Therefore, if surface conditions are the same, an anemometer with greater height records higher wind speed. Most of the Network's anemometers are mounted on the roof edge or corner of school buildings. When high speed wind approaches buildings with rectangular shape, which is most commonly seen in the study area, the airflow at the height of the upper one third to one quarter of a building is directed upward over the roof and accelerates. The airflow separates from the flat roof surface at the sharp edge of the roof. This separation causes suction on the roof and leeward wall and generates turbulent flow above the roof and leeward of the building. If the roof is long enough in the downwind direction, two kinds of airflow are generated. The primary flow is deflected above the roof but comes back down and reattaches to the roof near the edge of the leeward wall without changing direction and creates lee eddies in the lee of the building. The other is a turbulent flow which is produced between the reattaching airflow and the edge of the windward wall. The wind speed in this turbulent flow is considerably lower than that of both the airflow above and at the same elevation upwind. The wind direction becomes opposite to the regional one when the turbulent flow comes back down to reattach to the roof surface.

For small roofs where the air diverted up by the building comes back down beyond the roof, the turbulent airflow can go along the roof in the opposite direction over the entire roof. The speed of this turbulent airflow is also lower than that of the undisturbed airflow (Hosker 1985; Oke 1987; ASHRAE 1989). The airflow over the roof varies depending on building shape, roof pitch, wind speed and wind angle relative to the building. Mertens (2003) used a Computational Fluid Dynamics (CFD) calculation and investigated change in wind speed above the roof centre, edge and corner for different approaching wind directions relative to a windward wall of a rectangular building. He found that the average wind speed at the roof is slightly greater than the speed of undisturbed wind at the same height. Because the Network's anemometers mounted on the windward roof corner or at the windward roof edge are typically more than 1 m but less than 2 m high from the roof surface, they should avoid the turbulent zone and their wind measurement is most likely affected by accelerated airflow.

2.4 Wind pressure and windthrow

It is fairly common in Victoria that trees are uprooted or snapped by winds (Reyes and Tutsch 1999). This phenomenon is called windthrow. During the process of windthrow, not only are trees damaged, but also roads are blocked, electrical power is disrupted and buildings, cars and other objects are sometimes damaged. Mass (2008) stated that most of the damage to buildings and power lines is related not directly to wind itself but related to falling trees and called the Pacific Northwest tall trees "force multipliers for regional windstorms." Windthrow is a very complicated process, and there are many contributing factors, such as tree species, tree size, tree shape, porosity, tree leaf condition, soil type and its condition, and location (Gardiner and Quine 2000). However, the most obvious and significant control of windthrow is wind speed. The force per unit area produced by the wind blowing against a surface of an object is called wind pressure and is directly proportional to the square of the wind speed (Moran and Morgan 1994). Although air density is a minor variable compared to wind speed, it also contributes to the magnitude of wind pressure. Density is mainly a function of air temperature and air pressure and is inversely proportional to the former and proportional to the latter at a given elevation. Water vapour is also a control of air density though its effect is minor. The sensitivity of the method for calculating air density used in this study to the values of air temperature, air pressure and actual vapour pressure was determined. The method is most sensitive to air temperature, followed by air pressure, and least sensitive to vapour pressure (Figures. 2.1, 2.2 and 2.3).

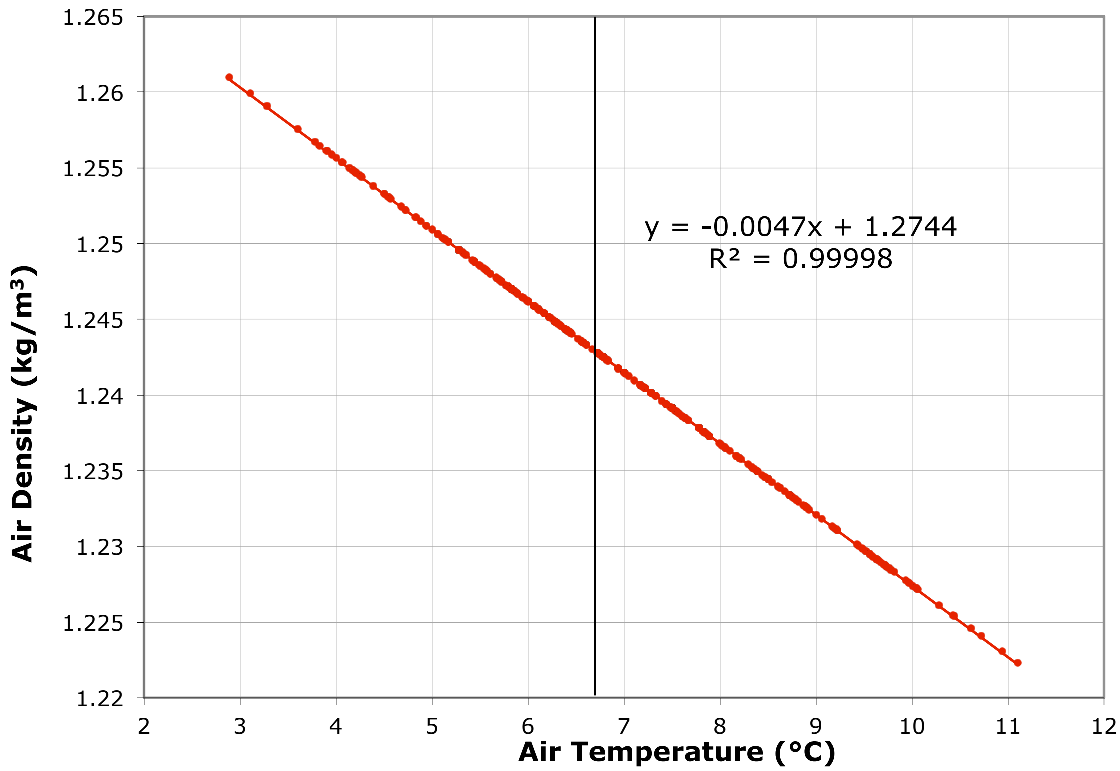

Figure. 2.1: Sensitivity of air density to air temperature. The solid vertical line within the graph indicates the median of all observed air temperatures used in the wind pressure calculations (6.82 °C).

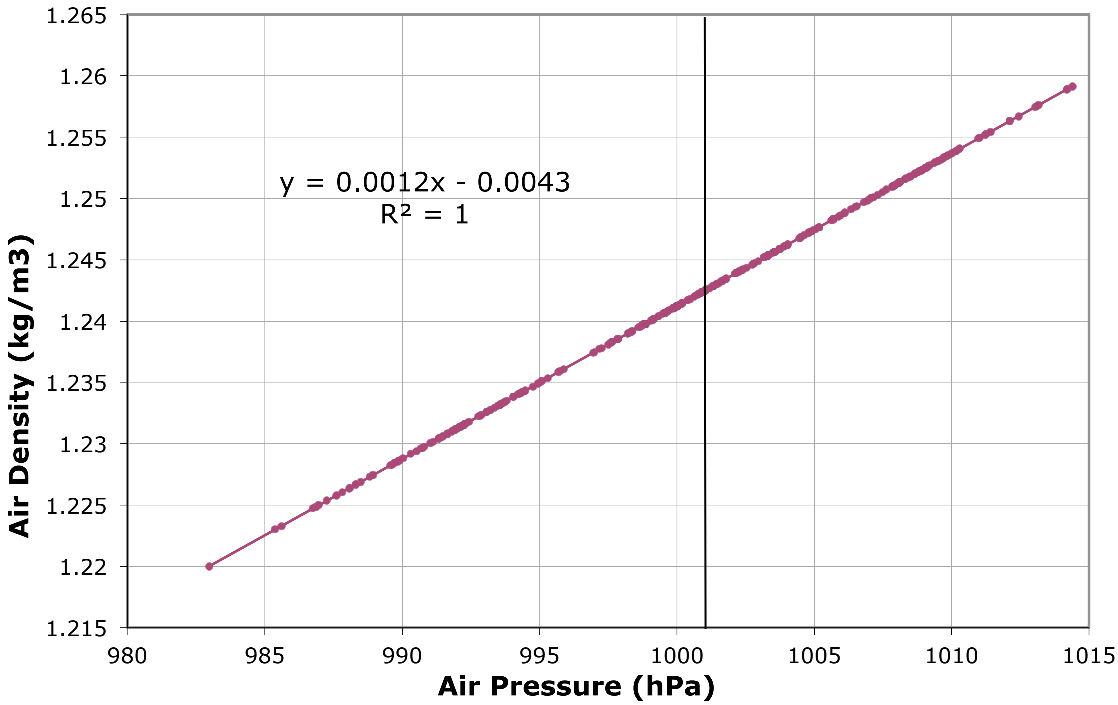

Figure 2.2: Sensitivity of air density to air pressure. The solid vertical line within the graph indicates the median of all observed air pressures used in the wind pressure calculations (1000.88 hPa).

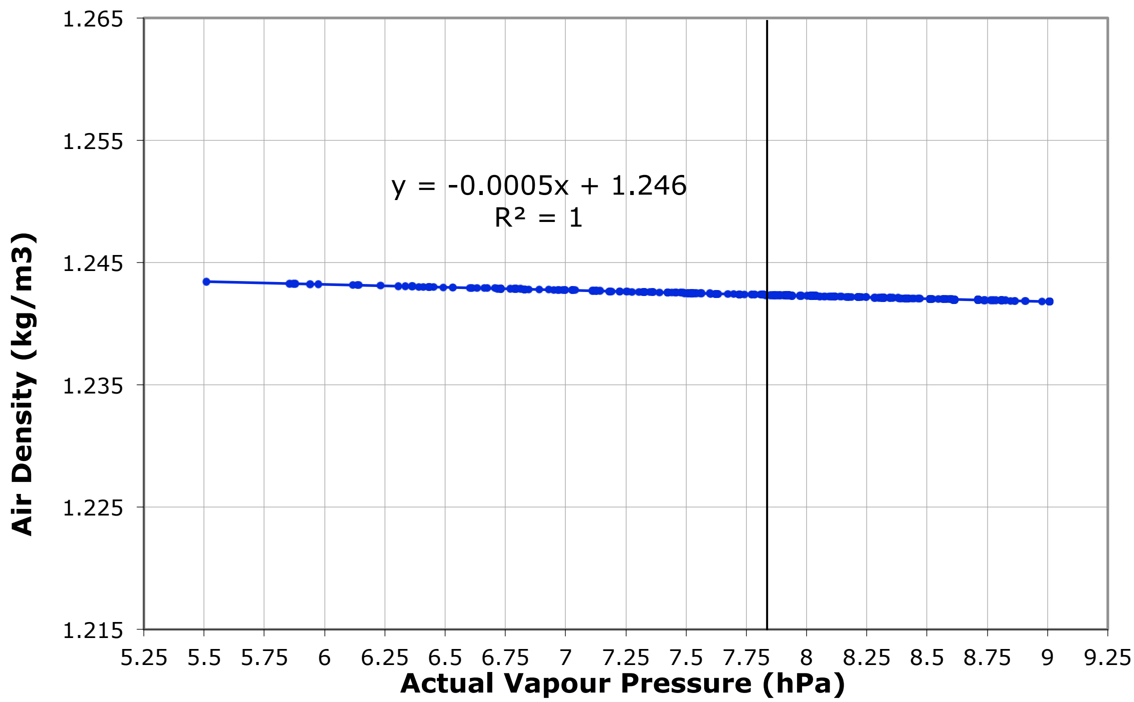

Figure 2.3: Sensitivity of air density to vapour pressure. The solid vertical line within the graph indicates the median of all observed vapour pressures used in the wind pressure calculations (7.83 hPa).

Gardiner and Quine (2000) studied threshold wind speed for overturning 50 year-old Sitka spruce with a top height of 19 m in a forest in Britain. Just like Douglas fir, Sitka spruce is a large coniferous evergreen tree found on North America's west coast including Vancouver Island. According to their calculation, the threshold wind speed is 27.4 m s^{-1} if soil type is brown earth and 23.8 m s^{-1} if soil type is gley. In addition, they found that the threshold wind speed for the tree in ploughed gley soil is lower than that for trees in gley soil with turf. Wider spacing between trees and thinning reduced threshold wind speed. They determined that a combination of these site and tree stand characteristics and a certain wind climate could yield a threshold wind speed of 17.6 m s^{-1}.

Although some conditions might differ depending on the location, Gardiner's and Quine's results can be used as a rough indicator of windthrow risk in Greater Victoria.

2.5 Summary

The winter mid-latitude cyclones which often bring strong winds to the study area form over the Pacific Ocean and are generated by a great temperature gradient. The counterclockwise circulation around the low pressure center determines the dominant wind direction of an area under the cyclones' influence. For the cyclones to develop and intensify upper atmosphere divergence is necessary. It helps maintain or strengthen a surface low pressure centre and pressure gradient by allowing surface converging air to rise and be carried away. Shortwaves cause warm and cold air temperature advection. These temperature advections aid vertical motion of air, which can deepen the trough, strengthen divergence and give energy for the cyclones to intensify. A cyclone reaches its maturity when an occluded front is formed. When cyclones have a bent-back occlusion, a region of great pressure gradient associated with the strongest winds is generated south of the low centre. Because movement of the occluded front, particularly of a bent-back occlusion, is slower than that of other fronts, cyclones with these fronts can cause greater damage. If a cyclone centre passes north of Victoria, the direction of the strongest winds will be from the range between southeast and southwest.

Topographic factors which affect wind speed in the study area are surface roughness, urban and rural differences, hills, valleys, escarpments, slopes and constrictions, and anemometer height and site conditions. Wind speed increases with smoother surface, windward slopes of hills and escarpments, the narrowest point of constrictions, and greater anemometer height. Around the windward roof edge of an isolated rectangular building, the accelerating upward airflow blows over the roof and separates to generate turbulent airflow above the flat roof surface. Speed of the turbulent airflow is significantly reduced compared to the airflow both above and upwind. Direction of the airflow on the roof in the turbulent zone can be opposite to the prevailing wind direction. If the anemometer is mounted on the edge or at the corner of the windward roof of the isolated rectangular building, it is most likely to be affected by the accelerating upward airflow.

Wind pressure is the force per unit area produced by the wind blowing against a surface of an object. It is a function of wind speed and air density and is directly proportional to the square of the wind speed. Major controls of air density are air temperature and air pressure while a minor control is vapour pressure. Air density is inversely proportional to air temperature and vapour pressure and proportional to air pressure. Falling tall trees caused by great wind pressure are associated with more wind damage than strong wind itself. Gardiner and Quine (2000) determined the threshold wind speed for overturning well-grown Sitka spruce to be 27.4 m s^{-1} for brown earth soil, 23.8 m s^{-1} for gley soil and 17.6 m s^{-1} for a vulnerable combination of site and tree stand characteristics and a certain wind climate.

Chapter 3

Methods

3.1 Study area and sub-regions

The study area for this research is the Capital Regional District of Victoria, British Columbia excluding Sooke and a large part of Metchosin (Figure 1.1). The study area was divided into 3 sub-regions of school districts 61, 62 and 63. However, it was necessary to redefine the area of school district 62 for the research purpose in this study. Despite the fact that the actual school district 62 covers a large area including Sooke and Port Renfrew, the weather stations utilized in this study are located only in the east portion of the district. Therefore, school district 62 mentioned in this study refers to an area that includes a part of the Highlands that belongs to school district 62, Colwood, Langford and a northeast part of Metchosin where Hans Helgesen Elementary School (Stn. ID 36) is located. The study area and the location of each weather station are shown in Figure 1.1 with official boundaries of the school districts. Station IDs, names, coordinates and elevations of weather stations in each school district are presented in Table A1. Examples of weather stations in residential and rural areas near Victoria's urban core are shown in Figures 3.1, 3.2, 3.3, 3.4, 3.5 and 3.6.

Figure 3.1: A weather station mounted on the roof of Central Middle School (Stn. ID 75) (Google Maps 2014a).

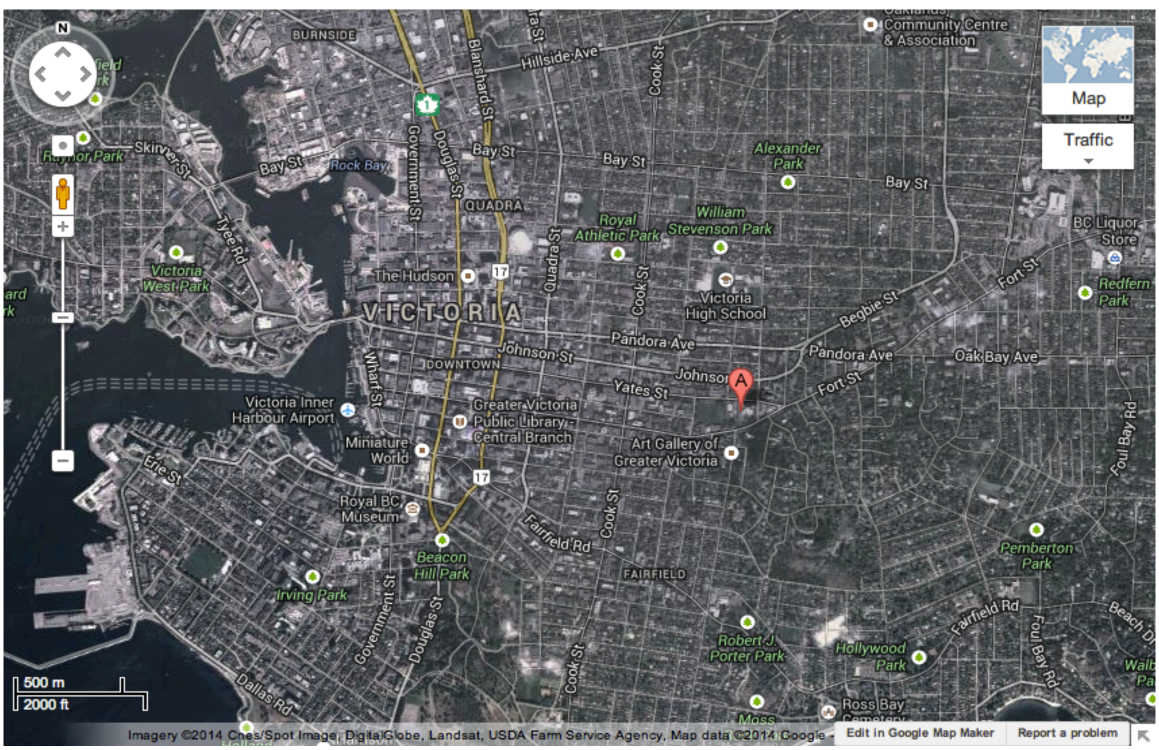

Figure 3.2: Central Middle School indicated by "A" is located near Victoria's urban core (Google Maps 2014b).

Figure 3.3: A weather station mounted on the roof of Sangster Elementary School (Stn. ID 31) (Google Maps 2014c).

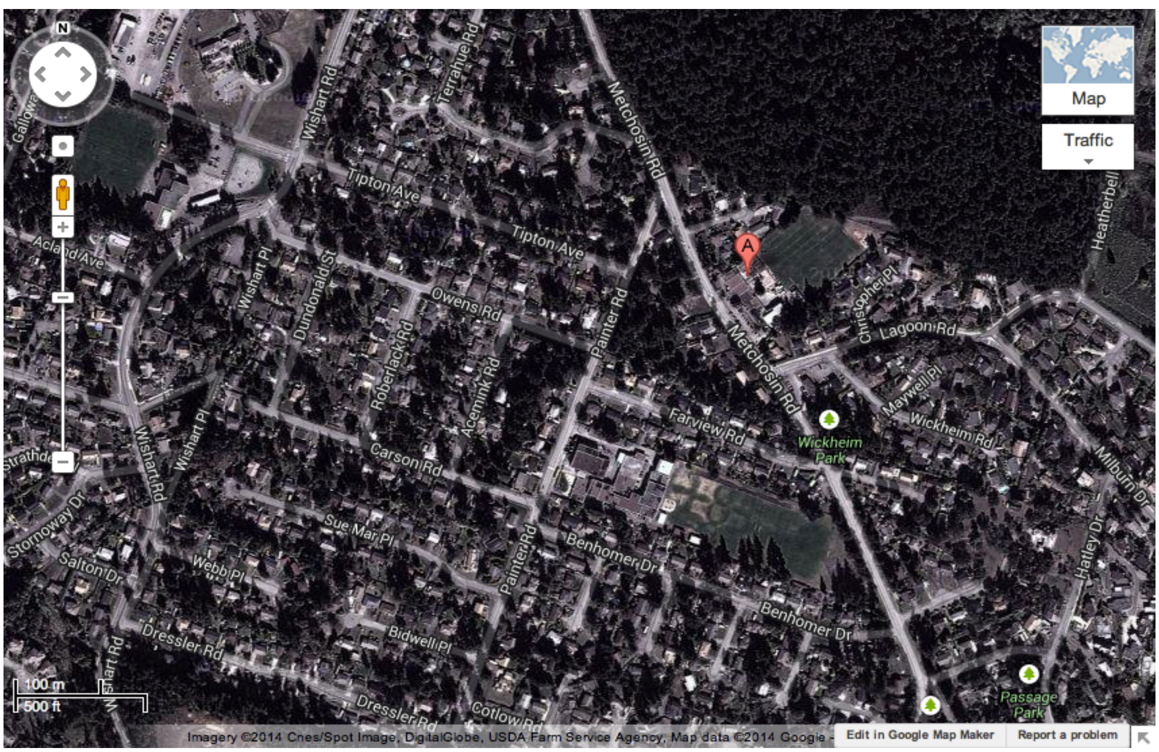

Figure 3.4: Sangster Elementary School indicated by “A” is located in a residential area (Google Maps 2014d).

Figure 3.5: A weather station mounted on the roof of Deep Cove Elementary School (Stn. ID 62) (Google Maps 2014e).

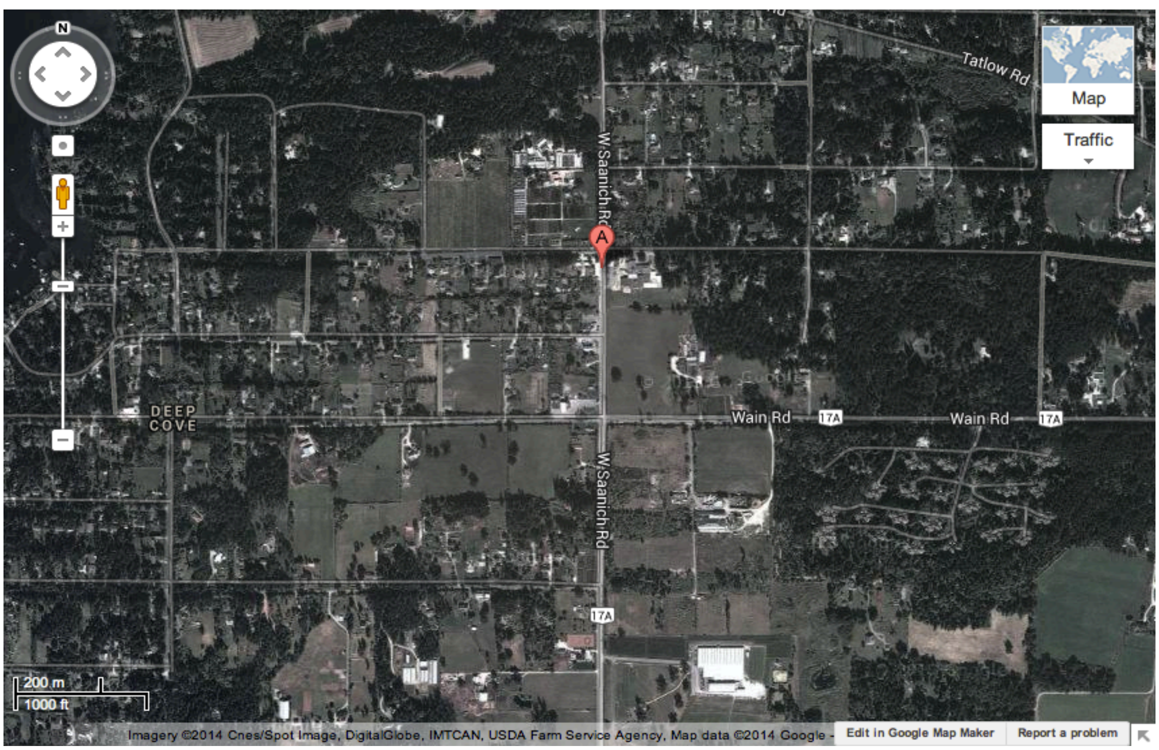

Figure 3.6: Deep Cove Elementary School indicated by “A” is located in a rural area (Google Maps 2014f).

The three school districts are chosen based upon their different land use, shoreline, relief and surface roughness. School district 61 (SD 61), which contains the urban core of Greater Victoria, is the most populous school district in the study area. It is residentially and commercially highly developed and has the least wooded area among all. Its shoreline encompasses the east and south sides of the school district. Major shoreline orientations are WNW-ESE, N-S and NW-SW. The relief of SD 61 is the lowest overall (Figure 1.1). Although the eastern part of a range of hills extends to the northwest part of the school district, the rest of the area is relatively plane with rolling hills. Because SD 61 is relatively plane and well developed, its surface roughness mainly comes from buildings.

School district 62 (SD 62) also has populous and well-developed residential, commercial and business areas in the middle east. The north and south parts of the school district are primarily rural residential areas, but the north part is characterized by large protected parkland whereas the south is characterized by agricultural land use. However, the agricultural area in this school district is relatively small. The shorelines of SD 62 are found on the northwest side with a N-S orientation and southeast side with a NNE-SSW orientation. SD 62 has the most significant relief among all, and areas with relief occupy a large portion of the school district (Figure 1.1). The range of hills is located in the north, and a plane area in the middle east beside the southeast shoreline is surrounded by hills and mountains with elevation of around 200 m to more than 300 m on its north and west sides and those with elevations of more than 200 m on its south side (Natural Resources Canada 2010a). Surface roughness of SD 62 is associated with agricultural land, buildings and tall evergreen trees. The numerous buildings and relatively large wooded lands with tall evergreen trees are located in the plane area in the middle part of the school district whereas the agricultural lands and many small wooded lands are seen in the plane areas in the south.

School district 63 (SD 63) is mainly agricultural and rural residential. Its residential, commercial and business areas are scattered in the school district and not as extensive as those in SD 61. The wooded areas can mostly be found in the south, especially southwest; middle west and north. The longest shoreline belongs to SD 63. The east, north and west sides of the school district are surrounded by the ocean. Its major orientations are N-S, NNW-SSE, NNE-SSW, NW-SE and NE-SW. SD 63 also has significant relief in its southwest and middle west, moderate relief in the south and relatively low relief in the north. Its major plane areas lie between those areas with the relief. SD 63's agricultural areas are mostly plane and have a much smoother surface than the well-developed areas with buildings and wooded areas with tall evergreen trees. In addition, Victoria International Airport is a prominent feature in the north of SD 63 providing a relatively large area with distinctly smooth surface.

In terms of the elevations of the weather stations, those located in the northeast of SD 61 tend to be at higher elevations than those located in the other part of the school district. Most of the weather stations' elevations in SD 62 are higher than those in SD 61 and SD 63. The range of weather station elevations in SD 63 is similar to that in SD 61, and the weather stations located near marine shorelines tend to have lower elevations than the others (Table A1).

3.2 Data

3.2.1 Sources of information on synoptic and mesoscale atmospheric conditions

Synoptic and mesoscale atmospheric conditions associated with the high wind speeds over the study area during the selected days were analyzed using *North American 500MB Analysis Hgts_Tmps Stn Plots*, *North American Surface Analyses* and *United States Surface North_West Analyses* from The National Centers for Environmental Prediction (NCEP), 500 hPa temperatures composite means from Earth System Research Laboratory (ESRL) and satellite images from Google Earth.

3.2.2 Climate data and cases

A source of climate data utilized in this study is the School-Based Weather Station Network (Figure 1.1). Since the first weather station of the Network started operating in Victoria in March 2002, the Network has been expanding to have over 100 weather stations mainly on a southern half of Vancouver Island and nearby islands. Each weather station measures various climate variables such as atmospheric temperature, atmospheric humidity, precipitation, UV Index, incoming solar radiation, wind speed, wind direction and atmospheric pressure. They are displayed on the Network's website (http://www.islandweather.ca/) and archived in a central database server at the University of Victoria (School-Based Weather Station Network 2012a; Weaver and Wiebe 2006).

Besides the Network data, Victoria Gonzales CS data from The National Climate Data and Information Archive were utilized to select the cases from the Network data. Victoria Gonzales CS was selected because it has excellent exposure to winds from southeast through southwest, which is typical of the strong winds during winter (Mass and Dotson 2010). In addition, topographic maps from Natural Resources Canada and the satellite images from Google Earth were used for analytical purposes.

The climate variables used in this study are wind speed, gust wind speed, wind direction, atmospheric temperature, atmospheric pressure and relative humidity measured on November 15, 2006; December 13, 2006; December 15, 2006; January 9, 2007; February 5, 2008 and February 7, 2008. The data of the last 3 climate variables were used for the calculation and analysis of air density.

3.2.3 Advantage of using wind data from the School-Based Network for this study

Two of the indisputable advantages of using the Network data are their high spatial and temporal resolutions. For example, when the plan of this study was made, the number of Environment Canada's weather stations that were providing hourly climate data in the study area was only 6 (Environment Canada 2011a). On the other hand, the number of the Network's weather stations was 65. Victoria's topography is rich in variation so that more weather stations can produce a more representative data set, which contributes to more accurate analyses and understanding of the wind distribution. In addition, the highest temporal resolution of Environment Canada's data was one hour whereas that of the Network data was one minute. This degree of resolution makes it possible to create data with lower resolutions from the original data (e.g. quarter-hourly and half-hourly data). Because wind speeds and wind directions can change rapidly following change in surface atmospheric conditions, the resolution of the Network data is a great feature that allows detailed analysis of changing winds. An additional definite advantage of the Network data was the inclusion of gust wind speed, which is another important climate variable for this study because of its implication for wind damage (Brasseur 2001). Therefore, the Network had the best obtainable data for this study, and without them this study would not have been feasible.

3.2.4 Weather station instrumentation

The weather stations in the School-Based Weather Station Network that collected the data for this study employ Davis Vantage Pro2 ™ Plus weather stations (School-Based Weather Station Network; Weaver 2006). They are solar powered and provide data every minute of climate variables including those mentioned above. The operating temperature is -40° to +65° C (Davis Instruments a), and the ranges of climate data displayed on console (Table 3.1) ensured that the data values utilized in this study were not limited by the ranges. Information on a calibration study of the Vantage Pro2 Plus weather station (Massen 2003) is also available via the website of the Network.

Table 3.1: Weather data specifications of the Davis Vantage Pro2™ Plus weather station. The listed climate variables in this table are the ones used in this study (Source: Davis Instruments).

Variable	Resolution	Range	Accuracy (+/-)
Barometric Pressure	0.1 hPa	540 to 1100 hPa	1.0 hPa
Outside Humidity	1%	0 to 100 %	3 %; 4 % above 90 %
Outside Temperature	0.1 °C	-40 ° to +65 °C	0.5 °C above -7 °C; 1 °C under -7 °C
Time	1 min.	24 hours	8 sec./month
Date	1 day	month/day	8 sec./month
Wind Direction	1°	0 to 360°	3°
Wind Speed (large cups)	0.5 m/s	1 to 67 m/s	greater of 1 m/s or 5 %

This study used the total of 65 weather stations operating in Greater Victoria. They were distributed over all three school districts: 43 weather stations in SD 61, 13 in SD 62 and 9 in SD 63. As a result, density of the weather stations was the highest in SD 61 (Figure 1.1; Table A1).

The conditions regarding the weather station site locations were unconventional and do not meet most of the Meteorological Service of Canada siting standards for meteorological observing sites (MSC 2001), which are in agreement with World Meteorological Organization (WMO) recommendations, individual instrument manuals, and manufacturer's recommendations (Tables 3.2 and 3.3). Among the weather stations whose data were utilized in this study, those which were not mounted on the roofs of schools were Swan Lake Nature Sanctuary (Stn. ID 2: a personal house), South Park Elementary School (Stn. ID 23: an antenna tower), the AChannel Studio (Stn. ID 41: AChannel headquarters), Butchart Gardens (Stn. ID 42: a lamppost in a parking lot) and Cal Revelle Nature Sanctuary (Stn. ID 71: a personal house). It should also be noted that the Marigold Elementary School weather station (Stn. ID 6) was actually mounted on nearby Spectrum High School.

Table 3.2: Siting standards for non-airport meteorological stations. The primary area is the area where the instruments or sensors are physically located, and the secondary area is an undisturbed zone surrounding the primary zone and provides protection (MSC 2001).

The site should be located:	
(i)	on open, level ground with a primary area at least 15m x 15m covered with short grass or at least on natural ground with a secondary turf covered area of at least 30m x30m, surrounded as by a single rail, cable, or chain link fence, and a protected area of 90m x 90m centered on the primary area.
(ii)	such that sensors shall be at a distance from vertical obstructions of four times the height of the obstruction for rain gauges, and two times the height of the obstruction for Stevenson screens.

(iii)	in an area which provides ease of access for the observer and for maintenance of instruments and the installation of electrical ducts.
Locations for sites which shall be avoided are:	
(i)	the top of hills
(ii)	in hollows, at the bottom of narrow valleys, and near hills or ridges, or cliffs
(iii)	near isolated ponds or streams
(iv)	near roads where snow from snow clearance operations, or dust, can affect the site
(v)	where there is excessive human or animal traffic
(vi)	where excessive drifting snow accumulates
(vii)	near vehicle parking areas
(viii)	where heat is exhausted by vehicles or buildings

Table 3.3: Siting standards for anemometers. The primary area is the area where the instruments or sensors are physically located, and the secondary area is an undisturbed zone surrounding the primary zone and provides protection (MSC 2001).

The site should be located:	
(i)	on open, level ground with a primary area at least 15m x 15m covered with short grass or at least on natural ground with a secondary turf covered area of at least 30m x 30m, surrounded as by a single rail, cable, or chain link fence, and a protected area of 90m x 90m centered on the primary area.
(ii)	such that the distance from vertical obstructions shall be at least ten times the height of the obstruction
(iii)	on an area which provides ease of access for maintenance and the installation of electrical ducts
Locations which shall be avoided are:	
(i)	the top of hills
(ii)	in hollows, at the bottom of narrow valleys, or near hills and ridges
(iii)	where future development of the airport is most likely to occur.

The unconventional site location conditions in the Network impose some limitations on its wind data because they make the wind data more susceptible to influence of the site-specific obstructions, terrain characteristics, and the height of the roofs where the weather stations are mounted. Therefore, it should be noted that there are local variations (or biases) in wind data from the Network that may cause deviations from regional wind patterns. Modifications occur in both speed and direction datasets, and they vary widely with: i) geographic location across the network in a very rough, largely urban region, and ii) where the instrument is sited on each school. Both modifications i and ii also vary with direction of the wind. For example, speed and direction of WSW wind at a weather station in the southwest of an urban region and those at a weather station in the northeast of the urban region can be very different from regional winds because of airflow around buildings and a channeling effect of a certain street. It is most likely that airflow around the edge and corner of the windward wall of buildings relative to WSW winds makes wind speed slightly higher than the undisturbed airflow at the same height above the ground, but airflow at the same site might decrease its speed when the site becomes the lee because of wind from opposite direction. The quantitative assessment of those influences on the wind data is too complex to be achieved so that the exact amount of the influence on the wind data cannot be known. However, the purpose of this study is not to measure a precise value of undisturbed wind speed at each weather station but to investigate the relative distribution of high wind speeds as they are affected by local site conditions in Greater Victoria. Therefore, some of the influences, especially of the terrain characteristics, on the data are actually desirable for this study. In addition, quality of the Network's wind data is considered to be acceptable because the weather station site locations were chosen with great care by the highly trained climatologists who did their best to minimize the effects of obstacles on the measurement (School-Based

Weather Station Network 2011a). The past and on going research using the Network's wind data, including Saenko (2008), support credibility of the data. Moreover, the fact that the weather stations were typically installed on the roofs of schools which were visible from the street and on the south-facing side rather than somewhere else on the building brings some degree of consistency regarding anemometer location conditions. Visual access from the street contributes to fewer obstructions, and the southerly location provides exposure to the strong southeast through southwest winds of main interest (Mass and Dotson 2010; School-Based Weather Station Network 2011a). Therefore, although analyses using the Network data require careful consideration of the effects of individual site location conditions on the data, their use for this study was considered to be appropriate.

3.2.5 Selection of the climate variables and cases

The climate variables used in this study are wind speed, gust wind speed, wind direction, atmospheric temperature, atmospheric pressure and relative humidity measured on November 15, 2006; December 13, 2006; December 15, 2006; January 9, 2007; February 5, 2008 and February 7, 2008. The data of the last 3 climate variables were used for the calculation and analysis of air density.

Prior to selecting the dates mentioned above, the following conditions were considered. First, the dates would be chosen from ones in winter when the frequency and intensity of mid-latitude cyclonic storms that produce the high wind speed events are greatest. Second, the dates should have a recorded wind speed of 61 km h^{-1} ($\approx$ 16.94 m s^{-1}) or more. The reason for the wind speed criterion is because Environment Canada defined very strong wind/gales as inland wind speed of 61 km h^{-1} ~ 90 km h^{-1} (= 25 m s^{-1}) (Environment Canada 2007). These winds become objects of wind warning if they are forecast or observed over the areas specified by Environment Canada (2011b). Third, the Victoria Gonzales CS wind data from The National Climate Data and Information Archive would be used as a reference to look for the dates to study. The data from the National Climate Data and Information Archive are readily accessible at Climate Data Online, considered to be reliable and widely used in Canada. Selecting the dates by referring to Environment Canada's hourly data was much easier and required far less time than going directly to the Network data measured every minute. Fourth, the number and distribution of weather stations should be sufficient to cover the Greater Victoria area on the selected days. The establishment of the School-Based Weather Station Network was relatively new when this study was planned, and the number of the weather stations which were operating within the Greater Victoria area was 1 in 2002, 2 in 2004 and 24 in 2005. It was the end of June 2006 when all of the 65 weather stations whose data were used in this study were operational. Therefore, although Victoria Gonzales CS recorded wind speed of 69 km h^{-1} on February 1 and 83 km h^{-1} on February 4, 2006, those dates before the end of June 2006 were not selected.

3.3 Methods

3.3.1 Analyses of wind distribution in the study area

The data collected at each weather station were affected by the weather station's unique immediate environment. Therefore, the basic approach of this study to the data is to look at them on the topographically distinct school district basis, level out the influence of extreme differences in immediate environments, and extract the common characteristics of the local winds. In order to find wind variability in the study area during specific time periods on the selected days, some basic statistics, such as mean wind speeds, mean wind directions, circular standard deviations, and frequency of occurrence of eight compass-point wind directions, were calculated for the school districts and/or some individual weather stations. The effects of topography on the spatial wind variation were examined qualitatively using topographic maps from Natural Resources Canada and satellite images from Google Earth which provide information on local topography. In addition, the daily maximum wind pressure was calculated for the weather stations, and the results are shown on maps in order to determine the areas susceptible to wind damage.

3.3.2 Data processing before calculations

All climate data from the School-Based Weather Station Network are stored in a MYSQL database. When the number of the downloaded data for a day was less than 1,440, the time periods when the data were missing during the day were identified, and the corresponding blank cells for the data values and times were created in their Excel files. This was necessary and done in order to make calculations using functions in Microsoft Excel, which are cell-location specific, easier. However, missing data were not replaced. Furthermore, even if some stations had missing data for a whole day or more, eliminating the stations from all the remaining case study days was not considered because completely losing the data from those stations means losing representativeness of the data set on the day when those stations had the data. This decision certainly would cause inconsistency among the selected days regarding the completeness of the data set. However, it was considered that providing statistics about the individual weather stations' wind speeds and time periods of missing data would make up for the problem and help readers critically evaluate the results.

3.3.3 Data quality and accuracy

The missing wind data and the missing data of air density variables at the time of the daily maximum gust wind speed at each weather station during the selected days are presented in Tables A2, A3, A4 and A5. Twenty-five out of 65 weather stations failed to record wind speed on Dec. 15, 2006 between 4:00 and 4:29. The number of the weather stations which failed to record wind speed data tended to reach the maximum during or after significant increases in wind speeds or around the daily maximum overall mean 30-minute wind speed in the entire study area (Figures 4.15, 4.18, 4.21, 4.24, 4.27 and 4.30). The overall percentage of missing data 30 minutes before and after the 30-minute period of the daily maximum overall mean 30-minute wind speed in the entire study area during the selected days was determined to be 13.17%. At a district level, the overall percentage of missing data for 1.5 hours around the times of the daily maximum district overall mean 30-minute wind speed during the selected days was 5.71% in SD 61, 33.76% in SD 62 and 18.85% in SD 63. Missing wind direction data occurred at the same time as the missing wind speed data at most of the weather stations. Those missing data, especially during the periods of high wind speeds, limited the analysis in this study.

When questionable data values were found, they were not used for calculations and analyses except for those cases where their effects on the analyses were negligible.

For example, if the questionable values were found during time periods of low wind speeds which are not the focus of this study, they were kept. However, if wind speed and/or wind gust speed recorded 0 m s^{-1} at a weather station during 1.5 hours around the primary peak time of the associated district overall mean wind speed, those data at the weather station for the whole day were eliminated. In addition, if a missing datum was found in gust wind speed at a weather station during the same period of time mentioned above, the weather station's entire data of gust wind speed for that day were also discarded.

3.3.4 Calculations of various means

Means of wind directions, air temperatures, air pressures, maximum gust wind speeds, a mean of an individual weather station's wind speeds during a 30-minute period and a mean speed of winds from a specific direction during a 30-minute period were calculated. On the other hand, "overall" means were calculated by taking the averages of already calculated means. For example, district overall mean 30-minute wind speeds were calculated by taking the averages of all individual weather stations' mean 30-minute wind speeds belonging to each school district. The reason why some means were calculated by taking the averages of the calculated means was because using raw data would make the calculation by the Excel function far more time consuming than using calculated means in some cases due to a large number of data. It was found that taking the averages of already calculated means could induce error, up to approximately 1 m s^{-1} for some overall mean wind speeds.

Wind directions are directional data whose 0 degrees and 360 degrees mean the same angle. Therefore, the mean wind directions and circular standard deviations were determined based on the directional statistical method described by Mardia (1972). For the mean wind directions:

$$\overline{C} = \frac{1}{n}\sum_{i=1}^{n}\cos\theta_i, \tag{1}$$

$$\overline{S} = \frac{1}{n}\sum_{i=1}^{n}\sin\theta_i, \tag{2}$$

where

$\overline{C}$ is the mean of cosines of wind directions,

$\overline{S}$ is the mean of sines of wind directions,

n is the number of observations,

θ_i is wind direction.

Then,

$$\overline{R} = \left(\overline{C}^2 + \overline{S}^2\right)^{\frac{1}{2}}. \tag{3}$$

$R = n\overline{R}$ is the length of the resultant, and $\overline{R}$ is the mean resultant length.

From the equations above,

$$\overline{C} = \overline{R}\cos\overline{x}_0, \tag{4}$$

$$\overline{S} = \overline{R}\sin\overline{x}_0, \tag{5}$$

where

$\overline{x}_0$ is the mean wind direction in radians.

To obtain $\overline{x}_0$, let

$$\bar{x}_0{}' = \arctan\left(\frac{\bar{S}}{\bar{C}}\right), \; -\frac{\pi}{2} < \bar{x}_0{}' < \frac{\pi}{2}, \tag{6}$$

therefore,

$$\bar{x}_0 = \bar{x}_0{}' \qquad \text{if } \bar{S} > 0, \; \bar{C} > 0, \tag{7}$$

$$\bar{x}_0 = \bar{x}_0{}' + \pi \qquad \text{if } \bar{C} < 0, \tag{8}$$

$$\bar{x}_0 = \bar{x}_0{}' + 2\pi \quad \text{if } \bar{S} < 0, \; \bar{C} > 0. \tag{9}$$

For the circular standard deviation:

$$S_0 = 1 - \bar{R}, \tag{10}$$

where

S_0 is the circular variance.

Because the range of S_0 is (0, 1), in order to relate S_0 to the standard deviation on the line, Mardia (1972) suggests using the following result for the wrapped normal distribution, which he considers “a natural adaptation of the linear normal distribution to the circle,”

$$1 - S_0 = e^{-\frac{1}{2}s^2}, \tag{11}$$

where

S^2 is variance of population values.

Then, the circular standard deviation, s_0, can be defined as

$$s_0 = \{-2\ln(1 - S_0)\}^{\frac{1}{2}}, \tag{12}$$

where the range of s_0 is $(0, \infty)$.

3.3.5 Calculations of daily maximum wind pressure

Daily maximum wind pressures were calculated for each weather station on all the selected days using the following equation:

$$p_w = 0.5\rho_a u^2, \quad (13)$$

where

p_w is wind pressure in kg m^{-1} s^{-2} (Pa);

ρ_a is air density in kg m^{-3};

u is wind speed in m s^{-1}.

In the School-Based Weather Station Network, both the wind speed and the gust wind speed are recorded every minute. The difference between them is that the stored wind speed is the average of wind speed measured for a period of one minute while the gust wind speed is the maximum wind speed recorded during the one minute period (School-Based Weather Station Network, 2011b). Because Equation (13) indicates that the dominant variable for wind pressure is the speed of wind u, data of gust wind speed were used in order not to underestimate the values of wind pressure. However, the square of u also implies that any local effects of roughness sub-layer flow modification will be compounded.

First, the daily maximum gust wind speed at each weather station was determined for all of the selected day using an Excel function called MAX, which returns the largest value in a set of values. Then, data values of the other climate variables needed to calculate the wind pressure were found at the corresponding time of the daily maximum gust wind speed.

The air density was calculated using the equation recommended by the Comité International des Poids et Mesures (CIPM) in 2007 (Picard *et al.* 2008). An advantage of using the CIPM-2007 equation is that the climate variables such as air temperature, air pressure and relative humidity can be utilized to calculate the air density. Another advantage is that the equation has frequently been studied, used and improved for years (Giacomo 1982; Davis 1992; Picard and Fang 2003; Picard *et al.* 2004; Picard *et al.* 2008).

The CIPM-2007 equation was developed based upon the equation of state of an ideal gas (Giacomo 1982) and has the following form:

$$\rho_a = \frac{pM_a}{ZRT}\left[1 - x_v\left(1 - \frac{M_v}{M_a}\right)\right], \tag{14}$$

where

ρ_a is the density of moist air in kg m^{-3};

p is the air pressure in Pa;

T is the thermodynamic temperature in K (= 273.15 + air temperature t in C);

x_v is the mole fraction of water vapour;

M_a is the molar mass of dry air in kg mol^{-1};

M_v is the molar mass of water vapour (= 18.01528 $\times$ 10^{-3} kg mol^{-1});

Z is the compressibility factor;

R is the molar gas constant (= 8.314472 J mol^{-1} K^{-1}).

The auxiliary equation for M_a is:

$$M_a = [28.96546 + 12.011\ (x_{CO2} - 0.0004)] \times 10^{-3}\ \text{kg mol}^{-1}$$

$$= 28.96546 \times 10^{-3}\ \text{kg mol}^{-1}, \tag{15}$$

where x_{CO2} is the mole fraction of carbon dioxide.

Because a measurement of x_{CO2} was not available, its value was assumed to be 0.0004, which is "a default value" in laboratory air (Picard *et al.* 2008) eliminating the effect of carbon dioxide on the molecular mass of dry air.

Applying the values of M_a, M_v and R, equation (14) reduces to:

$$\rho_a = \frac{0.003483740p}{ZT}\left(1 - 0.3780x_V\right). \quad (16)$$

The auxiliary equation for x_v is:

$$x_V = hf(p,t)\frac{p_{SV}(T)}{p}, \quad (17)$$

where

h is the relative humidity, whose range is $0 \le h \le 1$.

f is the enhancement factor calculated from:

$$f = \alpha + \beta p + \gamma t^2, \quad (18)$$

where

t is the air temperature in C;

α, β and γ are constants specified for the CIPM-2007 equation (Table 3.4).

$p_{SV}(T)$ in equation (17) is the saturation vapour pressure in pascals of moist air at air temperature (T) obtained from:

$$p_{SV}(T) = \exp(AT^2 + BT + C + \frac{D}{T}), \quad (19)$$

where

A, B, C and D are constants specified for the CIPM-2007 equation (Table 3.4).

The auxiliary equation for Z is:

$$Z = 1 - \frac{p}{T}\left[a_0 + a_1 t + a_2 t^2 + \left(b_0 + b_1 t\right)x_V + \left(c_0 + c_1 t\right)x_V^2\right] + \frac{p^2}{T^2}\left(d + e x_V^2\right), \quad (20)$$

where a_0, a_1, a_2, b_0, b_1, c_0, c_1, d and e are also constants specified for the CIPM-2007 equation (Table 3.4).

Table 3.4: Constant parameters specified for the CIPM-2007 equation for the determination of the density of moist air (Picard *et al.* 2008).

Vapour pressure at saturation $p_{SV}(T)$: $p_{SV}(T) = 1Pa \times \exp\left(AT^2 + BT + C + \frac{D}{T}\right)$	
A	1.2378847×10^{-5} K^{-2}
B	$-1.9121316 \times 10^{-2}$ K^{-1}
C	33.93711047
D	$-6.3431645 \times 10^{-3}$ K
Enhancement factor *f*: $f = \alpha + \beta p + \gamma t^2$	
α	1.00062
β	3.14×10^{-8} Pa^{-1}
γ	5.6×10^{-7} K^{-2}
Compressibility factor *Z*: $Z = 1 - \frac{p}{T}\left[a_0 + a_1 t + a_2 t^2 + (b_0 + b_1 t)x_V + (c_0 + c_1 t)x_V^2\right] + \frac{p^2}{T^2}\left(d + e x_V^2\right)$	
a_0	1.58123×10^{-6} K Pa^{-1}
a_1	-2.9331×10^{-8} Pa^{-1}
a_2	1.1043×10^{-10} K^{-1} Pa^{-1}
b_0	5.707×10^{-6} K Pa^{-1}
b_1	-2.051×10^{-8} Pa^{-1}
c_0	1.9898×10^{-4} K Pa^{-1}
c_1	-2.376×10^{-6} Pa^{-1}
d	1.83×10^{-11} K^2 Pa^{-2}
e	-0.765×10^{-8} K^2 Pa^{-2}

The ranges of air temperature and air pressure recommended for the use of the CIPM-2007 method to compute Z are from 288.15 K to 300.15 K and from 600 hPa to 1100 hPa, respectively (Giacomo 1982; Picard *et al.* 2008). On the other hand, the data ranges in this study are from 273.15 K to 284.25 K and from 983.0 hPa to 1014.4 hPa. Because the air temperature data were below the recommended range, an increase in uncertainty should be expected.

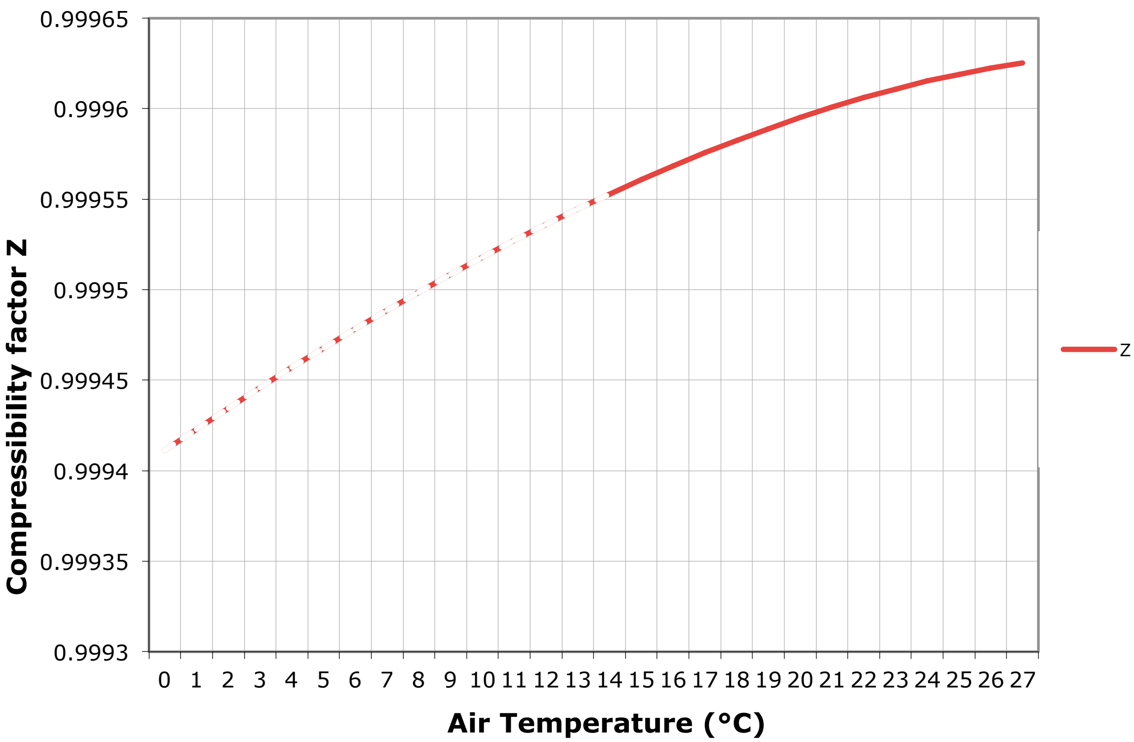

Figure 3.7: Compressibility factor *Z* as a function of air temperature (humidity = 80 % and air pressure = 1000.5 hPa). The solid line indicates *Z* for the recommended temperature range.

Figure 3.7 shows a relationship between the compressibility factor *Z* and the air temperature when relative humidity and air pressure stay constant at 80 % and 1000.5 hPa. The values of humidity and air pressure were chosen based on their averages in the data used in the wind pressure calculation. If the actual change in *Z* for the temperature between 2 °C and 12 °C is similar to the change estimated in Fig. 3.7, the value of Z^1 in the equation (16) increases 0.011007 % as the air temperature decreases from 12 °C to 2 °C while Z^1 increases 0.006450 % as the air temperature decreases from 27 °C to 15 °C. The rate of change of Z^1 with respect to the air temperature between 2 °C and 12 °C is almost 2.0 times as much as the rate of change of Z^1 with respect to air temperature in the recommended range. However, the values of Z^1 are small so that an increase of 0.011007 % can be negligible especially when the purpose of calculating the air density and subsequent daily maximum wind pressure is not to determine their precise values but their spatial distributions. Thus, it is assumed that the magnitude of the uncertainty would not significantly impair the spatial analysis.

3.4 Summary

The study area of Greater Victoria was divided into sub-regions of SD 61, SD 62 and SD 63 whose land use, marine shoreline, relief, surface roughness and elevation are different. The climate data were collected at 65 weather stations in the School-Based Weather Station Network on Nov. 15, 2006; Dec. 13, 2006; Dec. 15, 2006; Jan. 9, 2007; Feb. 5, 2008; and Feb. 7, 2008. Although the measurement site conditions of these weather stations were unconventional and the data set was found to be incomplete, their potentially negative effects on the analyses were considered acceptable and outweighed by advantages of high spatial and temporal resolutions of the Network data. Methods used to analyze wind variability in the study area are both qualitative and quantitative. In a qualitative approach, synoptic and mesoscale atmospheric conditions associated with the high wind speeds over the study area during the selected days were analyzed using various weather maps. In addition, maps and satellite images were utilized to determine regional and local topography. In a quantitative approach, simple statistics were used to extract information from the data. The main statistics used for the wind data were means, such as mean wind direction and mean wind speed. For air density calculation, the equation recommended by the Comité International des Poids et Mesures (CIPM) in 2007 (Picard *et al.* 2008) was employed.

Chapter 4

Results and analyses

4.1 Upper level synoptic atmospheric conditions

The general upper level synoptic atmospheric conditions on the selected days were examined and are summarized in Figure 4.1 and Table 4.1 using a satellite image from Google Earth (2011), 500 hPa level monthly composite mean air temperatures (ESRL 2012), and *North American 500MB Analysis Hgts_Tmps Stn Plots* (NCEP 2012) before and after the daily maximum overall mean 30-minute wind speeds in the entire study area. The time period of the 500 hPa level monthly composite mean air temperatures (ESRL 2012) is from 22:00 on the last day of the previous month to 22:00 on the last day of the month of interest. The temporal resolution of the *North American 500MB Analysis* is 12 hours, and the time when their data are collected is fixed at 4:00 and 16:00 Pacific Standard Time during winter. Therefore, the time difference between the *North American 500MB Analysis* and the daily maximum overall mean 30-minute wind speed is not consistent among selected days. For example, the daily maximum on Nov. 15, 2006 occurred between 19:30 and 19:59 so that the available charts of the *North American 500MB Analysis* closest to that time are the chart at 16:00 on Nov. 15, 3.5 hours before the daily maximum and at 4:00 on Nov. 16, 8 hours after the daily maximum. Although their temporal resolutions are coarse and the time frame before and after the daily maximum becomes inconsistent, they do provide a large scale picture of the synoptic atmospheric conditions.

Locations of the centres of the upper level low pressures associated with the troughs and ridges of the isobars over the study area before and after the daily maximum overall mean 30-minute wind speeds in the entire study area during the selected days are shown in Figure 4.1. Their initial and next locations after 12 hours are connected by a red straight line. However, the actual paths are unknown, and the red straight lines may not indicate the actual paths of the upper level lows. The upper level low pressure centres associated with the isobars over the study area were mainly located over the Gulf of Alaska, and there were upper level lows which moved in a southerly direction (Figure 4.1). A range of the 500 hPa heights of the upper level low centres before and after the daily maxima was approximately from 484 dam to 520 dam, and no specific trend of increase or decrease before and/or during the daily maxima was found. The troughs and their axes were consistently found over the northeast Pacific Ocean and to the west of the study area, respectively, before the daily maxima. A part of the northeast Pacific Ocean and the study area were under the divergence area where surface low pressures and storms form and develop. The 500 hPa level heights over the study area decreased before and/or during the daily wind speed maxima. The 500 hPa level air temperatures over the study area also decreased before and/or during the daily wind speed maxima and were mostly lower than the corresponding 500 hPa level monthly composite mean air temperature over the study area. Cold and/or warm air temperature advections and short waves associated with the temperature advection were found within the troughs, which can enhance divergence and intensify surface low pressures beneath (Aguado and Burt 2004).

Figure 4.1: Locations of the low pressure centres at 500 hPa around the time of daily maximum overall mean 30-minute wind speeds. Red line connects the initial location given by the L symbol and the location after 12 hours. The image (Google Earth 2011a) was modified by the author of this study based on the data from *North American 500MB Analysis Hgts_Tmps Stn Plots* (NCEP 2012).

Table 4.1: The upper level synoptic atmospheric conditions on the selected days (Source: NCEP 2012 and ESRL 2012). Parentheses indicate the time associated with the descriptions.

	Nov. 15, 2006	Dec. 13, 2006	Dec. 15, 2006	Jan. 9, 2007	Feb. 5, 2008	Feb. 7, 2008
The location of the low pressure centre closest to the study area at the 500 hPa-level	Over the Gulf of Alaska at 4:00 and 16:00	West of Haida Gwaii at 136°W and right above the surface low at 4:00 and the Gulf of Alaska at 16:00	Over the Gulf of Alaska on Dec. 14 at 16:00 and the south coast of Alaska on Dec. 15 at 4:00	Over the Gulf of Alaska at 4:00 and around Prince Rupert at 16:00	Over the south coast of Alaska which is also ESE of Anchorage at 4:00	SW of Banks Island at around 124.5°W and 72°N on Feb. 6 at 16:00 and Amundsen Gulf on Feb. 7 at 4:00
The 500 hPa height of the low pressure centre closest to the study area before and after the daily max. overall mean 30-min. wind speed (dam)	Before					
	484 (4:00 & 16:00)	511 (Dec. 12 at 16:00) 509 (Dec. 13 at 4:00)	506 (Dec. 14 at 16:00) 509 (Dec. 15 at 4:00)	510 (Jan. 8 at 16:00) 512 (Jan 9 at 4:00)	482 (Feb. 4 at 16:00) 506 (Feb. 5 at 4:00)	490 (Feb. 6 at 16:00)
	After					
	491 (Nov. 16 at 4:00)	506 (16:00)	514 in the NNW 520 in the ENE (Dec. 15 at 16:00)	515 (16:00)	503 (16:00)	489 (Feb. 7 at 4:00)
The location of the trough and ridge closest to the study area at the 500 hPa level before the daily max. overall mean 30-min. wind speed	Trough: the trough is almost circular over the entire North Pacific Ocean, but slight local trough existed SW of Vancouver Island whose axis extended from NNW to SSE between 125°W and 135°W Ridge: over between 100°W and 110°W in Canada and	Trough: over the NE Pacific Ocean and the west coast of North America (the axis of the trough is almost parallel to the longer axis of Vancouver Island and lies over the axis of the island) Ridge: over between 110°W and 130°W in Canada and	Trough: over around the west coast of North America (the axis of the trough extends from NNW to SSE between 120°W and 135°W) Another trough exists east of the first trough, and its axis lies almost along the eastern boarder of	Trough: over the NE Pacific Ocean (the axis of the trough extends from NE to SW between 135°W and 150°W) Ridge: over between 115°W and 125°W in Canada and the US (4:00)	Trough: over the NE Pacific Ocean (the axis of the trough extends from NNW to SSE between 130°W and 145°W) Ridge: over a little east of the west coast of North America (4:00)	Trough: over the NE Pacific Ocean (the axis of the northern trough extends from the low centre to WSW until 160°W and 54°N, and below 54°N the axis of another trough extends from north to south between 140°W and 145°W

	between 105°W and 115°W in the US (16:00)	110°W and 120°W in the US (4:00)	BC and in the mid west of the US Ridge: over central North America (between 100°W and 110°W) so that it is located in the east of the second trough (4:00)			Ridge: over along a little east of the west coast of North America (Feb. 6 at 16:00)
The 500 hPa height over the study area before and after the daily max. overall mean 30-min. wind speed (dam)	Before					
	552~546 (4:00) 540~534 (16:00)	552~546 (Dec. 12 at 16:00 p.m.) 540~534 (Dec. 13 at 4:00)	534~528 (Dec. 14 at 16:00) 528~522 (Dec. 15 at 4:00)	570~564 (Jan. 8 at 16:00) 564~558 (Jan. 9 at 4:00)	558~552 (Feb. 4 at 16:00 & Feb. 5 at 4:00)	546~540 (Feb. 6 at 4:00 & 16:00)
	After					
	540~534 (Nov. 16 at 4:00)	540~534 (16:00)	534~528 (Dec. 15 at 16:00)	534~528 (16:00)	534~528 (16:00)	534~528 (Feb. 7 at 4:00)
Air temperature range over the study area at the 500 hPa level before and after the daily max. overall mean 30-min. wind speed (°C)	Before					
	-15 ~ -20 (4:00 & 16:00)	-20 ~ -25 (Dec. 12 at 16:00) -25 ~ -30 (Dec. 13 at 4:00)	-20 ~ -25 (Dec. 14 at 16:00) -30 ~ -35 (Dec. 15 at 4:00)	-15 ~ -20 (Jan. 8 at 16:00) -20 ~ -25 (Jan. 9 at 4:00)	-20 ~ -25 (Feb. 4 at 16:00 & Feb. 5 at 4:00)	-20 ~ -25 (Feb. 6 at 4:00 & 16:00)
	After					
	-25 ~ -30 (Nov. 16 at 4:00)	-25 ~ -30 (16:00)	-35 ~ -40 (Dec. 15 at 16:00)	-20 ~ -25 (16:00)	-35 ~ -40 (16:00)	-30 ~ -35 (Feb. 7 at 4:00)
Monthly composite mean air temperature at 500 hPa level over the study area (°C)	-25 ~ -25.5 Nov. 2006	-23 ~ -23.5 Dec. 2006	-23 ~ -23.5 Dec. 2006	-22.5 ~ -23.5 Jan. 2007	-23 ~ -23.5 Feb. 2008	-23 ~ -23.5 Feb. 2008
Air temperature advection at 500 hPa level before the time of	Cold air advection and short waves within the trough axis (4:00 &	Significant cold air advection and short waves before and within	Exceptional cold air advection and short waves within the	Significant warm and cold air advection and short waves within the	Significant cold and warm air advection and short waves within the	Significant warm and cold air advection and short waves

the daily max. overall 30-min. wind speed (°C)	16:00)	the trough (4:00)	trough (Dec. 14 at 16:00 & Dec. 15 at 4:00)	trough (4:00)	trough (4:00)	within the trough (Feb. 6 at 16:00)

4.2 Mesoscale atmospheric conditions and the winds in the study area

The general mesoscale atmospheric conditions were examined using the *North American Surface Analysis* and *United States Surface North_West Analysis* (NCEP 2012) before and after the daily maximum overall mean 30-minute wind speeds in the entire study area. The temporal resolution of the charts is 3 hours. The main features of the conditions are summarized in Table 4.2.

First, the location of the centre of the surface low pressure associated with the front(s) passing over the study area was generally found in a region between 45°N and 55°N and between 120°W and 135°W three hours or less before the daily maximum overall mean 30-minute wind speed. It is a part of the region where the divergence at the 500 hPa level was located before the daily maximum. Second, the relative location of the surface low centre at the time of passing is north of the study area on all the selected days. This relative location causes the surface low pressures to favour strong winds mainly from the south part of the compass rose although the pressure pattern and wind direction can be affected by surface relief (Mass and Dotson 2010). Therefore, it significantly affects distribution of winds over the study area. Third, the time of the daily minimum mean air pressure in the entire study area and approximate time of the beginning of the change in mean wind direction in the entire study area to WSW were in good agreement except on Nov. 15, 2006 and Dec. 13, 2006. The minimum mean air pressure and the pressure tendency around the minimum are generally considered as a more reliable indicator of the frontal passage than the charts (Ahrens 1988; Aguado and Burt 2004). The change in the mean wind direction to WSW on Nov. 15, 2006 and Dec. 13, 2006 started about 2 hours and 1 hour after the daily minimum mean air pressure, respectively. Fourth, the relation between change in wind direction and the frontal passage over the study area was quite different from the one commonly described in introductory meteorology textbooks. Some textbooks state that winds veer from southeasterly to southwesterly after passage of a warm front, from southwesterly to northwesterly after that of a cold front and from southeasterly or southerly to westerly or northwesterly after that of an occluded front (Ahrens 1988; Moran and Morgan 1994; Aguado and Burt 2004). However, the dominant mean wind direction in the entire study area after passage of the cold or occluded front during the selected days was within a range of WSW, and no prominent and persistent change to a northwest direction was observed (Figures 4.13, 4.14, 4.16, 4.17, 4.19, 4.20, 4.22, 4.23, 4.25, 4.26, 4.28 and 4.29). As an example, location of a cold front and wind direction at the weather stations in the study area on Nov. 15, 2006 at 16:00 and 19:00 are shown in Figures 4.2 through 4.5. Fifth, different time periods between the time of the daily minimum mean air pressure in the entire study area and the time of the daily maximum overall mean 30-minute wind speed were found on the selected days. The longest time period was 9 hours on Dec. 13, 2006 whereas the shortest one was 0.5 hour on Jan. 9, 2007. Sixth, the magnitude of the central pressure of a surface low did not necessarily match the magnitude of wind speed associated with the surface low as Mass and Dotson (2010) showed in their study. Although the highest daily maximum overall mean 30-minute wind speed in the entire study area during the selected days occurred on Dec. 15, 2006, the central pressure of the surface low associated with that highest daily maximum was just the 4th lowest among the ones right before their associated daily maximums. On the other hand, the surface low on Dec. 13, 2006, which was associated with the second highest daily maximum wind speed, was found to have the lowest central pressure among all, which was also much lower than that on Dec. 15, 2006. Seventh, formation of new surface low pressure centres was found over Vancouver Island on Nov. 15, 2006, Jan. 9, 2007 and Feb. 7, 2008. All of them were formed before the daily maximum overall mean 30-minute wind speed.

Table 4.2: Mesoscale pressure and storm conditions affecting the overall mean maximum wind speed during the selected days (Source: NCEP 2012). Parentheses indicate the time associated with the descriptions.

	Nov. 15, 2006	Dec. 13, 2006	Dec. 15, 2006	Jan. 9, 2007	Feb. 5, 2008	Feb. 7, 2008
The location of the surface low centres associated with the front(s) passing over the study area	Around Quesnel at 13:00. Around Courtenay on Vancouver Island at 16:00. Around Lillooet at 19:00.	Off the west coast of Haida Gwaii at 4:00. Around Haida Gwaii at 10:00.	Nearshore, west coast of Vancouver Island on Dec. 14 at 19:00. Around Wyah Indian Reserve 3 on Vancouver Island at 22:00. A little east of Quesnel on Dec. 15 at 4:00.	Around Williams Lake at 10:00. Around Wyah Indian Reserve 3 on Vancouver Island at 13:00.	Southwest of Haida Gwaii at 4:00. Over Haida Gwaii at 10:00. Near the northeastern coast of Haida Gwaii at 13:00. Around Terrace at 16:00.	Northwest of Haida Gwaii on Feb. 6 at 22:00. Over Campbell River on Vancouver Island on Feb. 7 at 1:00.
The relative location of the surface low centre to the study area at the time of passing	North	North	North	North	North	North
Approx. time of the frontal passage over the study area based on the charts from NCEP	Sometime between 10:00~13:00 (warm) & 16:00~19:0 (cold)	Slightly before or at 4:00 (occluded)	A little after 19:00 on Dec. 14. (occluded) & a little after 0:00 on Dec. 15 (bent-back trough[1] (Mass and Dotson 2010))	Sometime between 13:00~16:00 (cold)	A little after 10:00 (weak warm) & little before 13:00 (cold)	At 1:00 (occluded)
General trend in mean air pressure in the entire study area	Decreasing until and steeply increasing after the daily min. at 15:33	Decreasing until and gradually increasing after the daily min. at 2:19	Steeply increasing after the daily min. at 0:00	Decreasing until secondary min. at 12:32, then a little increasing and decreasing until the daily min. at	Decreasing until and abruptly increasing after the daily min. at 10:29, then gradually decreasing until and	Slightly decreasing until and gradually increasing after the daily min. at 1:16

				13:46 then increasing again	increasing after the secondary min. at 12:58	
Approx. time of the beginning of the change in mean wind direction to WSW	Between 17:00~17:30	Between 3:00~3:30	0:30	Right before 14:00	Between 10:30~11:00	1:00
Time of daily max. overall mean 30-min. wind speed	19:30-19:59	11:00-11:29	4:00-4:29	14:00-14:29	15:30-15:59	3:30-3:59
Approx. time period between the daily minimum mean air pressure and daily max. overall mean 30-min. wind speed (hours)	4.5	9	4.5	0.5	5.5	2.5
The central pressure of the surface low pressures associated with the passing front(s) before and after the daily max. overall mean 30-min. wind speed (hPa)	Before					
	980 (16:00 & 19:00)	957 (1:00) 965 (4:00 & 7:00) 969 (10:00)	982 (1:00) 984 (4:00)	998 (13:00)	983 (4:00) 978 (10:00) 981 (13:00)	995 (1:00)
	After					
	986 (22:00)	973 (13:00)	979 (7:00)	989 (16:00)	982 (16:00)	995 (4:00)

Direction of the movement of the closest surface low to the study area	The low centre was located over around Quesnel at 13:00, and a new low centre formed over around Courtenay on Vancouver Island between 13:00 and 16:00. Then it moved to NE.	Slightly NE (very slow movement)	NE until 4:00 and then ESE until 7:00	The low centre was located close to Williams Lake at 10:00, and a new low centre formed over Wyah Indian Reserve 3 on Vancouver Island between 10:00 and 13:00. Then it rapidly moved NE between 13:00 and 16:00.	NE (slow movement)	The low centre was located NW of Haida Gwaii on Feb. 6 at 22:00, and a new low centre formed over Campbell River on Vancouver Island between Feb. 6 at 22:00 and Feb. 7 at 1:00. It moved NE until 4:00 and SSE the rest of the day

[1] Mass and Dotson (2010) use the term "bent-back trough/front" in their study. However, they clearly differentiate bent-back trough/front from the actual front. Therefore, a term 'bent-back trough' is used in this study rather than "bent-back trough/front" in order to avoid confusion.

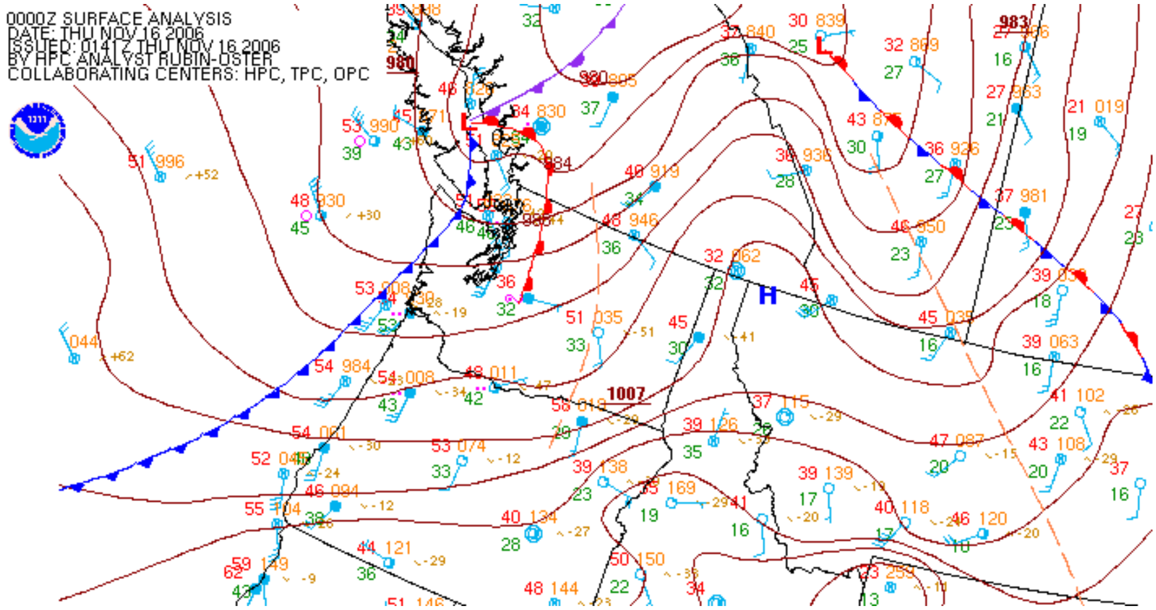

Figure 4.2: *United States Surface North-West Analysis* on Nov. 15, 2006 at 16:00 (NCEP 2012).

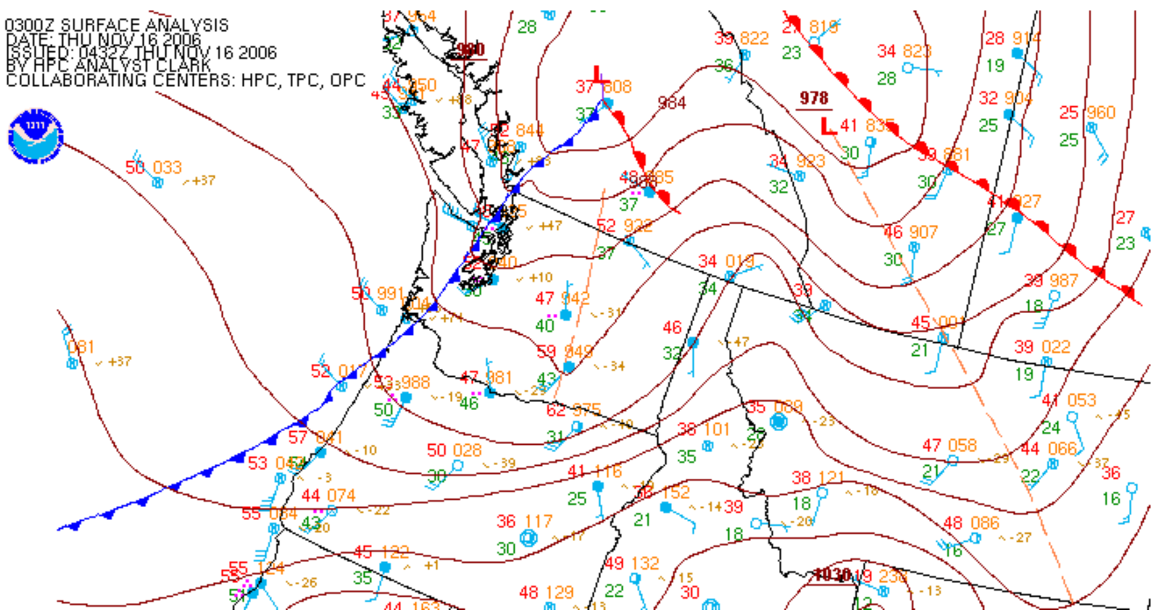

Figure 4.3: *United States Surface North-West Analysis* on Nov. 15, 2006 at 19:00 (NCEP 2012).

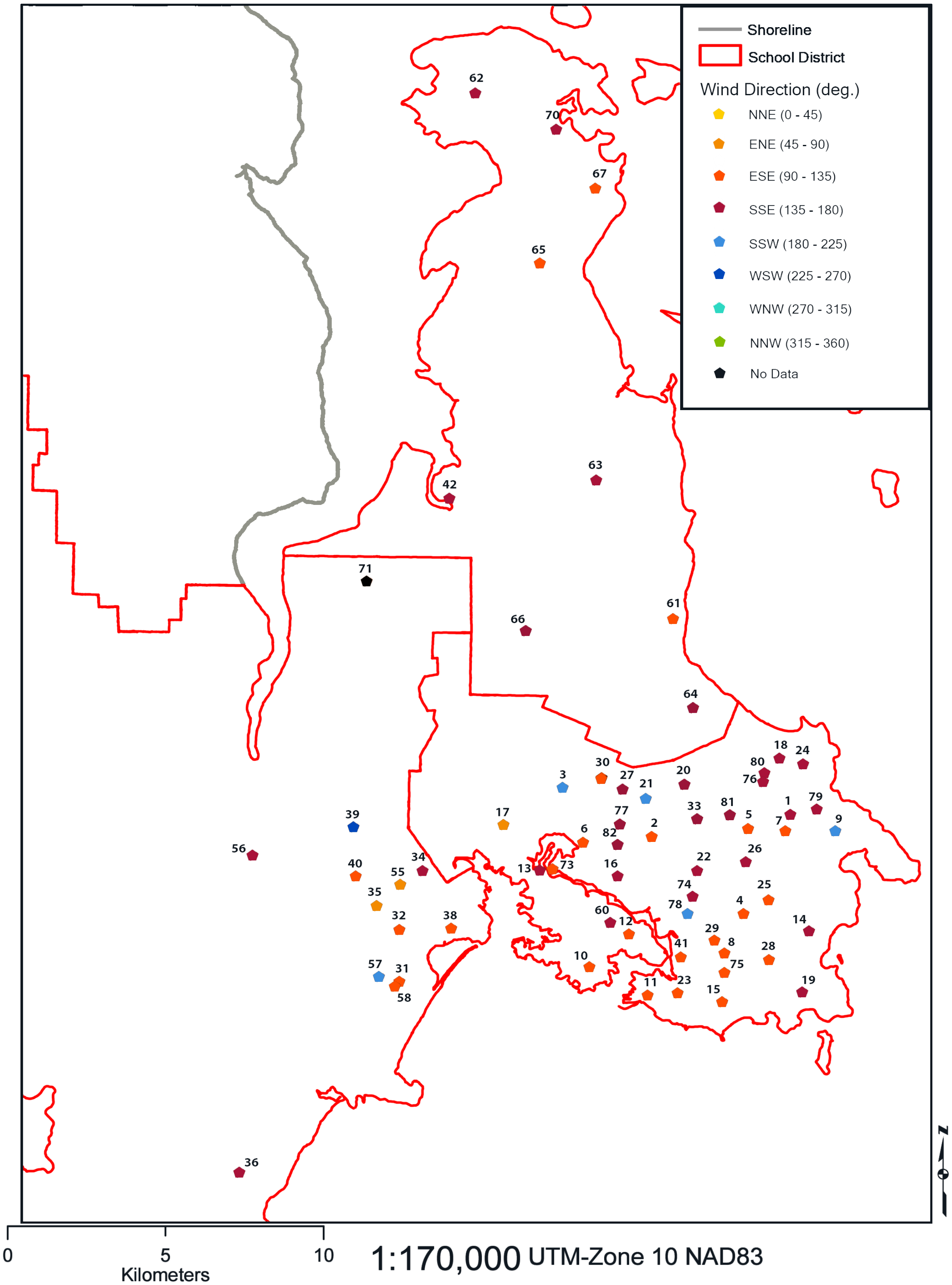

Figure 4.4: Distribution of wind direction over the study area on Nov. 15, 2006 at 16:00 before the passage of the cold front (Base map: Brendle-Moczuk 2010). The upper limit of each class of wind direction is exclusive. Redish colours indicate easterly components, and bluish colours indicate westerly components.

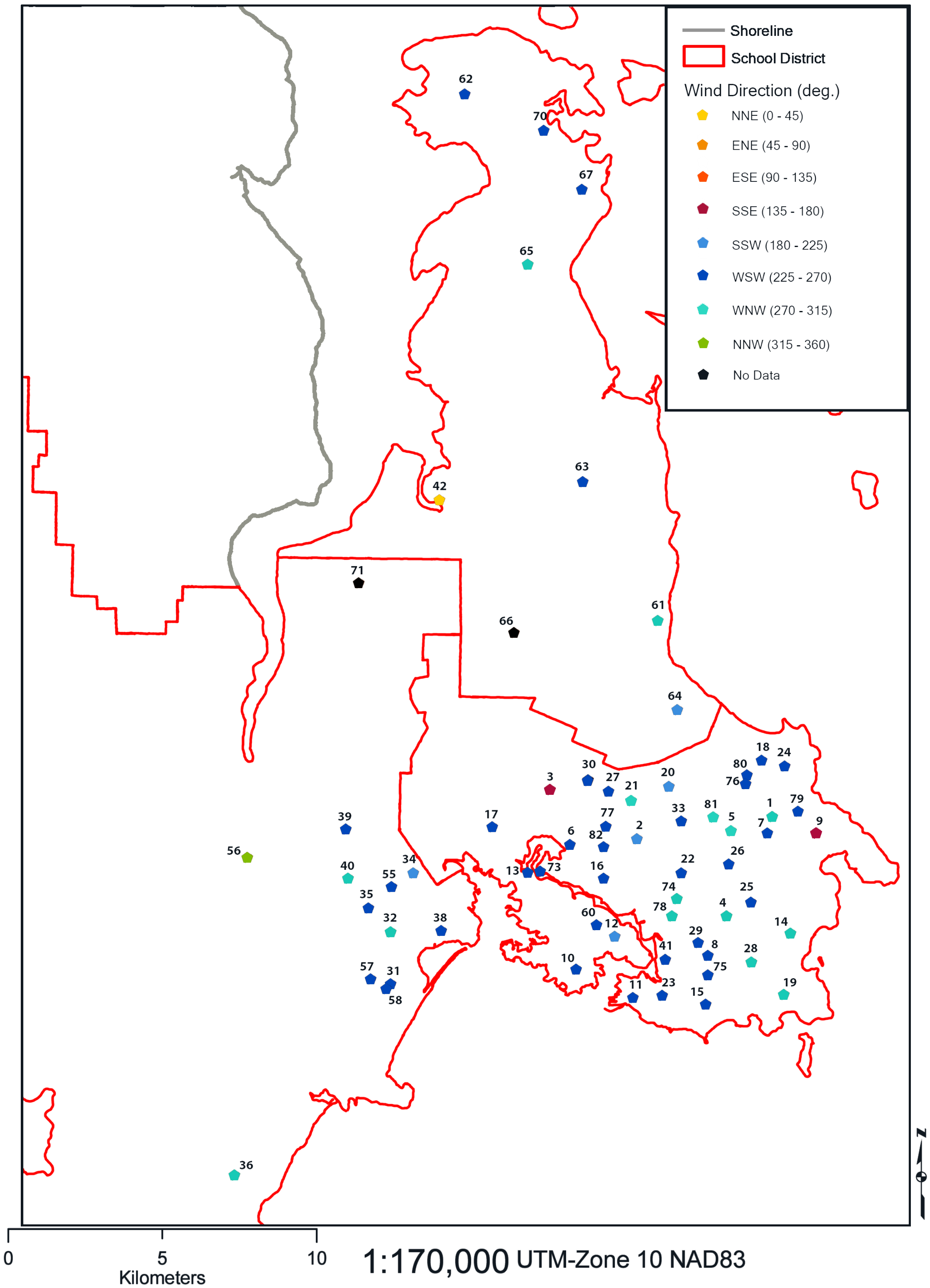

Figure 4.5: Distribution of wind direction over the study area on Nov. 15, 2006 at 19:00 after the passage of the cold front (Base map: Brendle-Moczuk 2010). The upper limit of each class of wind direction is exclusive.

A major cause of the dominance of WSW winds rather than northwesterly winds over the study area after passage of a cold or an occluded front during the selected days is considered to be relief. Mountainous Vancouver Island, which extends from the study area in the northwest direction, would make it difficult for the northwesterly winds to penetrate into the study area. On the other hand, the Strait of Juan de Fuca has a WNW-ESE oriented axis, and it is easy for the northwesterly winds to enter. The winds entering the Strait of Juan de Fuca are then funneled through the strait by the constriction of the relief of southern Vancouver Island and the Olympic Peninsula. After passing through the constriction, the winds spread out, and some of them come to the Greater Victoria area as southwesterly wind (McIntyre 1952). Because elevation of the Olympic Peninsula is higher than that of southern Vancouver Island especially to the southwest of the study area, there must also have been winds which overflow the constriction on the Vancouver Island side and passed over the southern tip of the island before reaching the study area. Those winds must have acquired a more westerly component in their directions and reached the study area as WSW winds. Location of a surface low pressure centre could also be a cause of dominant WSW wind in the study area because air circulation around a low pressure centre could determine general wind direction over an area under its influence. For example, if a low pressure centre is located northwest of the study area, the general direction of air circulation around the study area could become WSW even behind a cold or an occluded front just as the case on Dec. 13, 2006 (Figures 4.6 and 4.7). In terms of the WSW wind on Dec. 15, 2006, shift in wind direction to WSW accompanied by significant increase in wind speed in the study area occurred a little after 0:00 (Figures 4.19, 4.20 and 4.21). This indicates that these changes were not caused by passage of the occluded front but most likely a bent-back trough behind the occluded/cold front (Figure 4.10). After the passage of the bent-back trough, dominant wind direction off the west coast of Vancouver Island was NNW or WNW whereas that in the study area was WSW (Figures 4.11, 4.12 and 13; Table 4.2). Therefore, the major cause of the dominance of WSW winds over the study area rather than northwesterly winds after 0:00 on Dec. 15, 2006 is also considered to be relief.

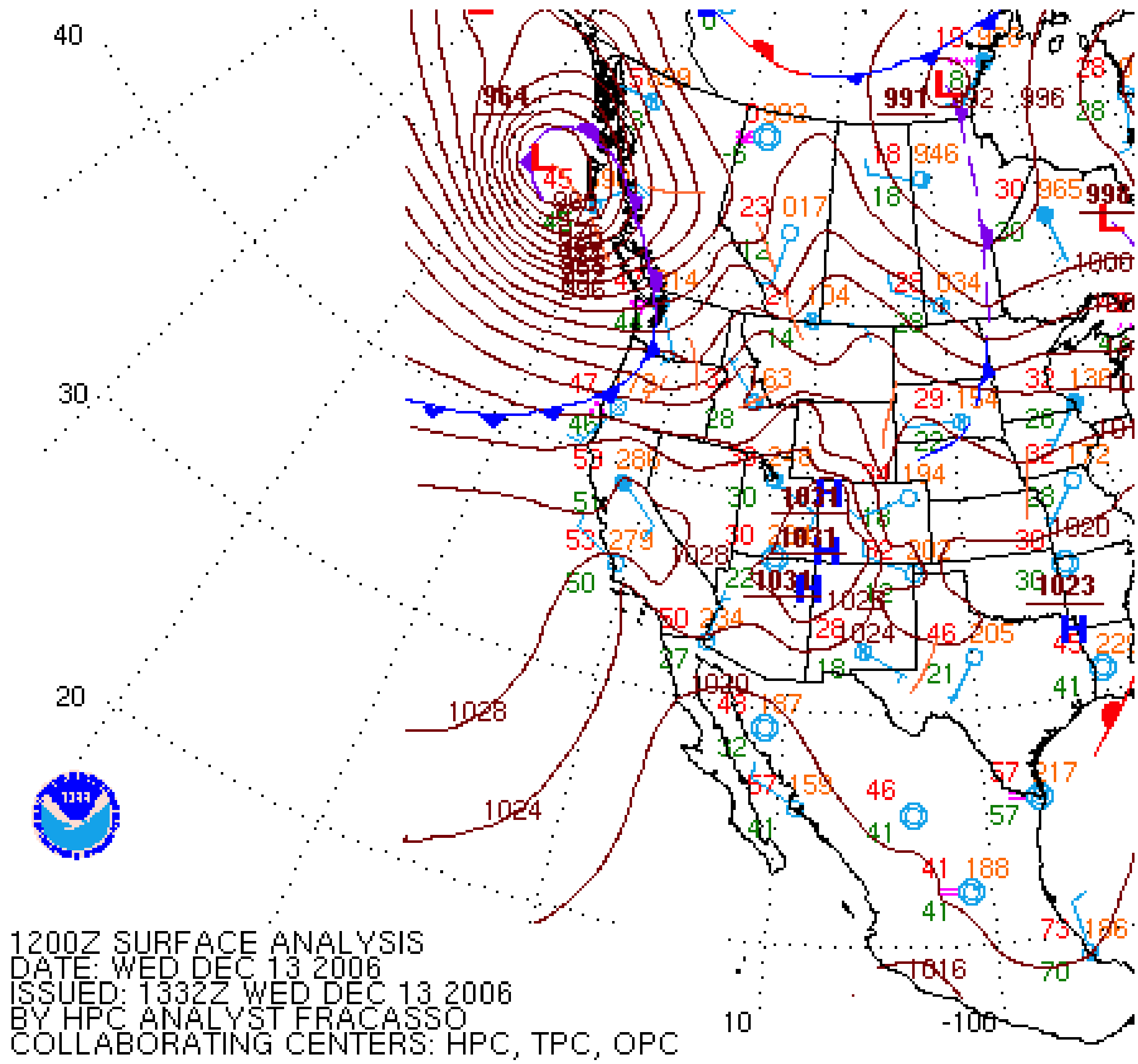

Figure 4.6: *North American Surface Analysis* on Dec. 13, 2006 at 4:00 (NCEP 2012).

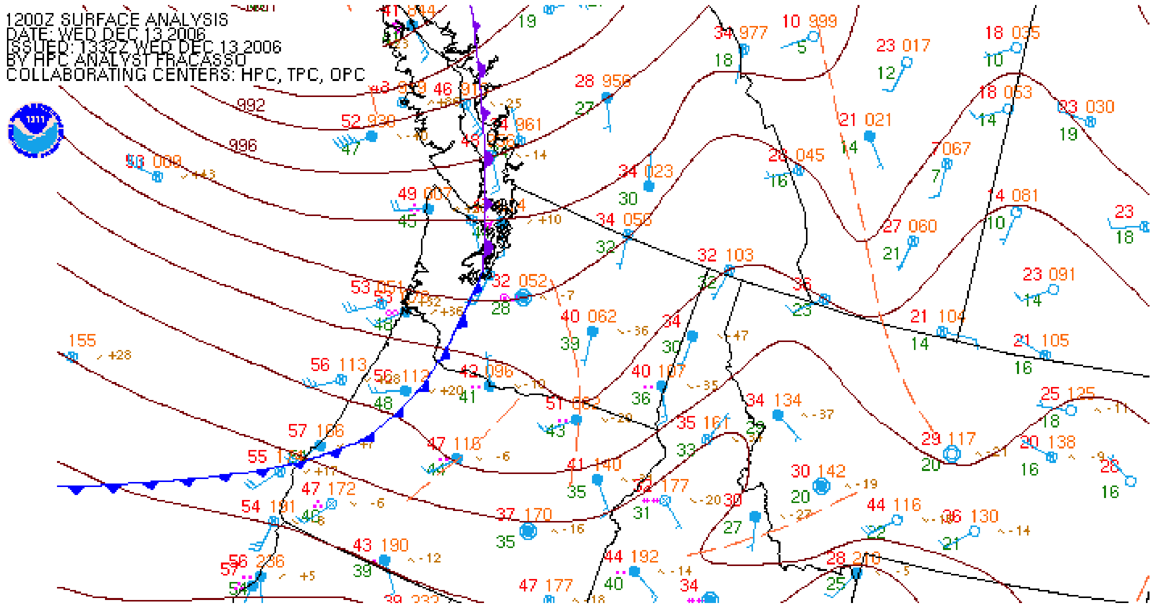

Figure 4.7: *United States Surface North-West Analysis* on Dec. 13, 2006 at 4:00 (NCEP 2012).

The formation of new surface low pressure centres over Vancouver Island on Nov. 15, 2006, Jan. 9, 2007 and Feb. 7, 2008 might be related to the movement of the upper level low pressure centres (Tables 4.1 and 4.2). All of them were formed during the southerly movement of the upper level low centres. It is considered that the southerly movement deepened the troughs of the isobars south of the upper level low centres and created a favorable condition for the formation of those new surface low centres under the upper level divergence region because deepening the trough increases the rate of decrease in upper level vorticity in the transition zone after the trough axis and enhances the divergence to draw more surface air upward (Aguado and Burt 2004). In addition, these new surface low centres were formed before the daily maximum overall mean 30-minute wind speeds in the entire study area so that their formation might have enhanced the magnitude of the daily maximums.

The possible causes of the temporal discrepancy between the daily minimum mean air pressure and approximate time of the beginning of the change in mean wind direction to WSW on Nov. 15, 2006 and Dec. 13, 2006 are not clear. In the case on Nov. 15, 2006, it might be related to the formation of the new surface low centre and/or change in mesoscale surface pressure fields around the study area whereas in the case on Dec. 13, 2006, the occlusion process and the orientation of the isobars might be related. The different time periods between the time of the daily minimum mean air pressure and the time of the daily maximum overall mean 30-minute wind speed is a matter of what caused the steeper pressure gradient, and how, over the study area after the daily minimum mean air pressure. Some factors that cause spatial variability of air pressure are vertical movement of air created by diverging and converging upper airflow, water vapour concentrations in the storm and air temperature (Moran and Morgan 1994). To identify the causes and understand the process which produced those observed results based only on the data used in this study is limited, and further investigation on these cases would be required.

4.3 Description of synoptic and mesoscale atmospheric conditions on Dec. 15, 2006

The winds on Dec. 15 were the strongest (Figures 4.15, 4.18, 4.21, 4.24, 4.27 and 4.30) and caused the most damage to the area under its passage among all on the selected days (BC Hydro 2007; Mass and Dotson 2010). Although the number of inactive weather stations was also the greatest on Dec. 15, it just proves how strong the winds were on that day (Tables A2, A3 and A4).

Some notable features that appeared in the 500 hPa level charts on Dec. 14 at 16:00 and on Dec. 15 at 4:00 were northeastward movement of the upper level low pressure centre accompanied by eastward propagation of a trough located southwest of Vancouver Island, multiple cold air advections toward the region above the surface low pressure centre and the study area from the west, and extraordinary short waves around the advections (Figures 4.8 and 4.9). The air temperatures of the upper air advections were -40°, -35° and -30° from west to east, and the isotherm of -30° was crossing isobars above the study area on Dec. 15 at 4:00. Aguado and Burt (2004) stated that cold air advection causes vertical and slightly rightward turning motions of air and that those air motions in turn cause the short waves, which enhance the divergence and thus intensify surface cyclones when the short waves are located down wind of a trough axis. The significant cold air advections and short waves which are depicted as small ripples superimposed on the longwaves around the intersections of isobars and isotherms in Figures 4.8 and 4.9 indicate that the process mentioned above might have taken place to create the powerful mid-latitude cyclone on Dec. 15, 2006.

The surface low pressure associated with the strong winds on Dec. 15, 2006 had a bent-back trough. It is a feature also found in another powerful Pacific Northwest cyclone which caused the Inauguration Day Windstorm in the U.S. on Jan. 20, 1993. These cyclones on Dec. 15, 2006 and Jan. 20, 1993 are considered the second and third most destructive windstorms that struck the Pacific Northwest in the past half century (Mass and Dotson 2010). The bent-back trough is associated with the greatest pressure gradient and thus, the strongest winds. It generally locates south or southwest of a surface low centre (Figures 4.10 through 4.12). It is important to consider the synergy between an actual front and the bent-back trough. It was documented that passing of the bent-back trough over Seattle Tacoma Airport on Dec. 15, 2006 cooled and further destabilized the air aloft where passing of the warm/occluded front had strengthened wind speeds and reduced vertical stability prior to the passing of the bent-back trough. This resulted in strong winds coming down to the surface from aloft until the time of maximum gusts (Mass and Dotson 2010). Likewise, after the passage of an occluded front, large pressure gradient associated with the bent-back trough came over Greater Victoria, and the similar synergy might have worked.

According to the analysis charts (NCEP 2012), the movement of the surface low centre between Dec. 14 at 22:00 and Dec. 15 at 4:00 was northeastward from over the southwest coast of Vancouver Island to a little east to Quesnel on the B.C. mainland. The central pressure during the same time period increased from 976 hPa to 984 hPa. In addition, the isobars of the bent-back trough south and southwest of the surface low centre were tightest on Dec. 14 at 22:00 and gradually loosened with time (Figures 4.10 through 4.12). The surface low centre was off the southwest coast of Vancouver Island and the occluded front was about to pass over the study area on Dec. 14 at 19:00. In the next 3 hours, the surface low centre reached the southwest coast of Vancouver Island, and the arched occluded front lay northwest clockwise through southeast of the study area. The bent-back trough extended from the middle west coast of Vancouver Island to off the west coast of Washington and Oregon in a NNE-SSW direction (Figure 4.10). Then, the surface low centre moved to mainland B.C., and the bent-back trough south of the surface low centre was located over the study area on Dec. 15 at 1:00 (Figure 4.11). Incidentally, Mass and Dotson (2010) state that the bent-back trough arrived in the Seattle area by 0:06

Pacific Standard Time. In the study area, the daily minimum mean air pressure was recorded at 0:00, and mean air temperature, mean wind direction (Figures 4.19 and 4.20) and overall mean 30-minute wind speed started changing significantly at around 0:30 (Figure 4.21). Although the surface low centre moved further northeast and the axis of the bent-back trough was also east of the study area on Dec. 15 at 4:00, the isobar spacing right above the study area became extremely narrow after the passing of the bent-back trough, and the overall mean 30-minute wind speed in the entire study area reached its daily maximum between 4:00 and 4:29 (Figure 4.12). It might be noteworthy that there might be slight inconsistency in interpretation of climate data between an analyst for the chart on Dec. 15, 2006 at 4:00 (Figure 4.12) and another for the previous two charts (Figures 4. 10 and 4.11).

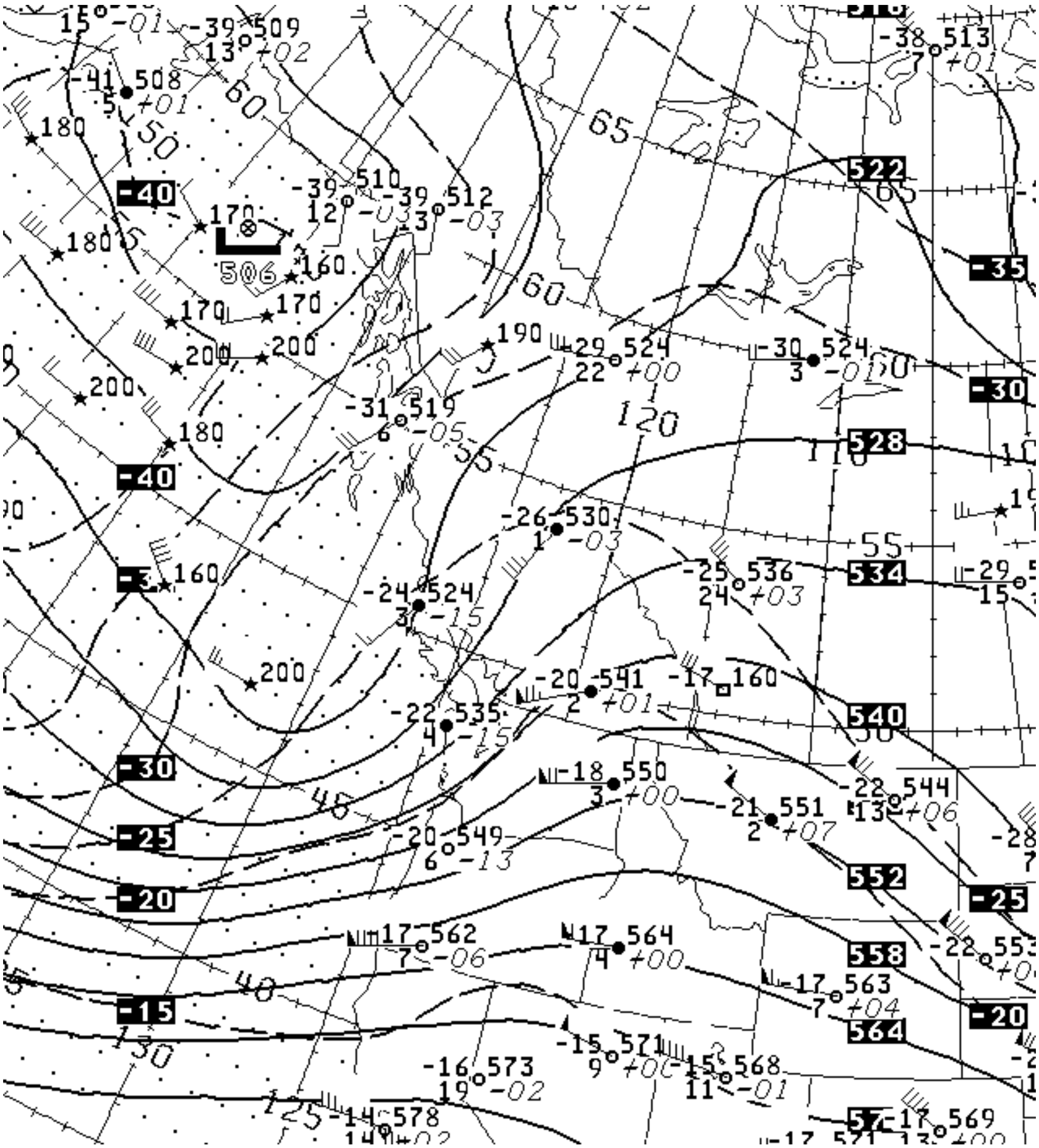

Figure 4.8: *North American 500MB Analysis Hgts-Tmps Stn Plots* on Dec. 14, 2006 at 16:00 (NCEP 2012).

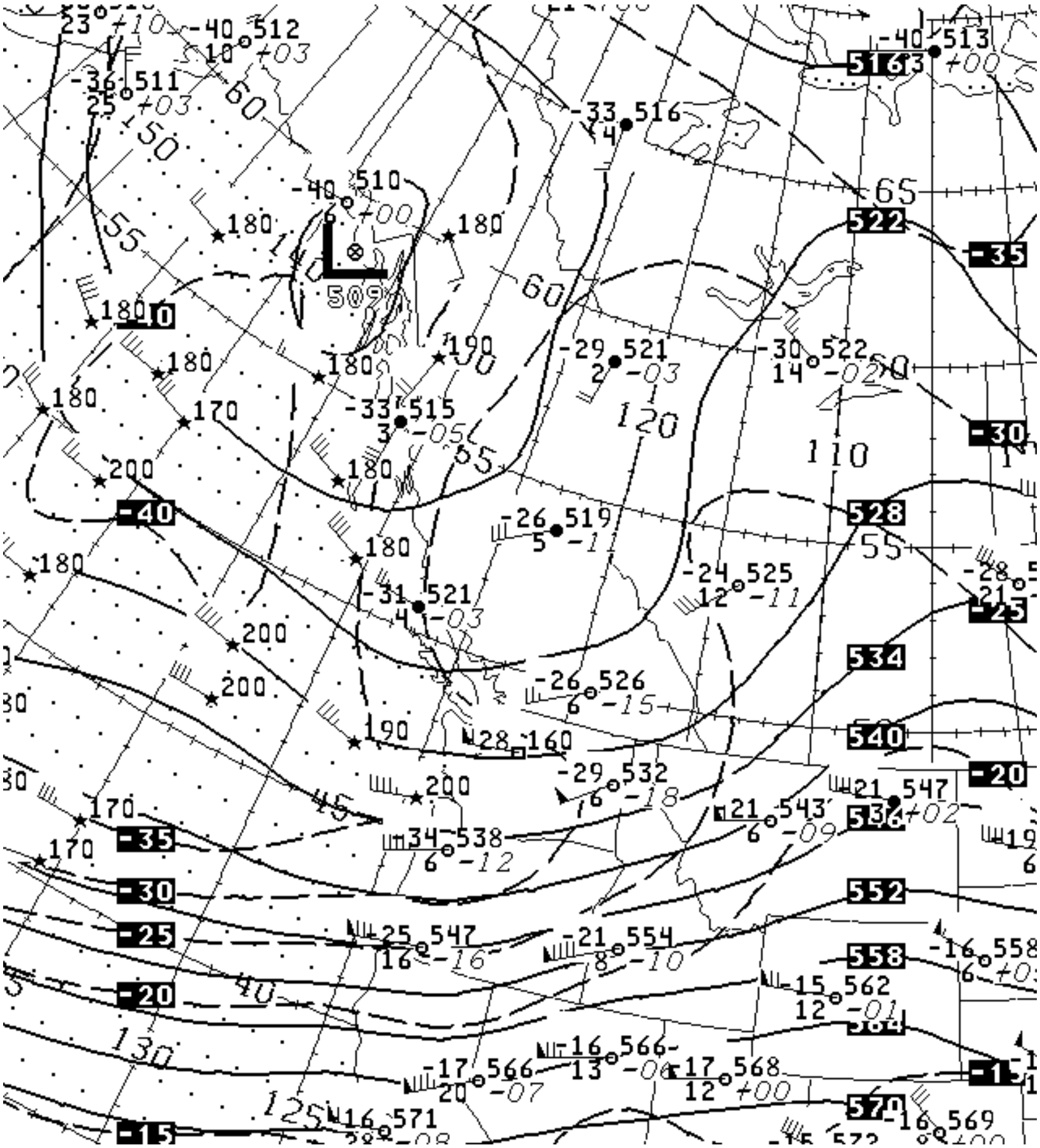

Figure 4.9: *North American 500MB Analysis Hgts-Tmps Stn Plots* on Dec. 15, 2006 at 4:00 (NCEP 2012).

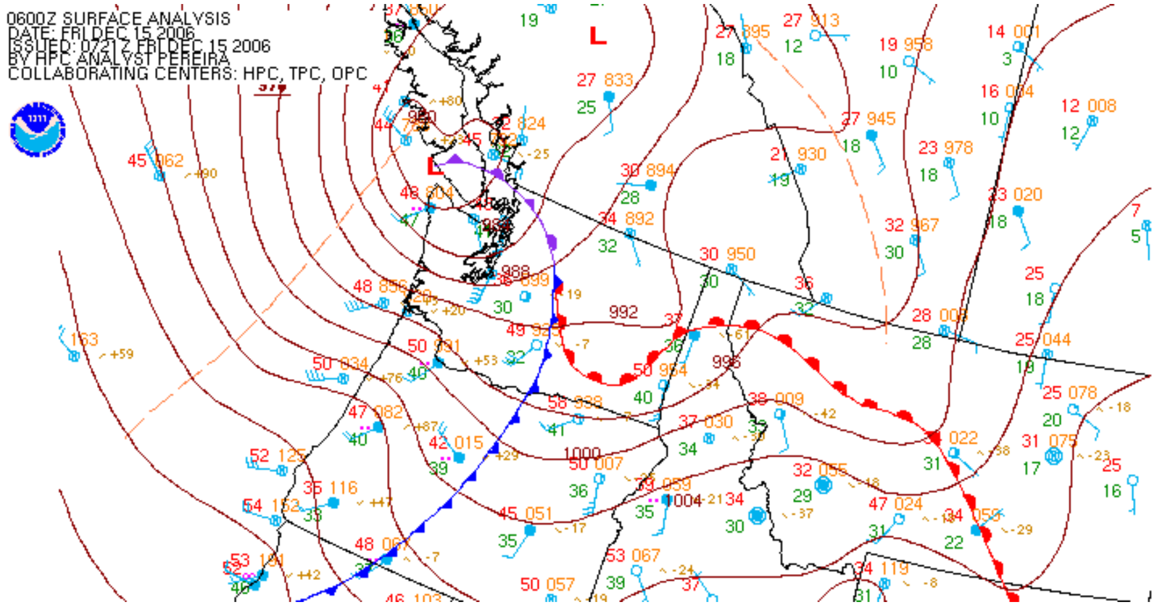

Figure 4.10: *United States Surface North-West Analysis* on Dec. 14, 2006 at 22:00 (NCEP 2012).

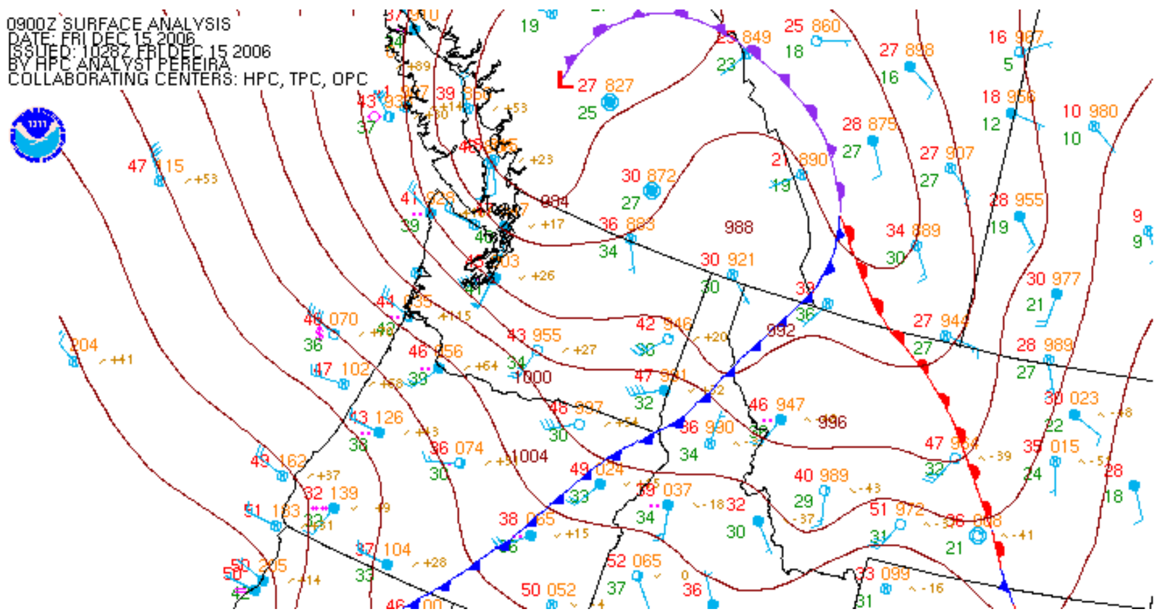

Figure 4.11: *United States Surface North-West Analysis* on Dec. 15, 2006 at 1:00 (NCEP 2012).

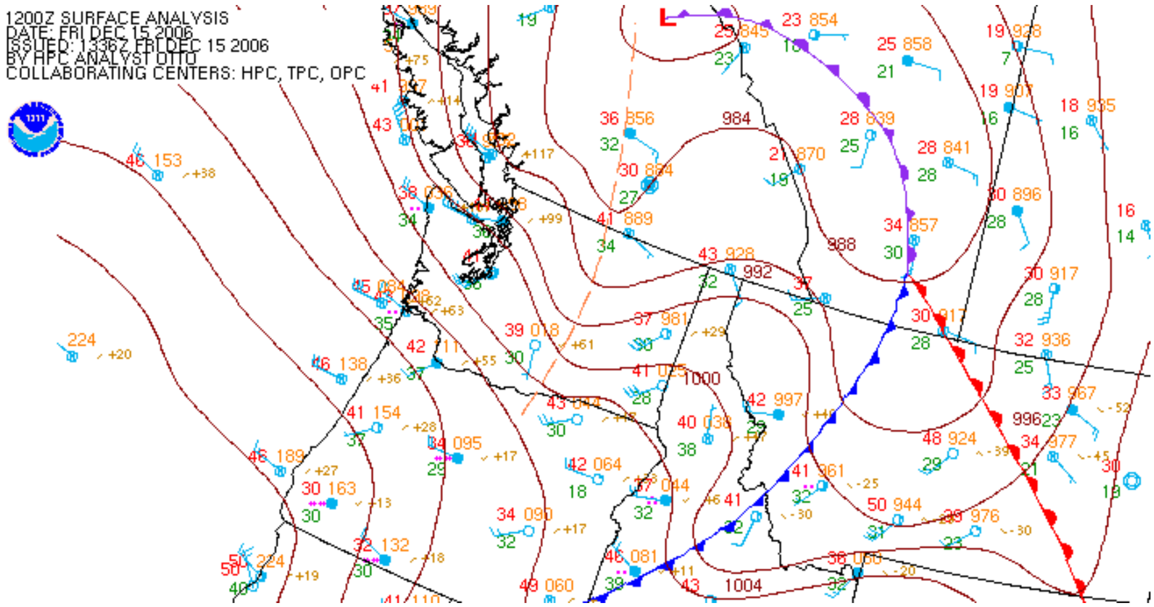

Figure 4.12: *United States Surface North-West Analysis* on Dec. 15, 2006 at 4:00 (NCEP 2012).

4.4 Summary of upper level synoptic atmospheric conditions

The synoptic 500 hPa level and mesoscale surface atmospheric conditions were examined, and some common features as well as minor differences were found among the selected days. Upper level low pressure centres located over the Gulf of Alaska and the troughs located to the west of the study area were generally observed before the daily maximum overall mean 30-minute wind speeds. In addition, cold and/or warm air temperature advection and associated short waves were found within the trough, and 500 hPa height and air temperature over the study area decreased before and/or during the daily maximums. At the mesoscale surface level, the centre of the low pressure associated with the front(s) passing over the study area was generally located west or northwest of the study area a few hours before the daily maximum and passed north of the study area. The time of the daily minimum mean air pressure in the entire study area and approximate time of the beginning of the change in mean wind direction to WSW in the entire study area were almost the same except on Nov. 15, 2006 and Dec. 13, 2006. The dominant mean wind direction in the entire study area after passage of the cold front, occluded front or bent-back trough was within a relatively narrow range around WSW despite mostly northwesterly winds behind these fronts and trough. General wind direction behind an occluded front near the study area on Dec. 13, 2006 was found to be WSW, and the location of the associated powerful low pressure centre was far northwest of the study area. Time periods between the time of the daily minimum mean air pressure in the entire study area and the time of the daily maximum overall mean 30-minute wind speed varied on the selected days. In addition, magnitude of the central pressure of a surface low did not necessarily match the magnitude of wind speed associated with the surface low. On Nov. 15, 2006, Jan. 9, 2007 and Feb. 7, 2008, formation of new surface low pressure centres over Vancouver Island was found before the daily maximum overall mean 30-minute wind speed. On Dec. 15, 2006, the study area recorded the highest daily maximum overall mean 30-minute wind speed as a whole among the selected days. At the 500 hPa level, exceptional cold temperature advection and short waves were observed within the trough above the surface low pressure and the study area. The surface low pressure associated with the highest daily maximum had the bent-back trough. However, the daily maximum occurred not at the time of passing of the bent-back trough over the study area but 3.5 hours later when the isobar spacing right above the study area became narrow.

4.5 Some features of winds, air density and its variables and wind pressure in the study area

4.5.1 Diurnal pattern of mean wind direction and speed

Knowledge of wind direction during severe wind conditions is necessary to assess areas most affected by the winds and those have the greatest wind damage potential. The most notable general trend in winds over the entire study area during the selected days was a change of the mean wind directions to WSW accompanied by sudden and significant increases in overall mean 30-minute wind speeds. This was followed by the daily maximums within several hours (Figures 4.13 through 4.30). The daily maximum overall mean 30-minute wind speeds occurred while the mean wind directions were generally within the range of WSW and when the range of circular standard deviations was narrow. This wind direction persisted over the study area for a while even after the daily maximums.

Some tendencies specific to each school district were also found. First of all, mean wind directions in SD 63 tended to be slightly more southerly than those in the other school districts (Figures 4.14, 4.17, 4.20, 4.23, 4.26 and 4.29). Therefore, even if the mean wind directions in SD 61 and SD 62 were within the range of WSW, the ones in SD 63 were frequently found within the range of SSW. Second, the change of mean wind directions to the range of WSW or SSW tended to take place slightly earlier in SD 62 and later in SD 63. Third, the sudden and significant increase in overall mean 30-minute wind speed associated with the change in wind direction in SD 63 tended to occur with less magnitude and at a later time than in the other school districts (Figures 4.15, 4.18, 4.21, 4.24, 4.27 and 4.30). Fourth, the increase in overall mean 30-minute wind speed from the lowest which occurred before the daily maximum to the daily maximum was usually greatest in SD 61. In addition, its overall mean 30-minute wind speed stayed higher than the other school districts' most of the time. Difference in the time of the occurrence of the daily maximum district overall mean 30-minute wind speed among the school districts was within 2.5 hours in most of the cases, but no specific temporal order was found.

There were features that differed among the selected days. First, the way the overall mean 30-minute wind speed changed after its daily maximum was different. Some identified patterns found within the time frame of a day were the sudden significant decrease on Nov. 15, 2006 (Figure 4.15) and Jan. 9, 2007 (Figure 4.24); the gradual decrease on Dec. 13, 2006 (Figure 4.18); and maintained lower but similar magnitude wind speed for many hours in SD 61 and recurrence of peaks with similar magnitude in SD 62 and SD 63 on Feb. 7 (Figure 4.30). The decrease in overall mean 30-minute wind speeds on Dec. 15, 2006 (Figure 4.21) was gradual, but it should be noted that the number of active weather stations after 1:30 in SD 62 and after 3:30 in SD 61 and SD 63 are much smaller for relatively long periods of time (Tables 4.5 and A2). Feb. 5, 2008 (Figure 4.27) has a gradual general decrease with multiple peaks. Second, timing of occurrence, wind direction and relative magnitude of the secondary peaks regarding the district overall mean 30-minute wind speeds were different among the selected days. For example, the secondary peaks on Nov. 15, 2006 occurred before the change of the mean wind directions to WSW so that the mean wind directions during those secondary peaks were mainly SSE, which ranges between 135° and 180° (Figures 4.13 and 4.14). On the other hand, the secondary peaks on the other days occurred after the change of mean wind directions to WSW or SSW. The magnitudes of secondary peaks in SD 61 were generally around 6 m s^{-1} or greater on the selected days. The secondary peaks in SD 62 on Feb. 7, 2008 and SD 63 on Nov. 15, 2006 and Feb. 7, 2008 had almost the same magnitude as the primary peaks. Similar to the case of SD 61 on Nov. 15, 2006 and Jan. 9, 2007, a notable decrease in the district overall mean 30-minute wind speed and lapse of time were observed between the primary and secondary peaks on Nov. 15, 2006 and Feb. 7, 2008.

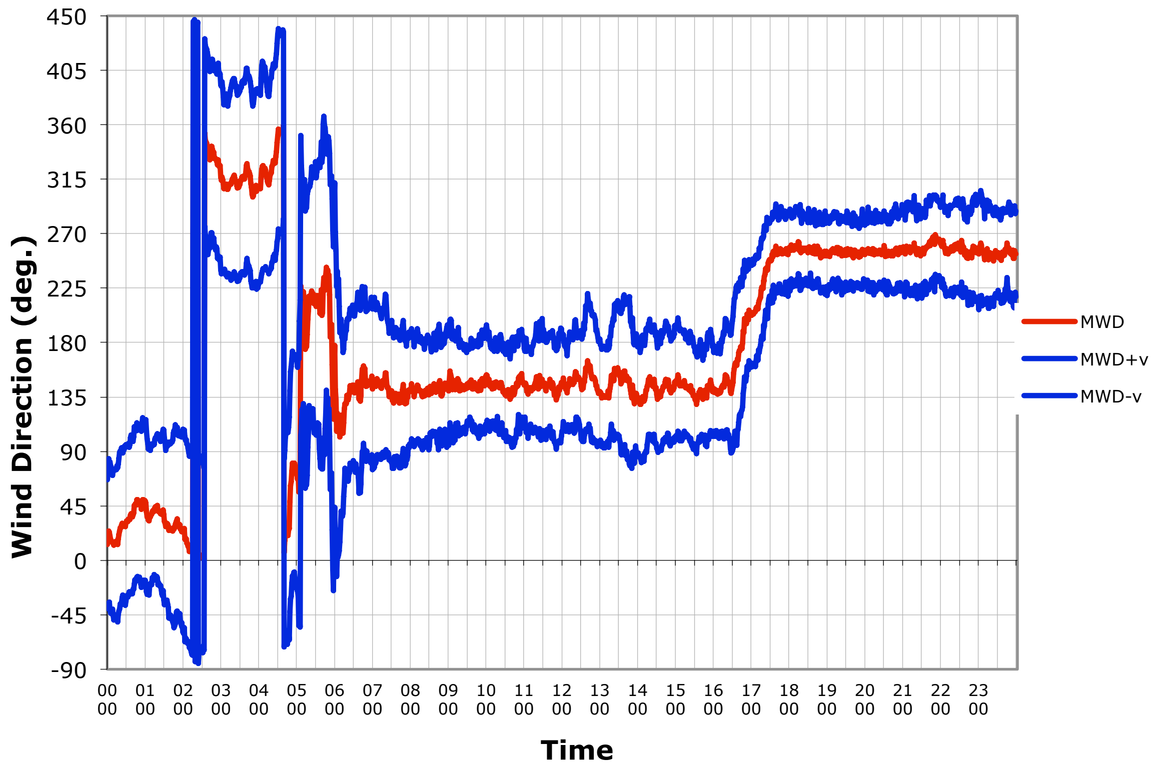

Figure 4.13: Mean wind direction in the entire study area and plus and minus one circular standard deviation on Nov. 15, 2006. MWD and v in legend are mean wind direction and one circular standard deviation, respectively.

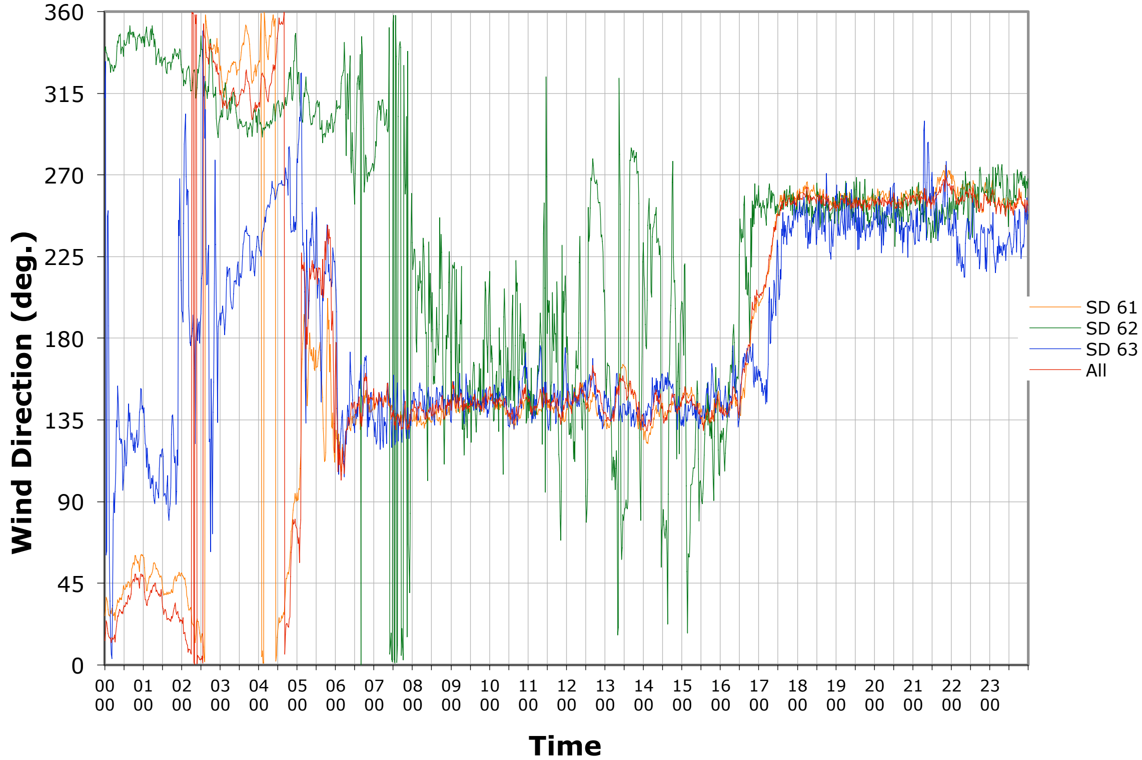

Figure 4.14: District mean wind directions on Nov. 15, 2006.

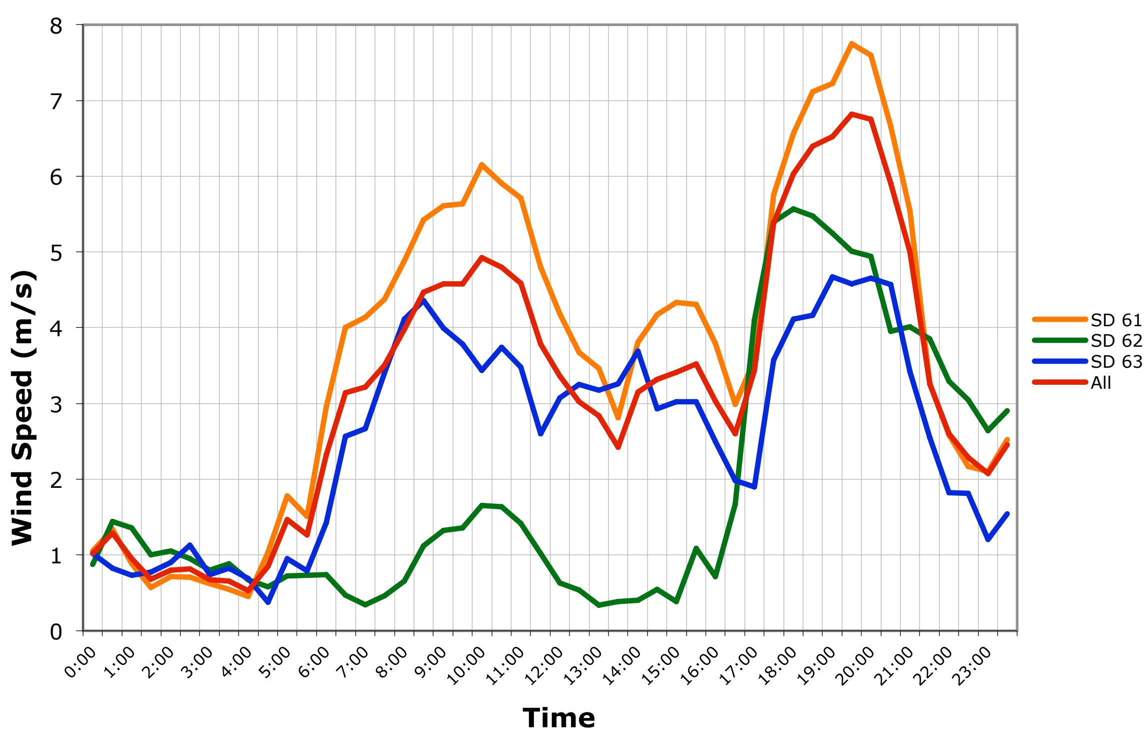

Figure 4.15: District overall mean 30-minute wind speeds on Nov. 15, 2006.

Table 4.3: The number of active weather stations, maximum mean 30-minute wind speed and minimum mean 30-minute wind speed in each school district during the time period of its daily maximum district overall mean 30-minute wind speed on Nov. 15, 2006.

School District	Nov. 15, 2006			
	Time period	Number of active weather stations	Max mean wind speed (m/s)	Min mean wind speed (m/s)
SD 61	19:30-19:59	43	14.34	2.43
SD 62	18:00-18:29	12	8.06	3.68
SD 63	19:00-19:29	8	7.13	3.01

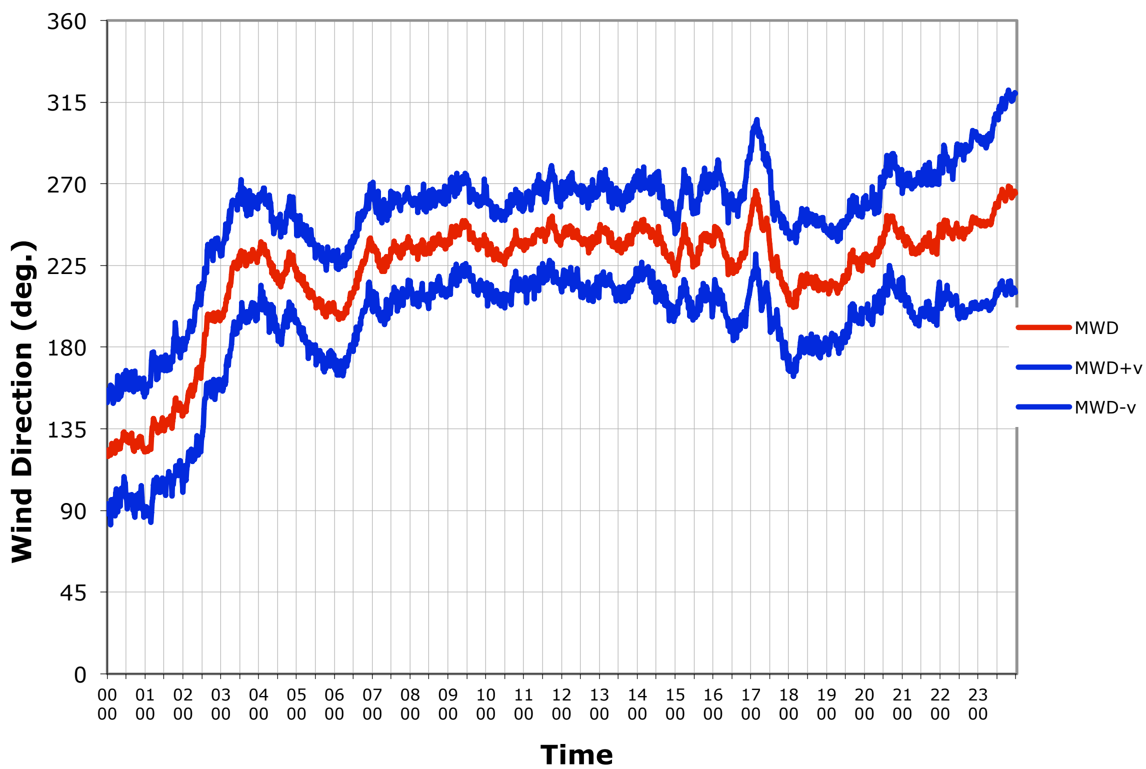

Figure 4.16: Mean wind direction in the entire study area and plus and minus one circular standard deviation on Dec. 13, 2006. MWD and v in legend are mean wind direction and one circular standard deviation, respectively.

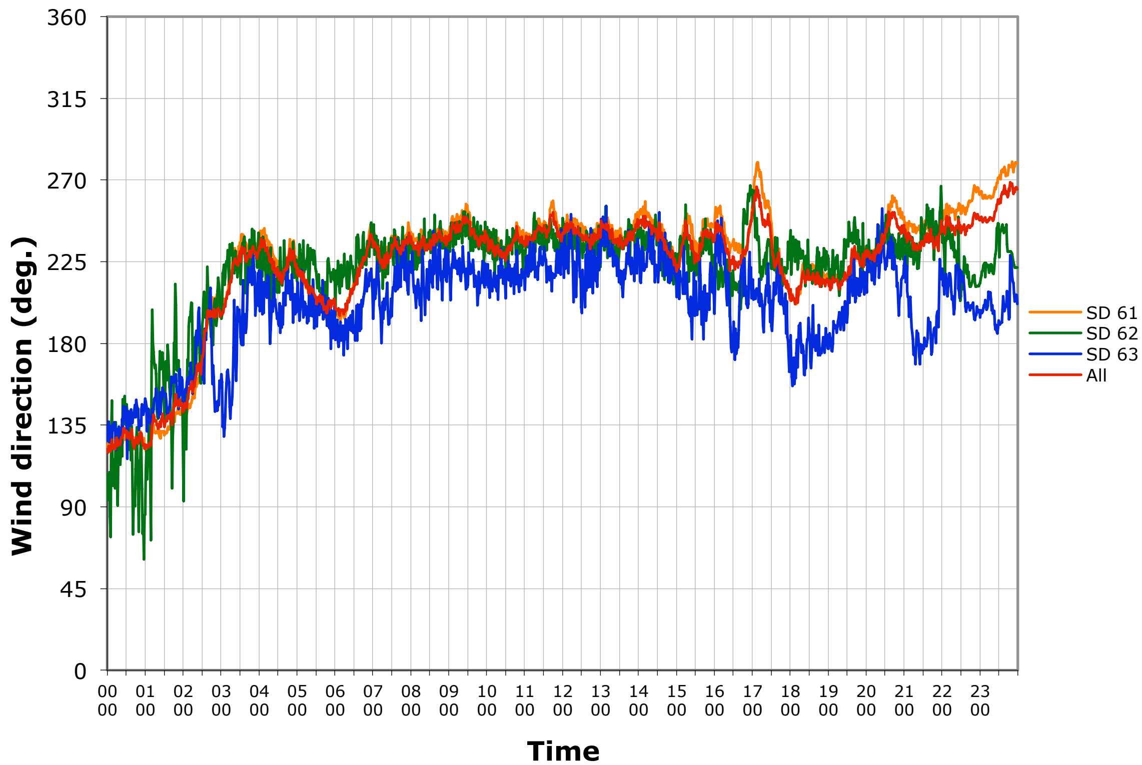

Figure 4.17: District mean wind directions on Dec. 13, 2006.

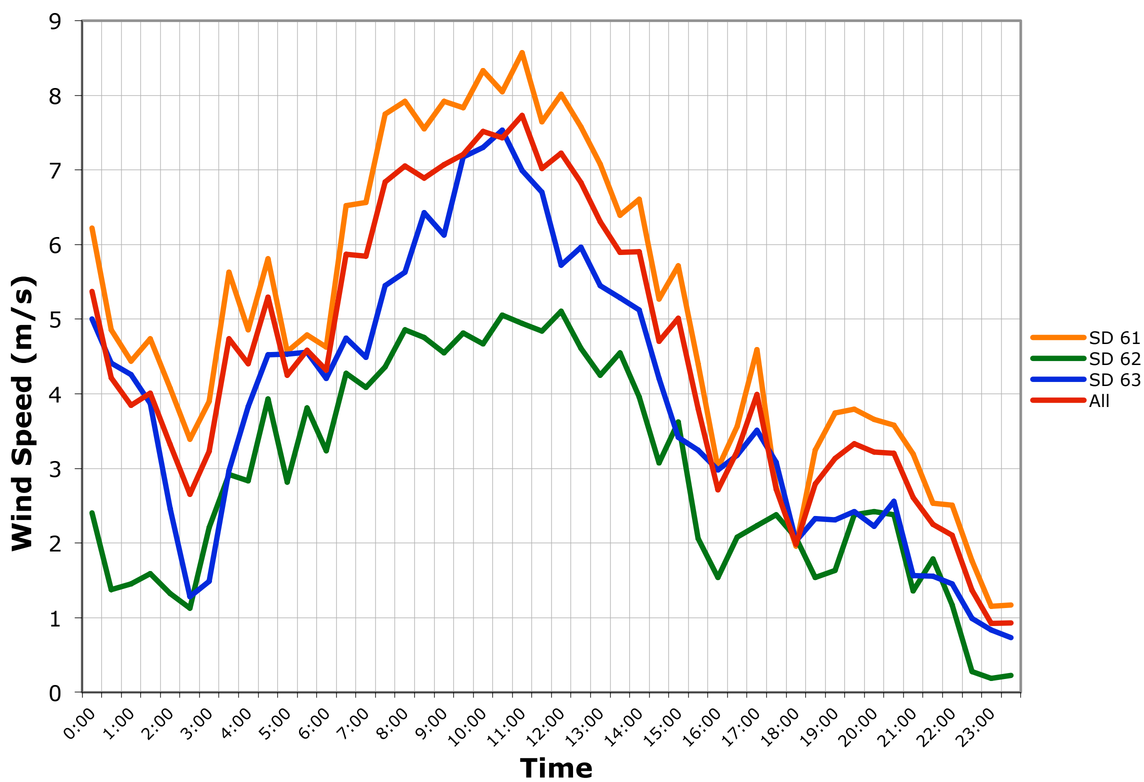

Figure 4.18: District overall mean 30-minute wind speeds on Dec. 13, 2006.

Table 4.4: The number of active weather stations, maximum mean 30-minute wind speed and minimum mean 30-minute wind speed in each school district during the time period of its daily maximum district overall mean 30-minute wind speed on Dec. 13, 2006.

School District	Dec. 13, 2006			
	Time period	Number of active weather stations	Max mean wind speed (m/s)	Min mean wind speed (m/s)
SD 61	11:00-11:29	41	15.13	1.98
SD 62	12:00-12:29	11	7.57	2.68
SD 63	10:30-10:59	6	10.90	4.71

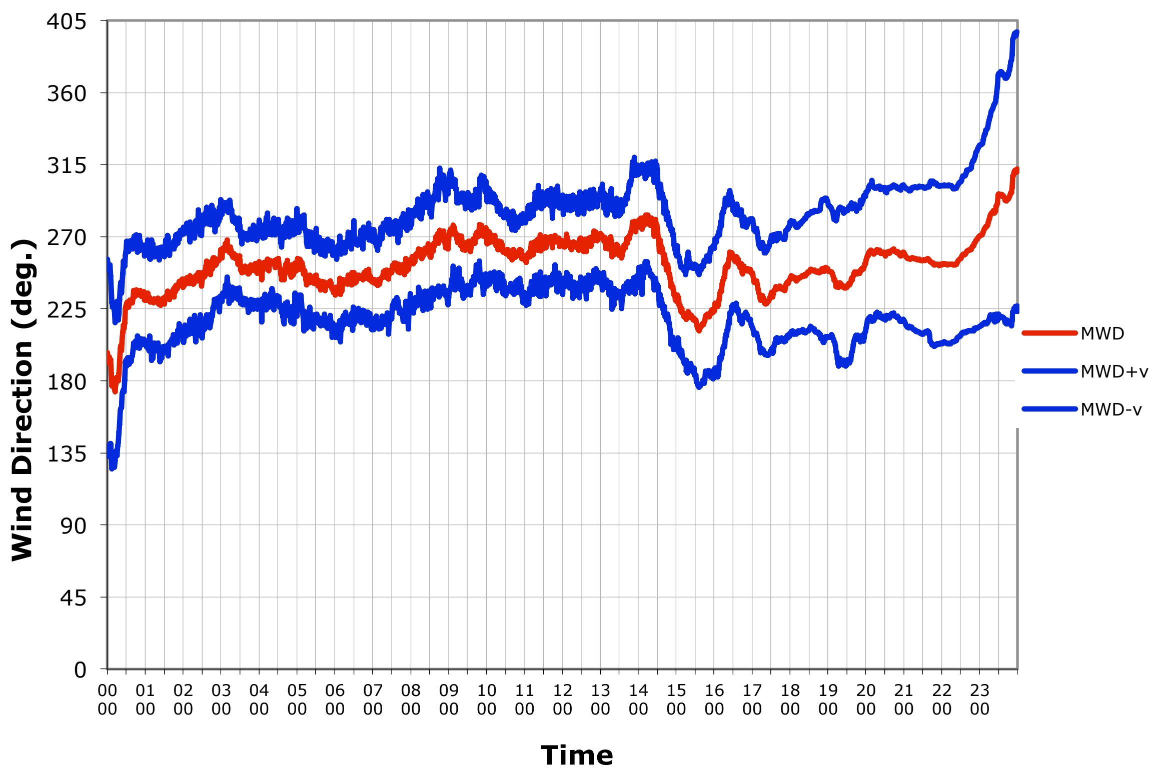

Figure 4.19: Mean wind direction in the entire study area and plus and minus one circular standard deviation on Dec. 15, 2006. MWD and v in legend are mean wind direction and one circular standard deviation, respectively.

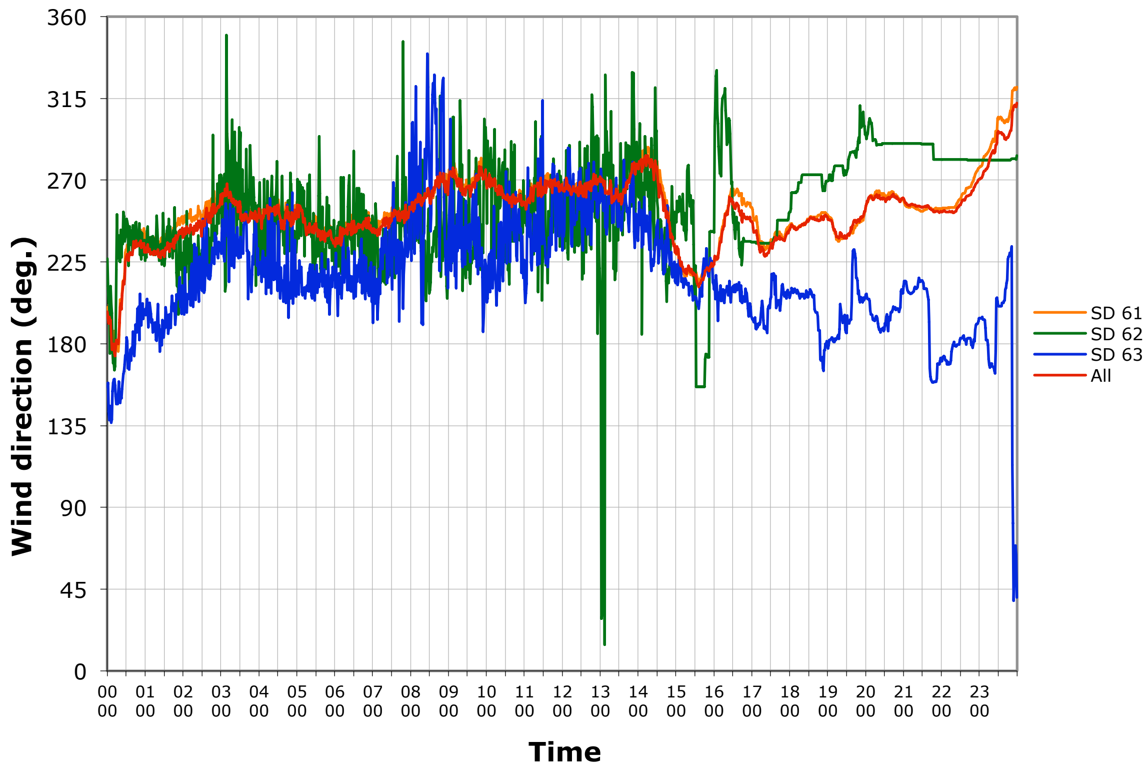

Figure 4.20: District mean wind directions on Dec. 15, 2006.

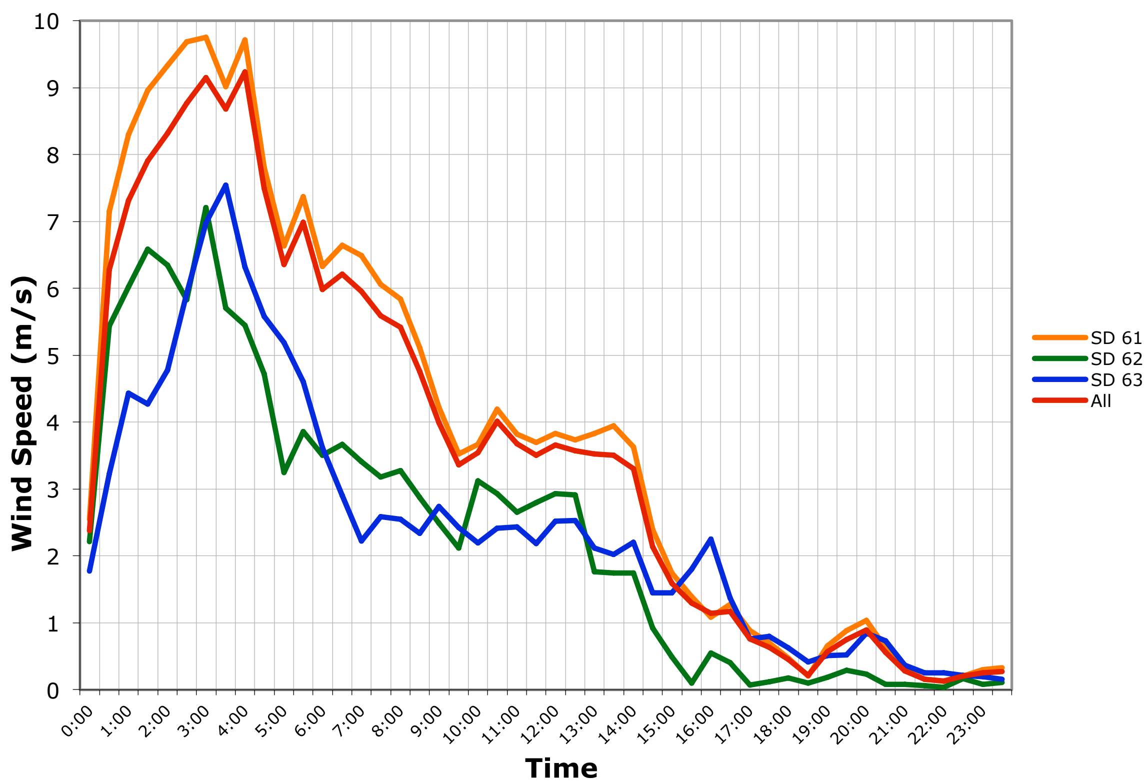

Figure 4.21: District overall mean 30-minute wind speeds on Dec. 15, 2006.

Table 4.5: The number of active weather stations, maximum mean 30-minute wind speed and minimum mean 30-minute wind speed in each school district during the time period of its daily maximum district overall mean 30-minute wind speed on Dec. 15, 2006. The Data at Frank Hobbs Elementary School (Stn. ID 9) in SD 61 were eliminated.

School District	Dec. 15, 2006			
	Time period	Number of active weather stations	Max mean wind speed (m/s)	Min mean wind speed (m/s)
SD 61	3:00-3:29	38	17.19	4.53
SD 62	3:00-3:29	3	8.65	5.97
SD 63	3:30-3:59	5	9.76	3.26

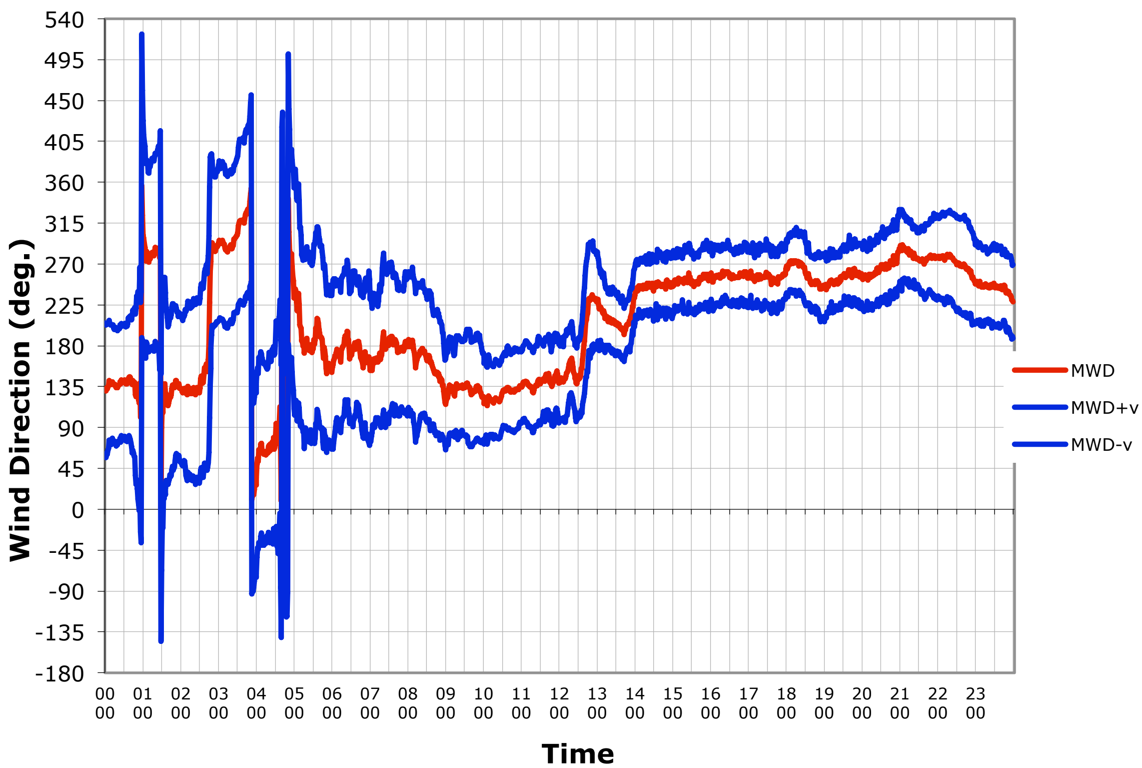

Figure 4.22: Mean wind direction in the entire study area and plus and minus one circular standard deviation on Jan. 9, 2007. MWD and v in legend are mean wind direction and one circular standard deviation, respectively.

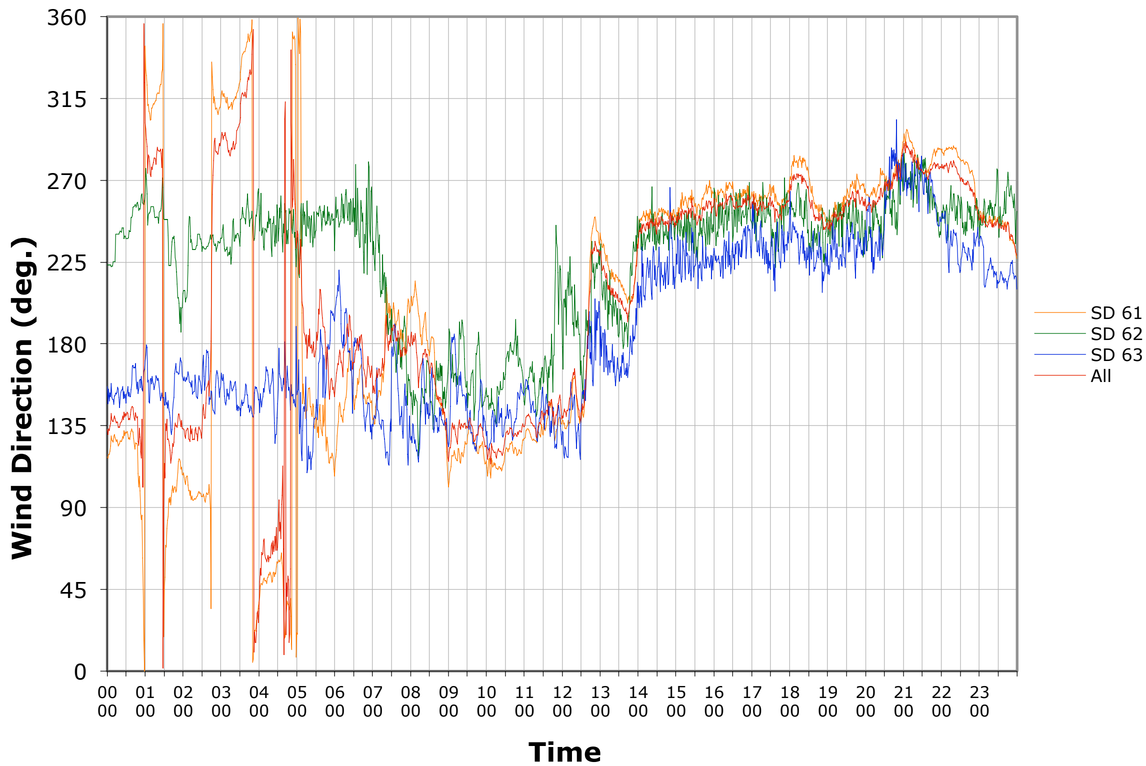

Figure 4.23: District mean wind directions on Jan. 9, 2007.

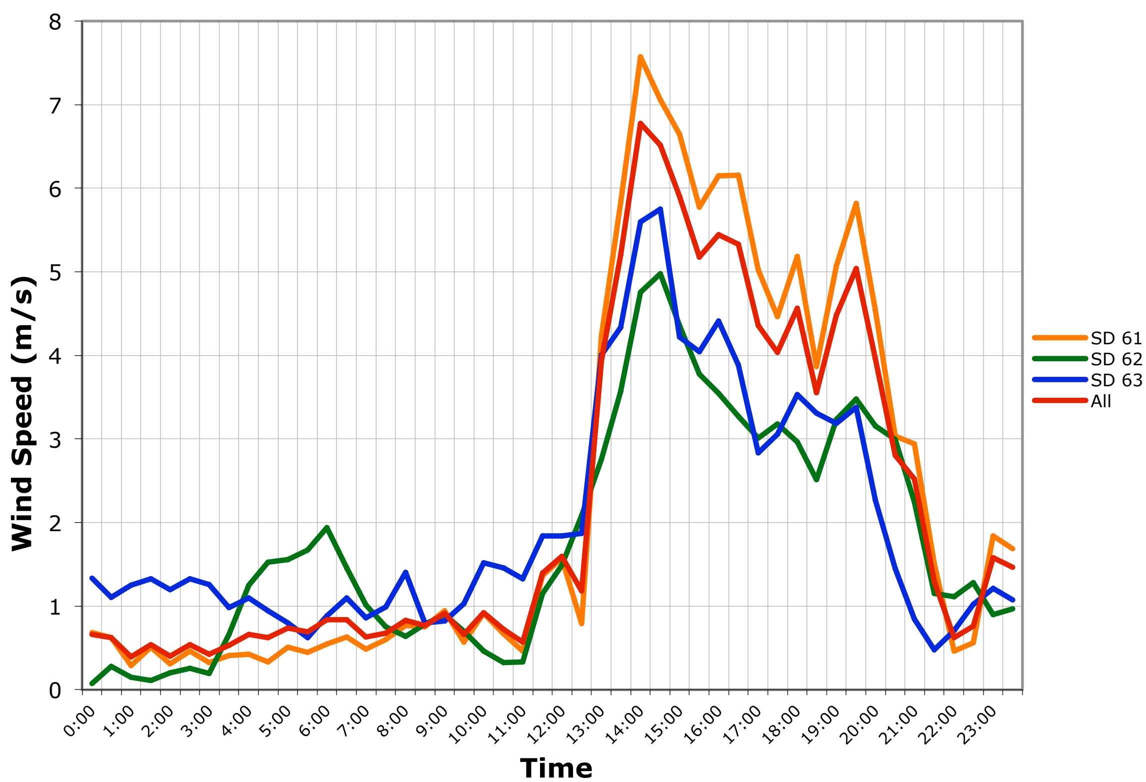

Figure 4.24: District overall mean 30-minute wind speeds on Jan. 9, 2007.

Table 4.6: The number of active weather stations, maximum mean 30-minute wind speed and minimum mean 30-minute wind speed in each school district during the time period of its daily maximum district overall mean 30-minute wind speed on Jan. 9, 2007.

School District	Jan. 9, 2007			
	Time period	Number of active weather stations	Max mean wind speed (m/s)	Min mean wind speed (m/s)
SD 61	14:00-14:29	41	12.67	2.20
SD 62	14:30-14:59	11	6.96	3.35
SD 63	14:30-14:59	8	8.48	2.61

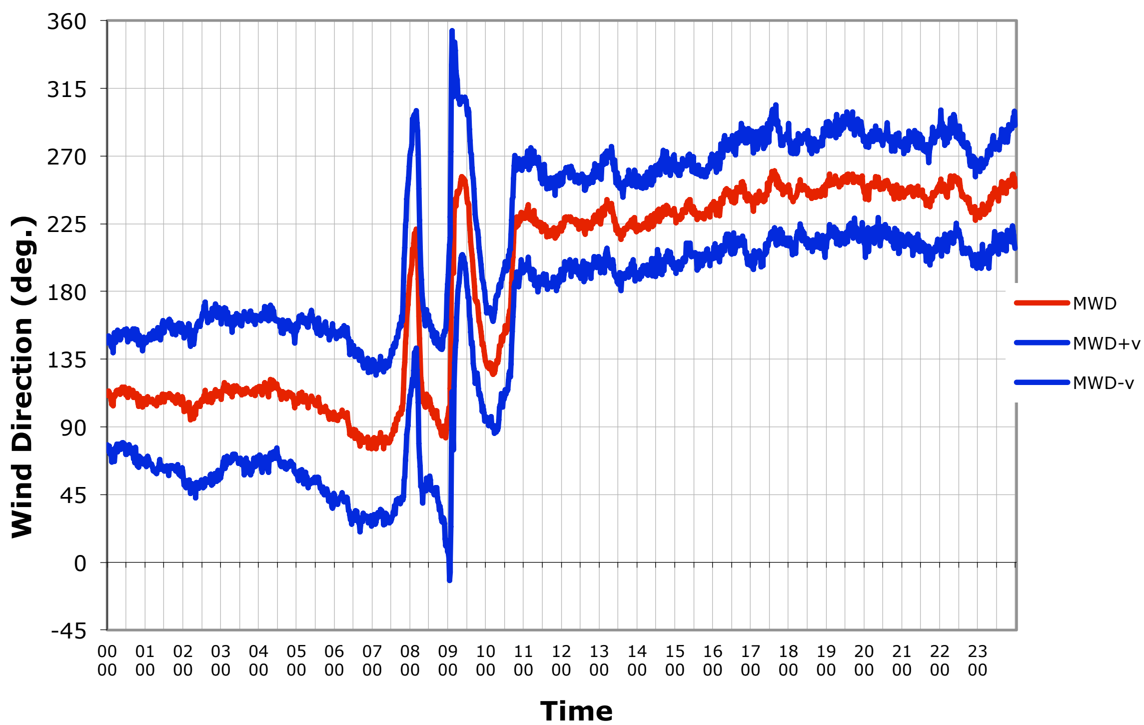

Figure 4.25: Mean wind direction in the entire study area and plus and minus one circular standard deviation on Feb. 5, 2008. MWD and v in legend are mean wind direction and one circular standard deviation, respectively.

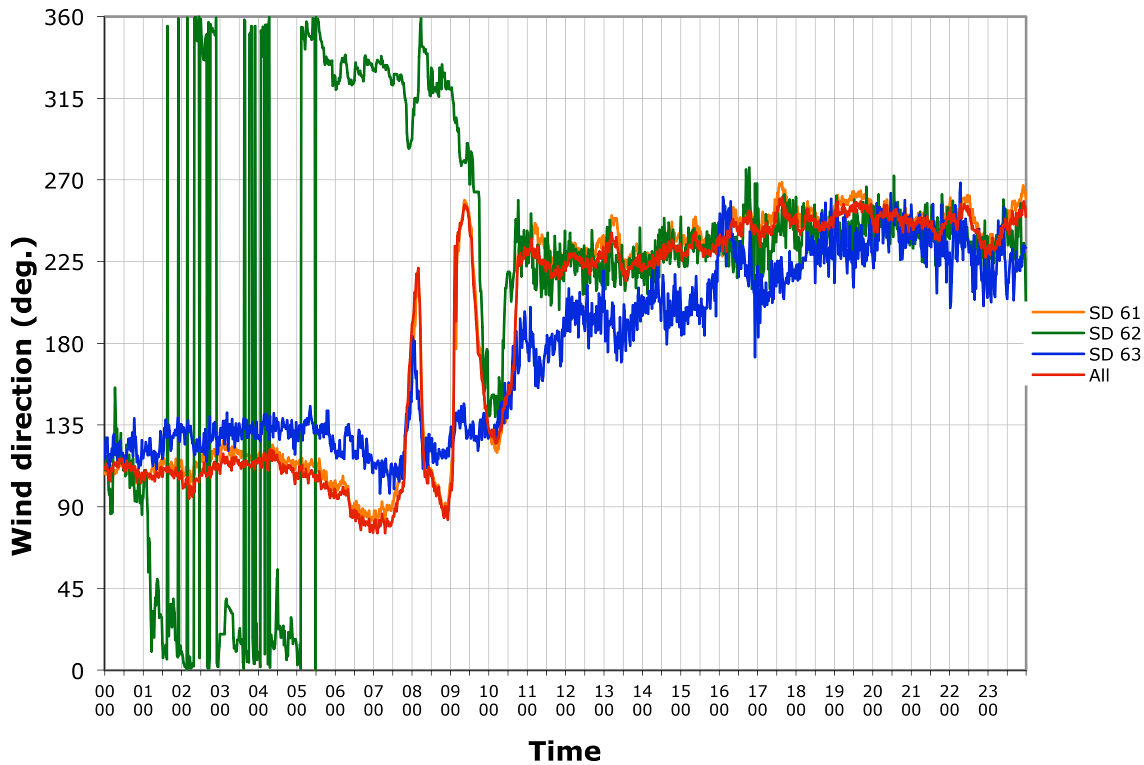

Figure 4.26: District mean wind directions on Feb. 5, 2008.

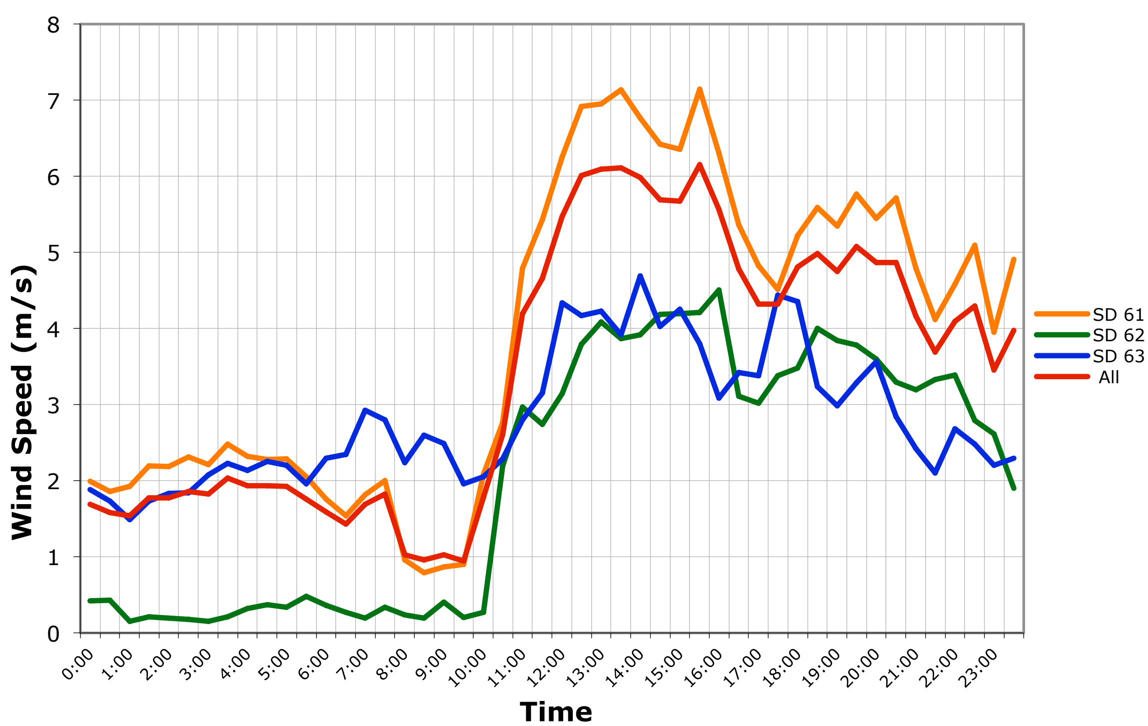

Figure 4.27: District overall mean 30-minute wind speeds on Feb. 5, 2008.

Table 4.7: The number of active weather stations, maximum mean 30-minute wind speed and minimum mean 30-minute wind speed in each school district during the time period of its daily maximum district overall mean 30-minute wind speed on Feb. 5, 2008.

School District	Feb. 5, 2008			
	Time period	Number of active weather stations	Max mean wind speed (m/s)	Min mean wind speed (m/s)
SD 61	15:30-15:59	41	11.88	1.28
SD 62	16:00-16:30	10	6.30	1.56
SD 63	14:00-14:29	9	7.34	2.78

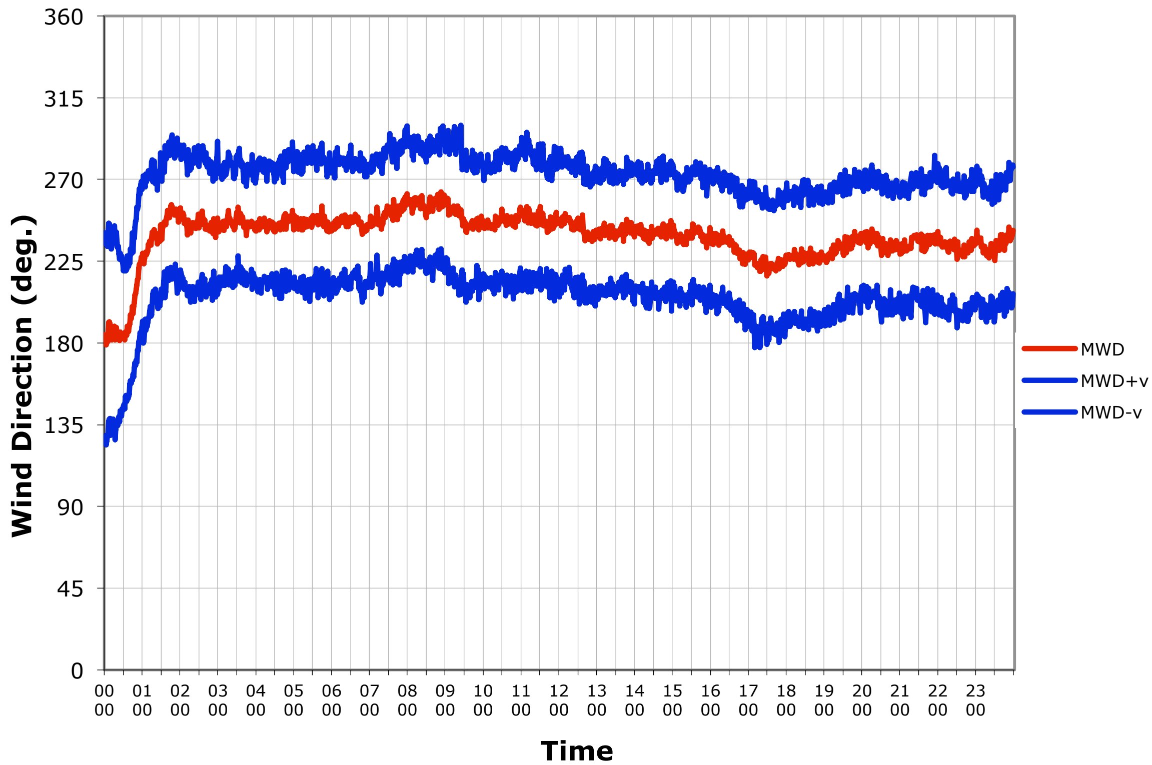

Figure 4.28: Mean wind direction in the entire study area and plus and minus one circular standard deviation on Feb. 7, 2008. MWD and v in legend are mean wind direction and one circular standard deviation, respectively.

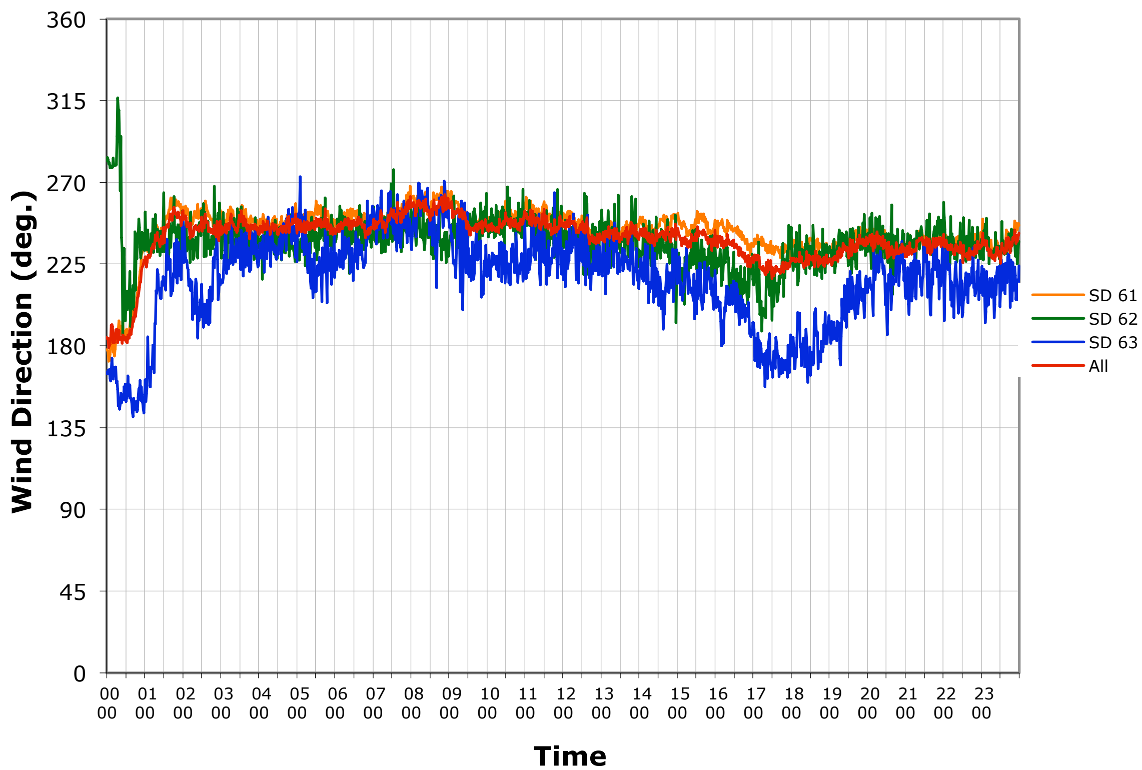

Figure 4.29: District mean wind directions on Feb. 07, 2008.

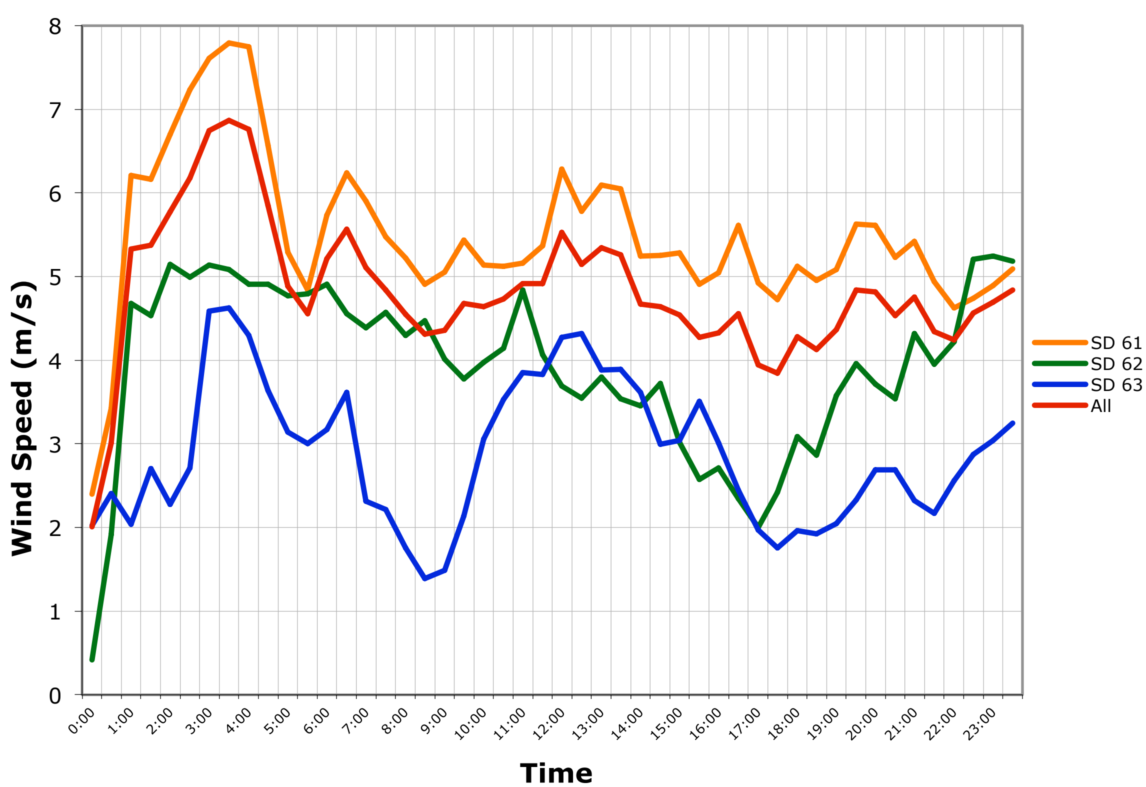

Figure 4.30: District overall mean 30-minute wind speeds on Feb. 7, 2008.

Table 4.8: The number of active weather stations, maximum mean 30-minute wind speed and minimum mean 30-minute wind speed in each school district during the time period of its daily maximum district overall mean 30-minute wind speed on Feb. 7, 2008.

School District	Feb. 7, 2008			
	Time period	Number of active weather stations	Max mean wind speed (m/s)	Min mean wind speed (m/s)
SD 61	3:30-3:59	41	14.03	1.79
SD 62	23:00-23:29	12	7.71	1.42
SD 63	3:30-3:59	9	6.93	2.43

4.5.2 General distribution of mean wind speed in the study area

The overall mean 30-minute wind speeds at the weather stations in each school district for the entire six days are shown in Table 4.9. The value was determined by calculating the average of the 30-minute wind speeds observed at a weather station during the 30-minute periods when the school district to which the weather station belongs recorded the daily maximum district overall mean 30-minute wind speed on the selected days. The maximum number of observations for a weather station is six, one for each case study day. For Dec. 15, 2006, the data recorded from 1:30 to 1:59 in SD 61, from 1:00 to 1:29 in SD 62, from 2:30 to 2:59 in SD 63 were used to minimize the effect of the amount of missing data.

School district 61 had the highest wind speeds. Thirty-three out of 43 weather stations in SD 61 recorded higher overall mean 30-minute wind speed than the highest in SD 62. Similarly, 28 out of 43 weather stations in SD 61 recorded the same or higher values than the highest in SD 63. In addition, magnitude of the highest overall mean 30-minute wind speed in SD 61 is close to double those of the highest ones in SD 62 and SD 63.

Table 4.9: Overall mean 30-minute wind speeds at the weather stations in each school district during the 30-minute periods when each school district recorded its daily maximum overall mean 30-minute wind speed during the selected days.

SD 61		SD 62		SD 63	
Stn. ID	Overall mean 30-minute wind speed (m/s)	Stn. ID	Overall mean 30-minute wind speed (m/s)	Stn. ID	Overall mean 30-minute wind speed (m/s)
25	13.74	58	7.19	67	7.53
75	12.00	40	7.09	63	6.92
23	11.44	34	6.95	62	6.72
8	11.28	35	6.19	70	6.67
22	10.01	39	5.77	66	5.04
4	9.66	38	5.36	61	4.60
6	9.60	32	5.30	65	4.10
15	9.35	55	5.25	64	3.43
81	9.25	56	4.98	42	3.22
60	9.14	31	4.81		
29	9.09	36	3.83		
21	9.09	57	3.54		
82	8.92	71	2.56		
78	8.48				
24	8.45				
16	8.40				
20	8.35				
11	8.29				
30	8.22				
77	8.16				
19	8.15				
80	8.14				
79	7.98				
12	7.98				
28	7.87				
18	7.85				
73	7.78				
27	7.53				
26	7.49				
33	7.49				
14	7.46				
2	7.45				
76	7.43				
7	6.81				
10	6.79				
1	6.28				
74	5.51				
41	5.39				
13	5.14				

5	4.07
3	3.70
9	2.65
17	2.02

The most dominant overall mean 30-minute wind speed class is 7.50-8.99 m s^{-1} in SD 61; 4.50-5.99 m s^{-1} in SD 62; and 6.00-7.49 m s^{-1} and 3.00-4.49 m s^{-1} in SD 63 (Figure 4.31). Nine, 4 and 4 classes were found in SD 61, SD 62 and SD 63, respectively. The main factors controlling the greater number of classes found in SD 61 than the other school districts are the higher incoming wind speeds because of close proximity to the south-facing shoreline and more diverse weather station site conditions due to the greater number of weather stations (Table 4.9).

The area with the highest overall mean 30-minute wind speeds in the entire study area was from south of downtown to northeast of downtown in SD 61 (Figure 4.31). Other areas in SD 61, such as north and south of the Gorge Waterway, and the north and northeast of the school district, also had higher wind speeds than those in the other school districts. Weather stations with lowest overall mean 30-minute wind speeds in SD 61 were found in the west and east ends. Although magnitudes of the wind speeds are much less than those in the high wind speed areas in SD 61, relatively high overall mean 30-minute wind speeds were observed in the middle and middle east of SD 62. The lowest, 2nd lowest and 3rd lowest overall mean 30-minute wind speeds in SD 62 were found in the northernmost, middle east and southernmost of the school district, respectively. The weather stations with the highest and the 2nd lowest are in close proximity to each other. In SD 63, a relatively high wind speed area was found in the north part of the school district. The weather station in the middle south also recorded relatively high overall mean 30-minute wind speed. Lowest ones were observed in the southwest, middle north and southeast of the school district. In general, most of the weather stations with wind speed less than 4.50 m s^{-1}, such as Cedar Hill Middle School (Stn. ID 5), Strawberry Vale Elementary School (Stn. ID 3) and Frank Hobbs Elementary School (Stn. ID 9) in SD 61; Hans Helgesen Elementary School (Stn. ID 36), Wishart Elementary School (Stn. ID 57) and Cal Revelle Nature Sanctuary (Stn. ID 71) in SD 62; and McTavish Elementary School (Stn. ID 65) and Butchart Gardens (Stn. ID 42) in SD 63, are located in the lee of local relief relative to WSW winds (Tables 4.9 and A1; Figure 1.1). Although local modification must have occurred in very low atmospheric boundary layer flow due to the unconventional weather station site location conditions, the magnitude and specific source of the modification cannot be known. The area with the highest overall mean 30-minute wind speeds in each school district is discussed later in this chapter (Section 4.8.2).

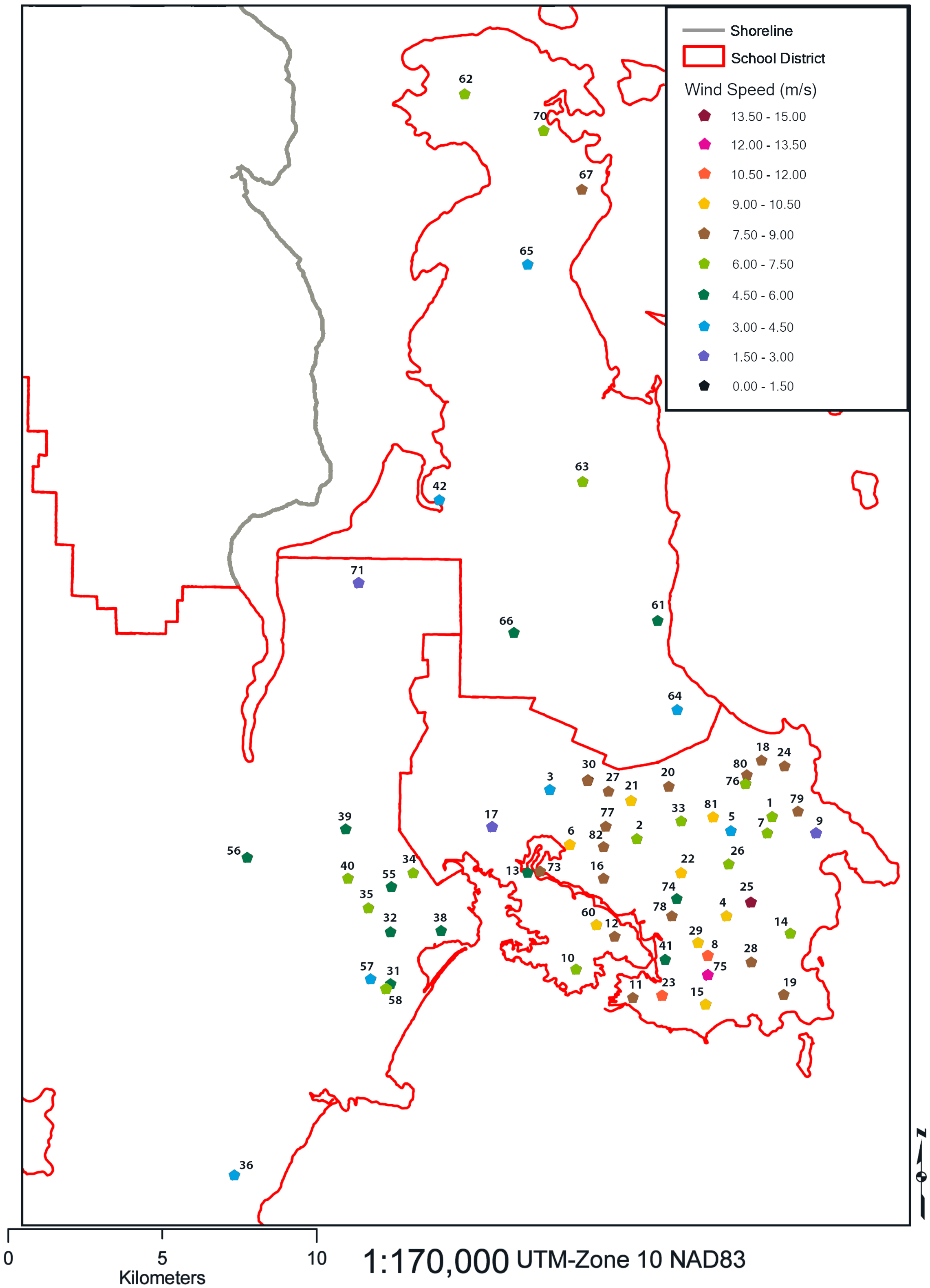

Figure 4.31: Distribution of overall mean 30-minute wind speed over the study area during the selected days (Base map: Brendle-Moczuk 2010).

4.5.3 Daily maximum gust wind speed

The daily maximum gust wind speed could occur at times other than at the primary peaks of the district overall mean 30-minute wind speeds (Figures 4.32 through 4.37). For example, 6 weather stations in SD 61 (Stn. IDs 1, 5, 13, 18, 19 and 27) and 3 weather stations in SD 63 (Stn. IDs 62, 64 and 65) recorded their daily maximum gust wind speeds not at the primary peak but near the secondary peak on Nov. 15, 2006 (Figure 4.32). In SD 62, one of the weather stations (Stn. ID 58) had its daily maximum gust wind speed twice on Jan. 9, 2007 at around 20:45 when its district overall mean 30-minute wind speed continued dropping from the second highest peak (Figure 4.35). On Feb. 7, 2008, 3 weather stations in SD 61 (Stn. IDs 12, 19 and 41) recorded their daily maximum gust wind speeds when their district overall mean 30-minute wind speed decreased by 2.00 m s^{-1} from its highest (Figure 4.37). The weather stations mentioned above had complete gust wind speed data on the associated days, so these results were not affected by their missing data (Table A4).

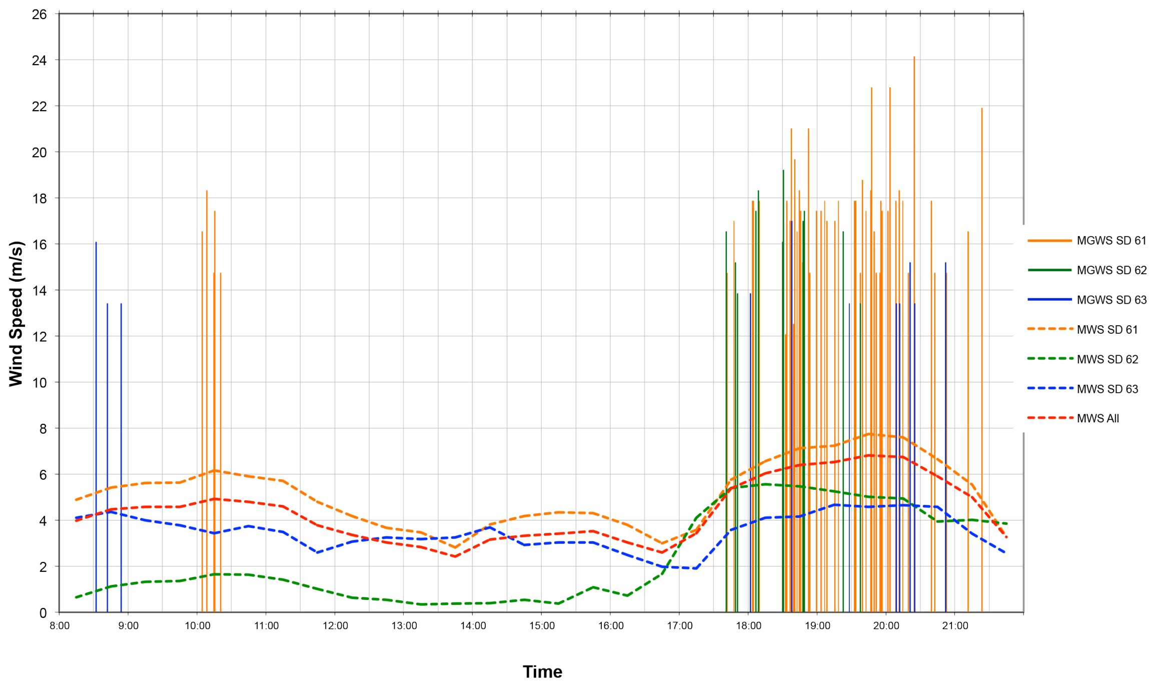

Figure 4.32: Overall mean 30-minute wind speeds (MWS) and occurrence of maximum gust wind speeds (MGWS) in all of the school districts on Nov. 15, 2006 between 8:00-21:59.

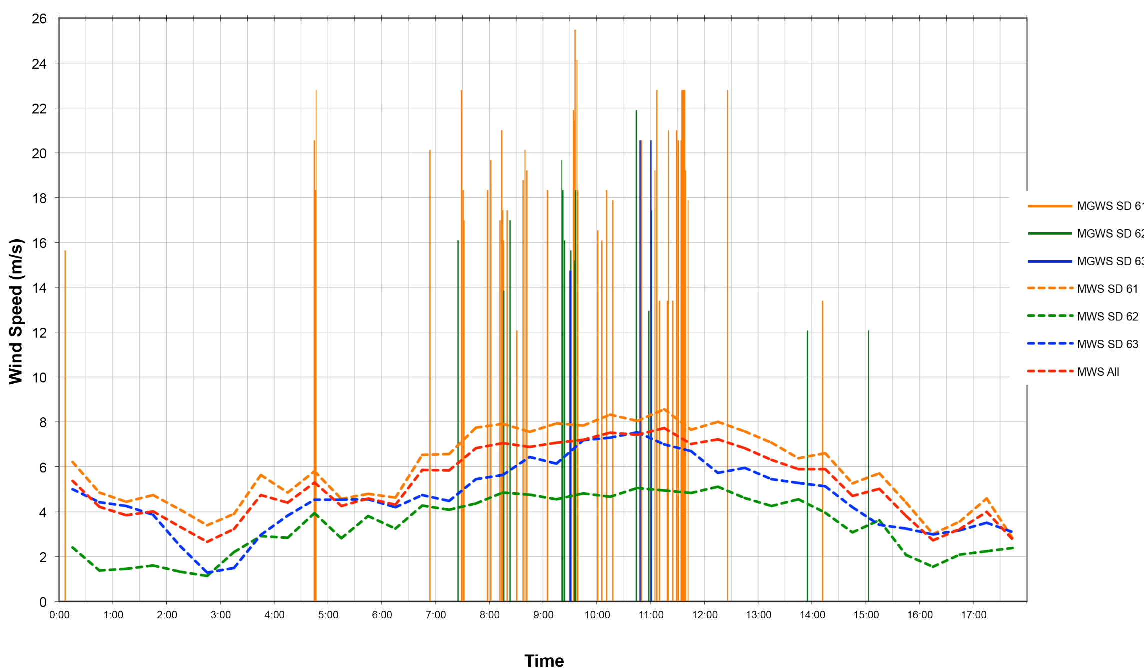

Figure 4.33: Overall mean 30-minute wind speeds (MWS) and occurrence of maximum gust wind speeds (MGWS) in all of the school districts on Dec. 13, 2006 between 00:00-17:59.

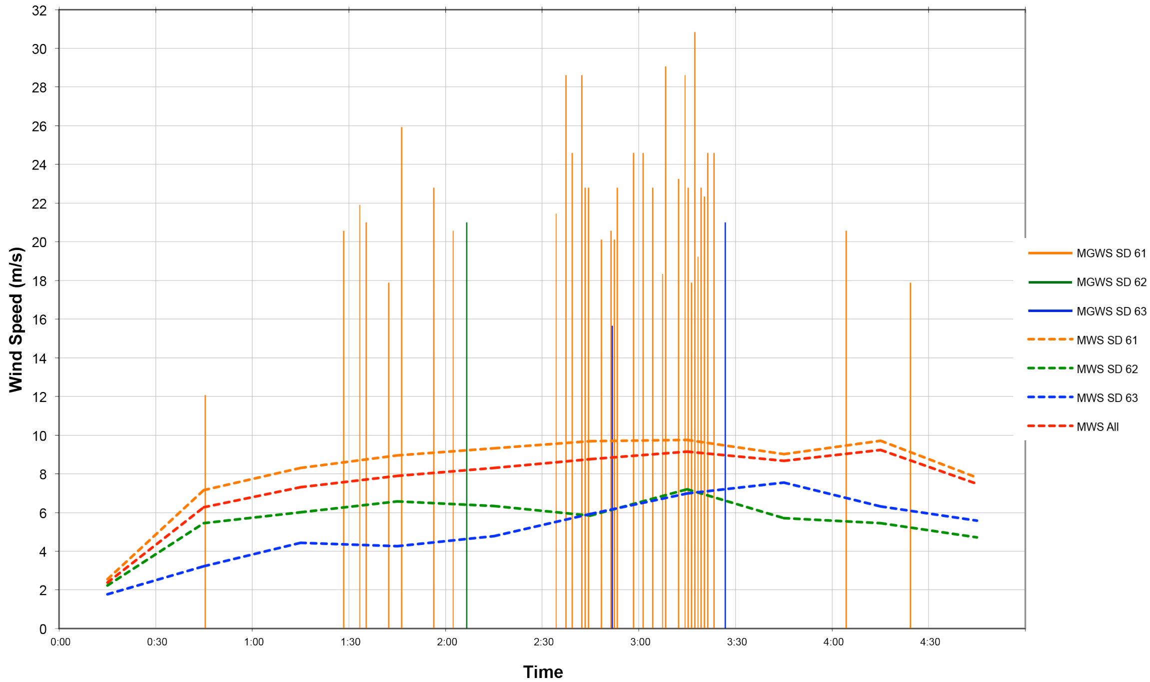

Figure 4.34: Overall mean 30-minute wind speeds (MWS) and occurrence of maximum gust wind speeds (MGWS) in all of the school districts on Dec. 15, 2006 between 00:00-04:59.

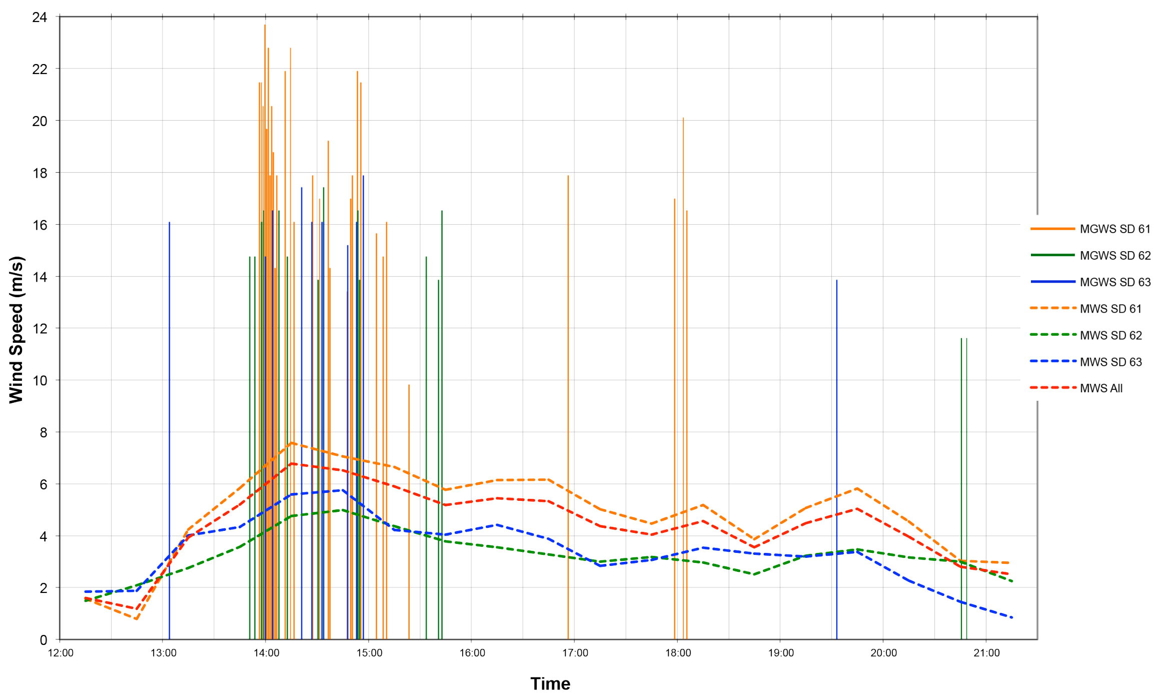

Figure 4.35: Overall mean 30-minute wind speeds (MWS) and occurrence of maximum gust wind speeds (MGWS) in all of the school districts on Jan. 9, 2007 between 12:00-21:29.

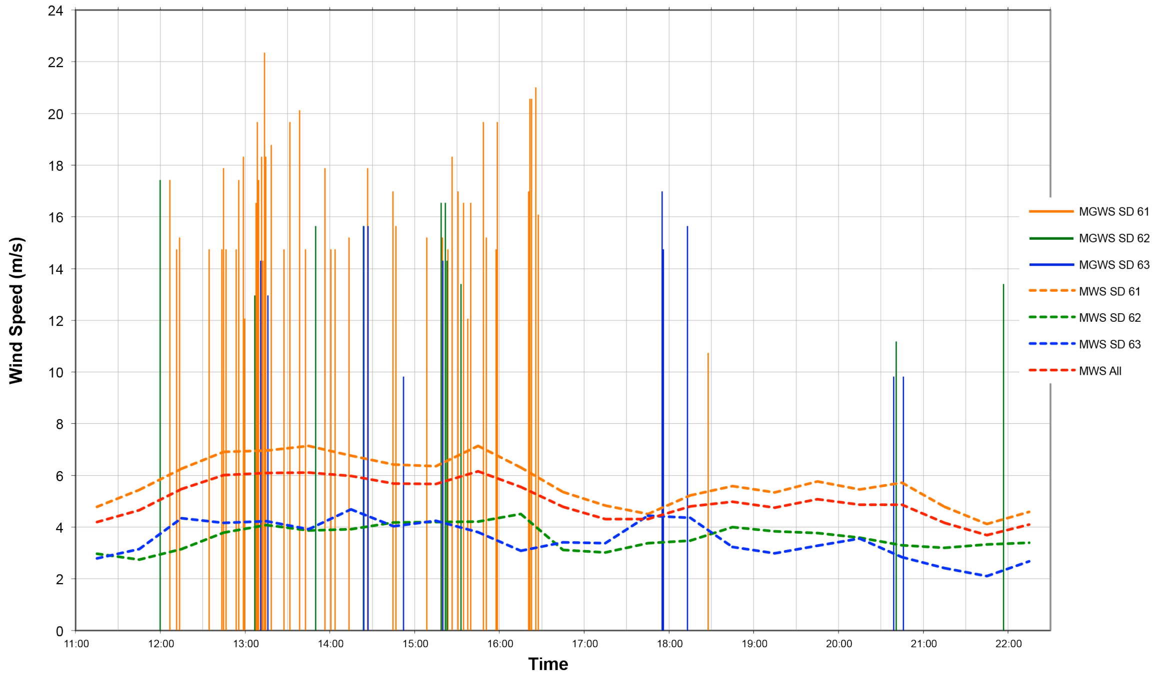

Figure 4.36: Overall mean 30-minute wind speeds (MWS) and occurrence of maximum gust wind speeds (MGWS) in all of the school districts on Feb. 5, 2008 between 11:00-22:29.

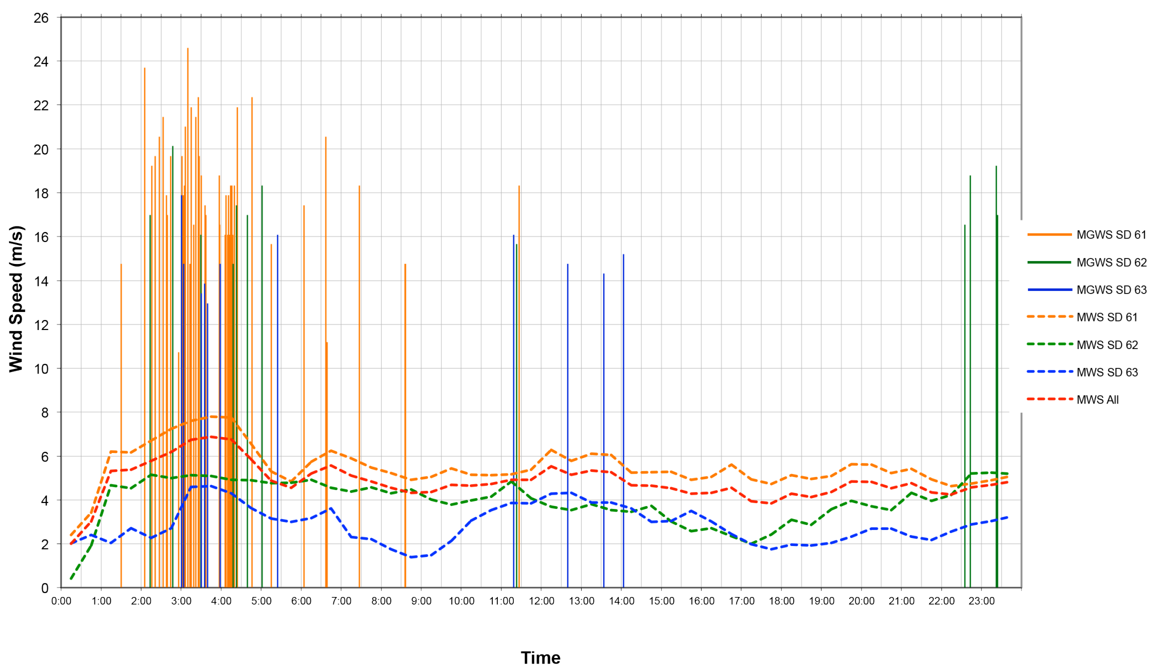

Figure 4.37: Overall mean 30-minute wind speeds (MWS) and occurrence of maximum gust wind speeds (MGWS) in all of the school districts on Feb. 7, 2008 between 00:00-23:59.

4.5.4 General distribution of gust wind speed in the study area

Distribution of daily maximum gust wind speed over the study area during the selected days is similar to that of the overall mean 30-minute wind speed. On Dec. 15, 2006, the number of valid weather stations was 34 in SD 61, 1 in SD 62 and 2 in SD 63. In SD 61, 8 classes were found, and the most dominant ones are 22.50-24.99 m s^{-1} and 20.00-22.49 m s^{-1} (Figure 4.39). The areas with high daily maximum gust wind speeds are basically the same as the ones for the overall mean 30-minute wind speed and mean daily maximum gust wind speed (Figures 4.31 and 4.38). The daily maximum gust wind speed is the daily highest of the gust wind speeds in the one minute periods at each weather station, and the mean daily maximum gust wind speed is the mean of 6 daily maximum gust wind speeds at each weather station. If a weather station has invalid gust wind speed data, a sample size of the mean daily maximum gust wind speed at the weather station becomes less than 6. Highest daily maximum gust wind speeds in the entire study area were found in the area surrounding downtown from north clockwise to south on its east side in SD 61. Several weather stations recorded the daily maximum gust wind speed over 25 m s^{-1}, and Lansdowne Middle School (Stn. ID 25) had the daily maximum above 30 m s^{-1} in that area. Braefoot Elementary School (Stn. ID 81), which is located in the middle northeast of SD 61, also recorded the daily maximum close to 30 m s^{-1} on Dec. 15. It is notably high, considering the weather station's records of overall mean 30-minute wind speed and mean daily maximum gust wind speed.

The distribution of mean daily maximum gust wind speed shows that most of the weather stations in the middle part of SD 62 recorded high mean daily maximums (Figure

4.38). In SD 63, the area with high mean daily maximum gust wind speed was found in the north and middle south.

The distribution patterns on Dec. 15, 2006 and during the other selected days indicate that although the areas with strong winds are basically the same during windstorms, the distribution patterns of weather stations with highest wind speeds within the areas can be different from one strong wind incident to another. One of the reasons might be the fact that every cyclone has a little different air circulation around its centre. However, it is unknown how much of the difference resulted from a large number of inactive weather stations after the sudden and significant increase in wind speeds on Dec. 15, 2006. It should also be noted that the actual magnitudes of the gust wind speeds on Dec. 15, 2006 could have been much greater than those shown on the map. As the distribution of the overall mean 30-minute wind speed, modifications occur in both speed and direction of the mean daily maximum and the daily maximum gust wind speeds. The modifications vary widely with: i) geographic location across the network in a very rough, largely urban region, and ii) where the instrument is sited on each school. Both modifications i and ii also vary with direction of the wind.

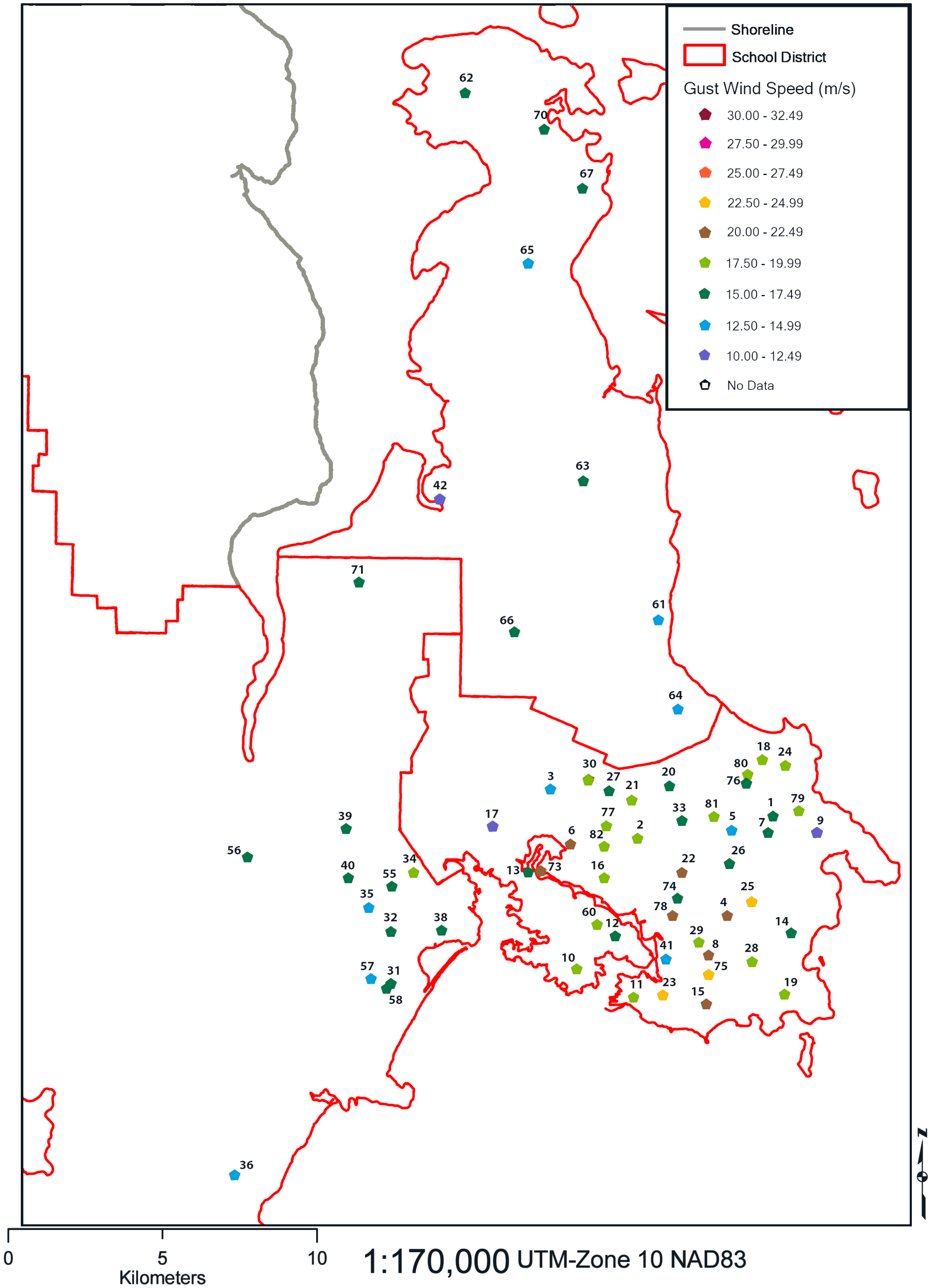

Figure 4.38: Distribution of mean daily maximum gust wind speed over the study area during the selected days except Dec. 15, 2006 (Base map: Brendle-Moczuk 2010).

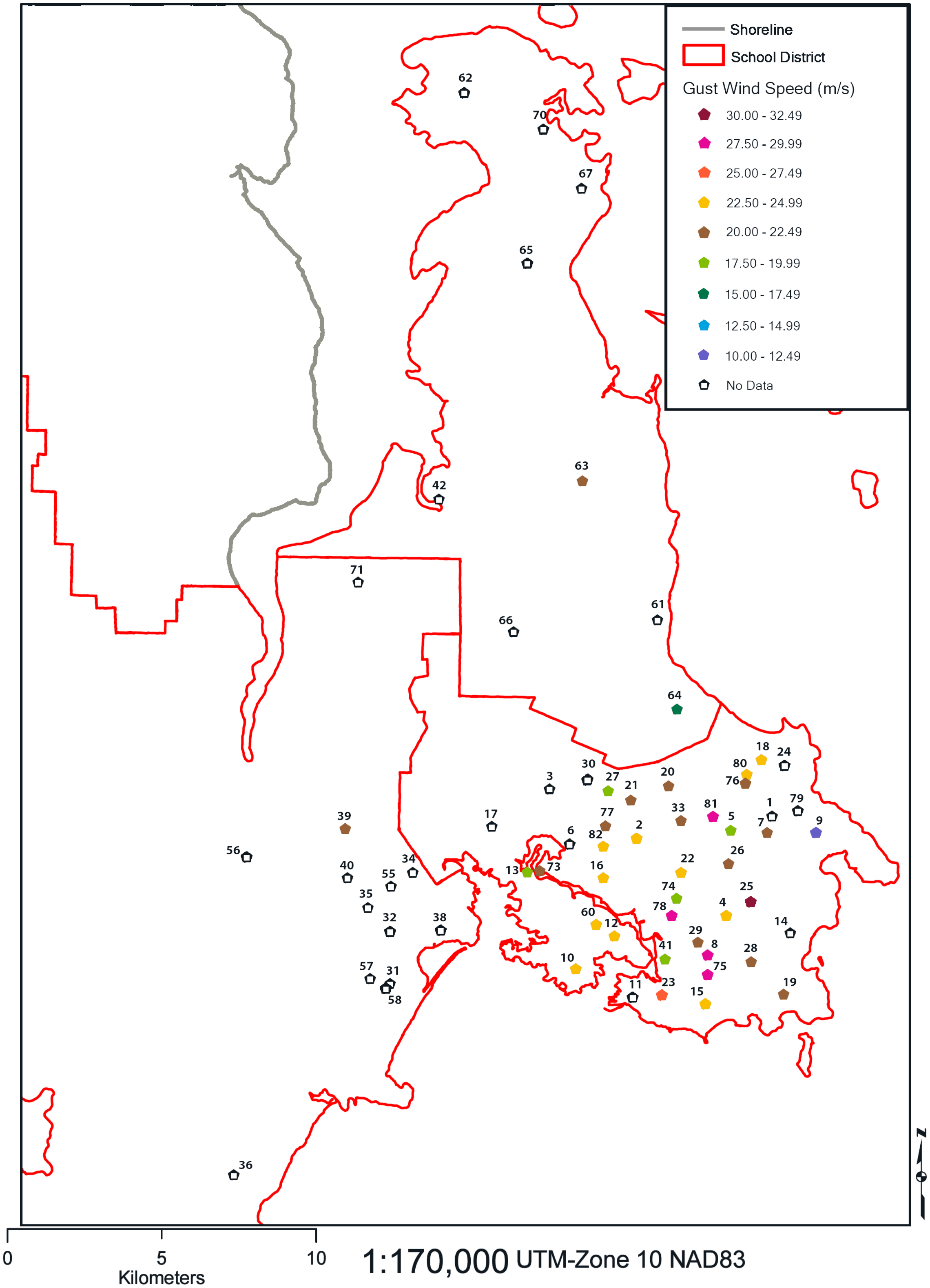

Figure 4.39: Distribution of daily maximum gust wind speed over the study area on Dec. 15, 2006 (Base map: Brendle-Moczuk 2010).

Table 4.10: Each weather station's record of mean daily maximum gust wind speed during the selected days except Dec. 15, 2006 and daily maximum gust wind speed on Dec. 15, 2006. The Stn. ID in orange, green and blue indicate weather stations in SD 61, SD 62 and SD 63, respectively.

Mean daily maximum gust wind speed (m/s) during the selected days except Dec. 15, 2006			Daily maximum gust wind speed on Dec. 15, 2006 (m/s)		
Class	Stn ID	Gust wind speed (m/s)	Class	Stn ID	Gust wind speed (m/s)
22.50-24.99	25	22.80	30.00-32.49	25	30.85
	23	22.53	27.50-29.99	8	29.06
	75	22.53		75	28.61
20.00-22.49	8	21.81		78	28.61
	6	20.83		81	28.61
	4	20.47	25.00-27.49	23	25.93
	73	20.45	22.50-24.99	2	24.59
	15	20.30		4	24.59
	22	20.30		15	24.59
	78	20.21		22	24.59
17.50-19.99	81	19.58		12	23.25
	80	19.49		10	22.8
	11	19.04		16	22.8
	16	18.89		18	22.8
	29	18.86		60	22.8
	82	18.69		80	22.8
	77	18.51		82	22.8
	34	18.51	20.00-22.49	19	22.35
	30	18.42		7	21.9
	24	18.42		29	21.9
	60	18.15		20	21.46
	2	18.03		33	21.01
	79	17.99		39	21.01
	18	17.88		63	21.01
	21	17.88		21	20.56
	10	17.79		28	20.56
	28	17.79		73	20.56
	19	17.61		77	20.56
15.00-17.49	12	17.43		26	20.12
	20	17.43		76	20.12
	40	17.25	17.50-19.99	74	19.22
	63	17.08		13	18.33
	33	16.99		5	17.88
	38	16.99		27	17.88
	76	16.90		41	17.88
	7	16.81	15.00-17.49	64	15.65
	58	16.65	10.00-12.49	9	12.07
	32	16.63	No Data	1	

	67	16.63		3	
	14	16.63		6	
	39	16.54		11	
	55	16.18		14	
	1	16.18		17	
	27	16.09		24	
	62	16.09		30	
	56	15.87		31	
	26	15.87		32	
	66	15.80		34	
	70	15.76		35	
	74	15.76		36	
	71	15.65		38	
	31	15.42		40	
	13	15.20		42	
12.50-14.99	65	14.98		55	
	5	14.84		56	
	36	14.53		57	
	61	14.42		58	
	41	14.39		61	
	3	14.31		62	
	35	14.19		65	
	64	13.86		66	
	57	13.77		67	
10.00-12.49	42	12.30		70	
	17	12.16		71	
	9	11.40		79	

4.5.5 Air density and associated climate variables

Means of air density, air temperature and air pressure measured at weather stations in each school district at the times of the valid daily maximum gust wind speed during the selected days are summarized in Table 4.11. The 20 highest station mean air densities, lowest air temperatures and greatest air pressures at the times of their daily maximum gust wind speed during the selected days are presented in Table 4.12. Because the majority of weather stations in SD 62 and SD 63 don't have valid daily maximum gust wind speed on Dec. 15, 2006 (Figure 4.39), those weather stations don't have the climate data mentioned above on that day, either. The tables provide means of actually observed air temperatures and air pressures, and of air densities calculated based on more than one observed climate variable, and the standard deviations of these means. They also provide the ranges of their values in the study area. SD 62 had highest air density, lowest air temperature and greatest air pressure as a whole among the school districts at the time of the valid daily maximum gust wind speed.

Table 4.11: District mean air density, air temperature and air pressure at the times of the valid daily maximum gust wind speed at each weather station on the selected days.

	SD 61	SD 62	SD 63
Mean air density (kg/m^3)	1.239	1.247	1.242
Standard deviation (kg/m^3)	0.012	0.014	0.013
Mean air temperature (°C)	7.16	6.19	7.21
Standard deviation (°C)	1.63	1.59	1.53
Mean air pressure (hPa)	999.8	1002.5	1001.9
Standard deviation (hPa)	6.5	7.7	6.9

Table 4.12: The 20 highest mean air densities, lowest mean air temperatures and greatest mean air pressures at the times of the valid daily maximum gust wind speed during the selected days. Orange, green and blue indicate SD 61, SD 62 and SD 63, respectively.

Air Density (kg/m^3)		Air Temperature (°C)		Air Pressure (hPa)	
Stn. ID	Mean of Air Densities (kg/m^3)	Stn. ID	Mean of Air Temperatures (°C)	Stn. ID	Mean of Air Pressures (hPa)
56	1.256	71	4.69	56	1008.1
71	1.254	36	4.79	42	1006.2
42	1.252	34	5.71	35	1006.1
35	1.252	66	5.82	71	1005.9
36	1.251	56	5.86	67	1005.0
66	1.250	74	5.97	40	1004.3
34	1.250	35	6.09	66	1003.5
40	1.249	42	6.23	62	1003.3
74	1.246	58	6.30	34	1002.7
57	1.246	40	6.31	57	1002.6
3	1.245	17	6.34	32	1002.5
58	1.245	9	6.36	41	1002.0
17	1.245	3	6.42	61	1002.0
75	1.244	31	6.43	3	1001.6
32	1.244	21	6.47	12	1001.6
79	1.243	57	6.51	70	1001.5
31	1.243	26	6.54	75	1001.5
60	1.242	75	6.57	19	1001.5
18	1.242	18	6.57	22	1001.4
29	1.242	79	6.61	24	1001.4

4.6 Wind pressure

4.6.1 Threshold wind pressure for windthrow

Threshold wind pressures for windthrow for brown earth soil, gley soil and the very vulnerable combination of site and tree stand characteristics and a certain wind climate were calculated based on Gardiner's and Quine's (2000) threshold wind speed values for overturning and stem breakage and the mean air density (1.241 kg m^{-3}) at the time of daily maximum gust wind speeds at all of the Greater Victoria weather stations during the selected strong wind days. Threshold wind pressures were 465.8 kg m^{-1} s^{-2} for brown earth soil, 351.4 kg m^{-1} s^{-2} for gley soil and 192.2 kg m^{-1} s^{-2} for the very vulnerable combination.

4.6.2 Daily maximum wind pressures observed in the study area

Although the results studied in Britain may not be applicable to windthrow in Greater Victoria, they can be considered as a rough indicator of areas susceptible to windthrow. The timing and distribution of maximum wind pressure is similar to that of the major control, wind gust speed. The 7 highest daily maximum wind pressures on each selected day were all recorded at weather stations in SD 61 (Table 4.13). The difference in magnitude between the highest daily maximum wind pressure recorded in SD 61 and that in SD 62 and SD 63 exceeds 100 kg m^{-1} s^{-2} on all the selected days. The study area, especially SD 61, had exceptionally high wind pressure on Dec. 15, 2006. On that day, 10 and 5 weather stations in SD 61 recorded wind pressure over 351.4 kg m^{-1} s^{-2} and 465.8 kg m^{-1} s^{-2}, respectively. It was the only day when the study area had station wind pressures over 465.8 kg m^{-1} s^{-2}. The highest daily maximum wind pressure in the entire study area was observed at Lansdowne Middle School (Stn. ID 25) in SD 61. It was 587.5 kg m^{-1} s^{-2}, which was greater than the threshold wind pressure of 465.8 kg m^{-1} s^{-2} for brown earth soil by approximately 120 kg m^{-1} s^{-2}. Although the total number of the weather stations with the daily maximum wind pressure over 192.2 kg m^{-1} s^{-2} in the study area is lower on Dec. 15, 2006 than that on Dec. 13, 2006, it is most likely that the total number on Dec. 15, 2006 would have exceeded that on Dec. 13, 2006 if all of the weather stations in the study area had had the valid maximum gust wind speed data.

Table 4.13: The daily maximum wind pressures which exceeded the threshold wind pressure of 192.2 kg m^{-1} s^{-2} for the very vulnerable combination of site and tree stand characteristics and a certain wind climate. Orange, green and blue indicate SD 61, SD 62 and SD 63 respectively.

The daily maximum wind pressure (DMWP) (kg m^{-1} s^{-2})											
Nov. 15		Dec. 13		Dec. 15		Jan. 9		Feb. 5		Feb. 7	
Stn. ID	DMWP	Stn. ID	DMWP	Stn. ID	DMWP	Stn. ID	DMWP	Stn. ID	DMWP	Stn. ID	DMWP
25	358.7	25	398.7	25	587.5	23	345.7	73	313.9	23	374.6
75	320.1	78	358.8	8	521.1	75	325.2	25	278.7	75	347.6
8	319.6	75	322.9	75	505.6	81	320.5	75	267.8	8	310.9
23	296.4	23	321.4	78	505.1	8	299.3	8	267.2	22	298.3
6	270.6	22	321.4	81	504.9	25	299.2	4	253.9	11	285.6
15	269.7	80	321.0	23	413.9	78	287.4	80	245.1	25	284.4
4	236.7	6	318.7	22	374.4	6	283.7	15	245.0	15	273.5
32	226.9	34	297.7	15	373.6	30	283.5	23	243.1	4	263.4
22	217.1	4	294.4	4	373.0	21	263.0	29	233.9	73	261.6
18	207.2	8	283.0	2	372.5	80	261.0	82	221.6	58	251.1
80	207.1	73	282.7	12	333.4	11	260.2	16	220.5	28	240.0
34	206.0	33	272.6	80	321.8	4	255.1	22	212.3	60	238.9
10	205.6	15	272.3	18	321.3	22	238.9	60	212.3	78	238.9
78	197.1	82	271.2	82	321.2	10	230.7	81	210.2	34	233.6
24	197.0	16	271.1	60	321.1	18	218.4	78	200.7	40	222.8
29	196.8	79	261.6	16	321.1	77	217.6	28	200.5	77	219.3
76	196.6	24	261.1	10	320.8	15	217.5	12	199.5	29	218.9
81	196.1	29	260.8	19	307.6	82	207.0			12	210.4
11	195.2	63	260.7	7	295.8	16	206.9			32	210.2
		81	260.6	29	295.2	2	206.8			19	209.9
		67	259.8	20	284.4	29	199.6			24	209.2
		77	259.2	63	272.8	65	198.8			81	208.5
		21	249.4	39	272.4	24	198.4			7	208.1
		39	239.7	33	271.6	20	198.1			82	198.5
		76	239.0	77	263.1					30	198.4
		18	238.5	73	260.5					33	198.3
		30	228.5	28	260.4					66	198.3
		2	228.0	21	259.9						
		27	227.1	76	250.0						
		20	217.1	26	249.7						
		56	208.0	74	228.3						
		58	207.8	13	207.4						
		19	207.3	5	198.9						
		11	206.9	41	197.4						
		60	206.6	27	196.4						
		14	197.9								
		28	197.4								
		12	197.4								

61	197.4

Distribution of mean daily maximum wind pressures over the study area during the selected days except Dec. 15, 2006 shows that there are 27 weather stations with mean daily maximum wind pressure equal to or above 192.2 kg m^{-1} s^{-2} but no weather station with that equal to or over 351.4 kg m^{-1} s^{-2} (Figure 4.40). The area which recorded higher mean daily maximum wind pressures than the others and might be most susceptible to windthrow is the same as that of wind speed, the south half of SD 61, especially areas south and east of downtown. Although 26 out of 43 weather stations in SD 61 had mean daily maximum wind pressure above 192.2 kg m^{-1} s^{-2}, it was only Crystal View Elementary School (Stn. ID 34) that exceeded the lowest threshold in SD 62, and there was no such weather station in SD 63. However, as already shown in Table 4.13, it does not mean that SD 62 and SD 63 are safe from the potentially damaging wind pressure. Several weather stations in these school districts had it once or more during the selected days.

On Dec. 15, 2006, most of the weather stations with daily maximum wind pressure equal to or over 351.4 kg m^{-1} s^{-2} are located in the east half of SD 61. Most of the weather stations with daily maximum equal to or over 465.8 kg m^{-1} s^{-2} are located around downtown, more specifically from its north clockwise to east of downtown (Figure 4.41). Lansdowne Middle School (Stn. ID 25), which recorded the highest daily maximum on the day, is one of them and is situated northeast of downtown.

Thus, given the observed data, the areas with the highest wind speed and gust wind speeds are most susceptible to windthrow. However, a caution should be made that these wind pressure distributions (Figures 4.40 and 4.41) contain compounded local effects of roughness sub-layer flow modification because of the squared term of gust wind speed (Equation 13).

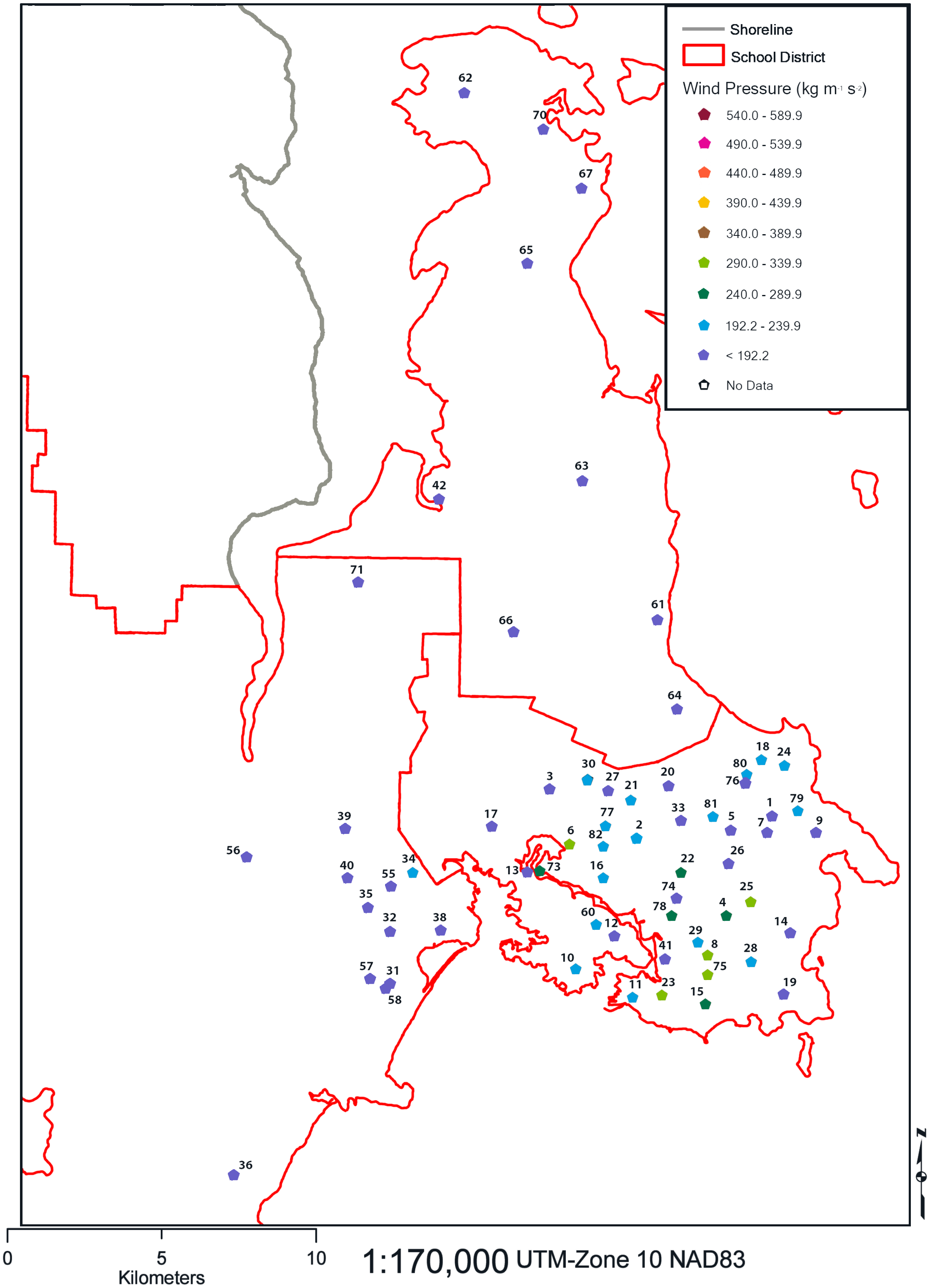

Figure 4.40: Distribution of mean daily maximum wind pressures over the study area during the selected days except Dec. 15, 2006 (Base map: Brendle-Moczuk 2010).

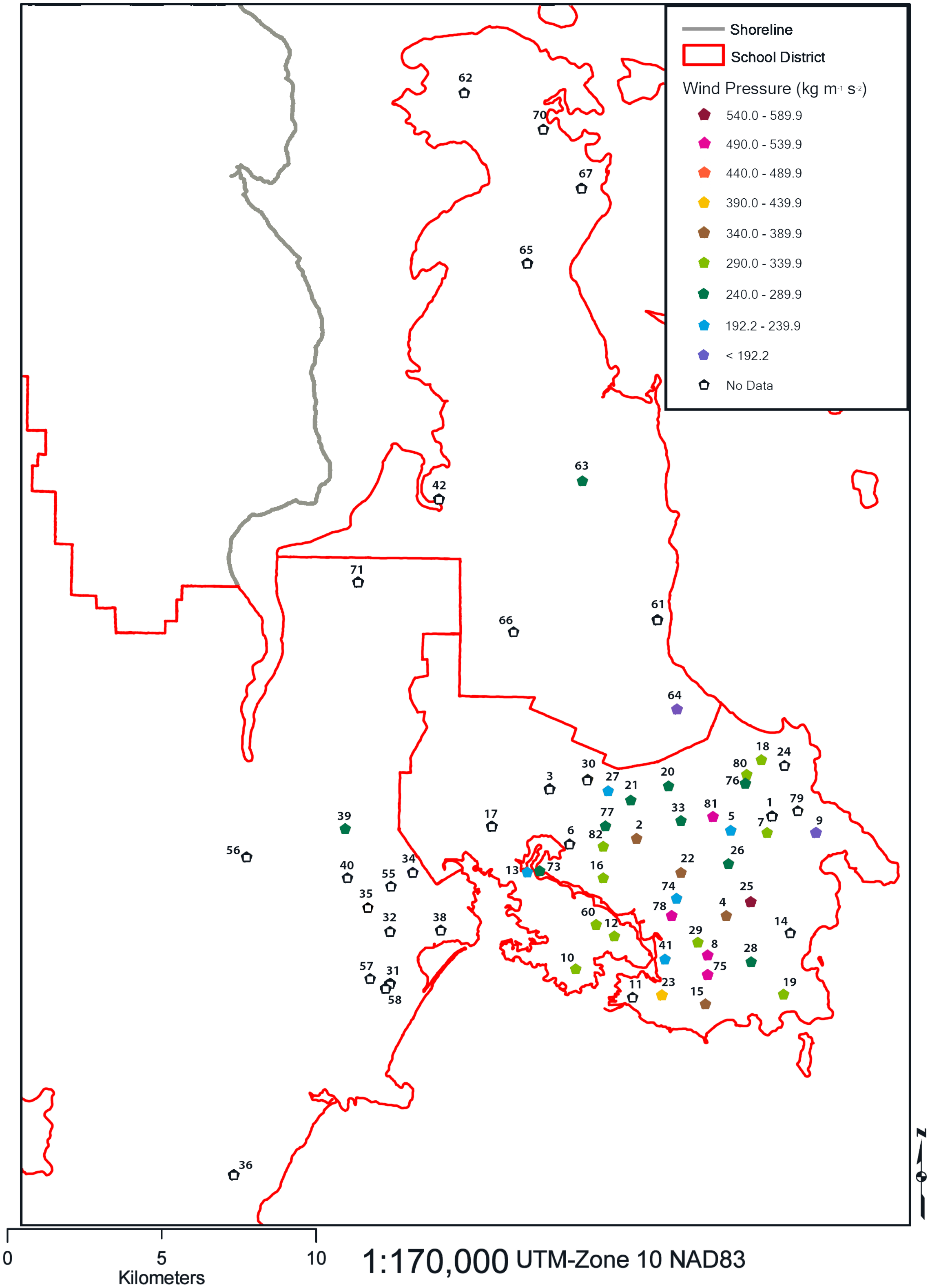

Figure 4.41: Distribution of daily maximum wind pressure over the study area on Dec. 15, 2006 (Base map: Brendle-Moczuk 2010).

4.7 Summary of some features of winds, air density and its variables and wind pressure in the study area

Change of the mean wind direction to WSW accompanied by sudden and significant increase in wind speed was found in the study area as a whole during the selected days. The magnitude of increase in mean wind speed to its daily maximum was usually highest in SD 61. The change in mean wind direction occurred slightly earlier in SD 62 and slightly later in SD 63. In addition, the mean wind direction in SD 63 tended to be more southerly than that in the other school districts.

Three patterns of change in the mean wind speed after the daily maximum during the selected days were: a sudden or gradual decrease, maintained certain speed, and recurrence of peaks with a similar magnitude after a lapse of time.

The daily maximum gust wind speeds were found both before and after the time periods of their associated daily maximum district overall mean 30-minute wind speeds in all the school districts on all the selected days.

Mean air density, air temperature and air pressure at the weather stations at the time of their valid maximum gust wind speed during the selected days were highest in SD 62, lowest in SD 62 and highest in SD 62, respectively.

The spatial distribution patterns in the study area were generally the same among overall mean 30-minute wind speeds during the selected days, mean daily maximum gust wind speed and wind pressure during the selected days except Dec. 15, 2006, and daily maximum gust wind speed and wind pressure on Dec. 15, 2006.

If the lowest threshold wind speed for windthrow based on Gardiner and Quine (2000) is considered, the area which is most susceptible to windthrow in the entire study area would be the area surrounding downtown from north clockwise to south on its east side. The secondary area would be the north and south of the Gorge Waterway and Gordon Head in SD 61. In SD 62, the most susceptible area would be the middle part of the school district, more specifically a northern half of Langford and Colwood. In SD 63, the areas would be in northern North Saanich, and around Keating Elementary School (Stn. ID 63) in the middle south of Central Saanich.

4.8 Wind characteristics of each school district and influence of topography during the daily maximum district overall mean 30-minute wind speed

4.8.1 Generalized high wind speed distribution and influence of topography among school districts

As presented earlier, different timing of change in district mean wind direction to WSW and different magnitude of resulting wind speed peak of district overall mean 30-minute wind speeds on the arrival of WSW wind were found among the school districts during the selected days (Figures 4.14, 4.15, 4.17, 4.18, 4.20, 4.21, 4.23, 4.24, 4.26, 4.27, 4.29 and 4.30). SD 62 tended to have the change in district mean wind direction earlier whereas SD 63 tended to have it later than the others. The associated initial increase in district overall mean 30-minute wind speeds was greatest in SD 61 most of the times whereas the increase in SD 63 tended to occur with less magnitude and at later time than the other school districts.

The wind directions divided into eight compass directions and their corresponding mean wind speeds during six 30-minute periods when each school district recorded daily maximum overall mean 30-minute wind speed are summarized in Table 4.14. For

December 15, 2006, the data recorded from 1:30 to 1:59 in SD 61, from 1:00 to 1:29 in SD 62, from 2:30 to 2:59 in SD 63 were used to minimize the effect of the amount of missing data. This usage of the data is the same in Tables 4.14 through 6.1. WSW wind had a high percentage occurrence and high mean wind speed in all school districts, but dominance of WSW wind is particularly notable in SD 61. The percentage occurrence and mean speed of WSW wind in SD 62 and SD 63 are more comparable to each other and much lower than those in SD 61. In addition, the distribution of wind directions in SD 62 and SD 63 spreads more around WSW. What distinguished SD 62 from the other school districts is the highest percentages of WNW and NNW winds among the school districts. On the other hand, SD 63 had the highest total percentage of winds from the south half of the compass rose. An even more noticeable feature of SD 63 in Table 4.14 would be the winds with east components. Not only was the total percentage occurrence of the winds from the east half the highest among the school districts, but also most of the mean wind speeds from the east half were the highest. It is considered that SD 63's more southerly district mean wind directions than the other school districts' shown earlier reflect this tendency of higher occurrence of winds with east components (Figures 4.14, 4.17, 4.20, 4.23, 4.26 and 4.29).

Table 4.14: Percentage and mean wind speed of each wind direction during the six 30-minute periods which recorded the daily maximum district overall mean 30-minute wind speed during the selected days (Figures 4.15, 4.18, 4.21, 4.24, 4.27 and 4.30). The units of missing data in the parentheses in each school district are minutes. MWS is mean wind speed.

Wind direction	SD 61		SD 62		SD 63	
	%	MWS (m/s)	%	MWS (m/s)	%	MWS (m/s)
NNE	0.17	2.12	0.30	2.42	0.57	3.06
ENE	0.04	2.64	0.30	1.34	1.28	2.70
ESE	0.04	2.38	1.06	1.96	3.97	3.30
SSE	0.43	4.36	4.41	3.01	9.36	3.95
SSW	15.12	7.12	27.08	5.54	31.47	6.20
WSW	71.49	8.36	49.24	5.51	45.43	5.71
WNW	12.20	7.20	15.82	5.02	6.80	4.09
NNW	0.50	2.77	1.77	3.74	1.13	2.62
Note	Missing data: Stn. 3 (30), 9 (60), 11 (22), 13 (16), 16 (30), 73 (30), 79 (30).		Missing data: Stn. 31 (32), 35 (120), 36 (35), 38 (60), 39 (30), 58 (61) 71 (30).		Missing data: Stn. 42 (30), 61 (30), 62 (26), 65 (59), 66 (33), 70 (31).	

All of these observed differences seem to relate to one or more of the geographic and topographic conditions of the study area, such as the relative location of each school district within the study area, each school district's distance from an area around the east end of the Strait of Juan de Fuca from where WSW winds come, topography of the likely paths for WSW wind to reach each school district, and topography within each school district.

SD 61 is not the school district closest to the area around the east exit of the Strait of Juan de Fuca, but its south boundary, which is located just north of the east exit, faces the sea. Because the WSW wind's path to SD 61 is much smoother than those to the other school districts, especially those directly from the sea, the speed of incoming WSW wind in SD 61 would be the greatest among the school districts (Figure 4.31; Table 4.14). In addition, the south boundary is long in the WNW-ESE direction, which is almost perpendicular to WSW wind; the area near the south boundary lacks significant relief to create large leeward areas; and relatively many weather stations are located close to the sea. Therefore, SD 61 is very sensitive to speed of WSW wind, and as a result SD 61's initial increase in its overall mean 30-minute wind speed on the arrival of WSW wind was usually greatest among the school districts. Furthermore, unlike SD 62 and SD 63, SD 61 is short in the north-south direction and has almost no prominent relief which is great enough to cause WSW wind deceleration and deviation from its direction (Figure 1.1). Thus, strong WSW wind can pass through SD 61 without losing much of its speed and direction, which led to its dominance in SD 61.

SD 62 occupies the westernmost and southernmost parts of the study area and extends toward the southwest. Therefore, the arrival of WSW wind tended to occur slightly earlier in SD 62 than the other school districts. However, SD 62 is separated from the sea in the south by a part of Metchosin, East Sooke and Sooke, which are woody and hilly and located south and southwest of the school district. Topography within SD 62, which is characterized by the most significant relief, the most wooded area with tall evergreen trees and the least plane area among the school districts, is also unfavourable for WSW wind to maintain their speed and direction. In addition, the distance between the southernmost and northernmost weather stations in SD 62 is more than twice as long as that in SD 61. The plane area in the middle of the school district where most of the weather stations are located is surrounded by many hills except for its east side which is a marine shoreline running almost parallel to WSW wind. Although the relief can create areas with high wind speeds around it, it can also produce areas with low wind speeds on lee sides. Moreover, winds can be channeled into a certain direction around the significant relief. Subsequent lower daily maximum and lower mean wind speed and occurrence of WSW wind than SD 61's (Table 4.14) resulted from WSW wind's speed loss before its arrival in SD 62 and further speed loss and deviation from its direction during a trip over the rough and complex topography within the school district. The highest percentage occurrence of strong WNW and NNW winds in SD 62 is discussed later in detail (Section 4.8.2).

SD 63, which occupies the central and north parts of the Saanich Peninsula, is located northeast of SD 62 and north of SD 61 sharing its south boundary with these school districts (Figure 1.1). The area southwest of SD 63 has prominent relief including that in SD 62. Therefore, the path of WSW wind to SD 63 is not only the longest, but also the roughest among the paths to the school districts. These are factors which caused the arrival of WSW wind and associated wind speed increase to occur later with smaller magnitude in SD 63. Both the significance and distribution of relief in the school district seem to be moderate if they are compared to those in SD 61 and SD 62. The relief created by hills is seen in the south, middle west and north areas of the school district. The wooded areas with tall evergreen trees are mainly around this relief and the lakes near the southern boundary. These high relief and wooded areas could also contribute to deviating WSW wind from its direction and lowering SD 63's mean wind speeds by providing shelter for the weather stations in their lee. However, SD 63 also has large smooth-surfaced relatively plane areas whose west and east ends are marine shorelines. Because of the mixture of relief and open plane lands readily accessible from the sea, SD 63 has areas of shelter and of deviated wind directions from WSW as SD 62 and the areas of relatively high wind speeds as SD 61. SD 63's lower occurrence of WSW wind than SD 61's and mean wind speeds comparable to SD 62's despite the longer and rougher paths to SD 63 than that to SD 62 can be attributed to these topographic features. On the other hand, the shape and topography of SD 63 seem to be favourable for the winds from the east half of the compass rose. When SD 63 was under the influence of ESE or SSE wind, its district overall mean 30-minute wind speeds tended to be much higher than those in SD 62 and could be even higher than those in SD 61, though the magnitude of the wind speeds was generally much lower than that of southwesterly winds (Figures 4.14, 4.15, 4.17, 4.18, 4.20, 4.21, 4.23, 4.24, 4.26, 4.27, 4.29 and 4.30). The higher percentage occurrences of the winds from the east half and south half of the compass rose during the six 30-minute periods which recorded the daily maximum district overall mean 30-minute wind speed are discussed later in the next section.

4.8.2 Generalized high wind speed distribution and influence of local topography within each school district

Although the overall district mean 30-minute wind speeds of SD 61 are almost always the highest among the school districts (Figures 4.15, 4.18, 4.21, 4.24, 4.27 and 4.30), unequal distribution of wind speed was found within the district (Figure 4.31). If the weather stations in the school district are divided into those in the north half and the south half, the average of the overall means of six mean 30-minute wind speeds at each weather station during the time periods of the daily maximum district overall mean 30-minute wind speeds is higher in the south half than the north half (Table 4.15). The contributing factors are closer proximity to the sea and gradually increasing elevation inland, which give better exposure to the WSW wind for the weather stations in the south half.

Within the south half of SD 61, the area with particularly high wind speed extends from north of Beacon Hill to around Lansdowne Middle School (Stn. ID 25), including the weather stations of South Park Elementary School (Stn. ID 23), Victoria High School (Stn. ID 8), Central Middle School (Stn. ID 75) and Oaklands Elementary School (Stn. ID 4) (Table 4.15; Figure 4.31). It was found that wind distribution in this area was more WSW oriented than that in the entire school district (Table 4.16). The topographic features of this area are well developed residential and business sectors, the gentle hills on the north and south of the area and slightly increasing slope toward an area around Lansdowne Middle School (Figures 1.1, 4.42 and 4.43). The increasing slope can provide better exposure to the WSW winds. In addition, these two hills on the north and south might create a little constriction for the winds flowing through the area between them, which can also increase wind speed of the area (Oke 1987). The immediate environment of these weather stations is fairly open, especially on the west side, and their anemometers are mounted on the roof of three-story buildings or equivalent so that their anemometers have great exposure to winds. Lansdowne Middle School, which recorded the highest mean wind speed most often among all the weather stations in the entire study area, has an increasing slope upward toward the school from the south and southwest, great height of the anemometer from the ground and an exceptionally large open schoolyard extending approximately 370 m from the anemometer to the southwest (Figure 4.44). Saenko (2008) also found the highest wind speeds and wind power at Lansdowne Middle School.

Table 4.15: The average of overall mean 30-minute wind speeds at the weather stations in the north and south halves of SD 61 during the daily maximum district 30-minute mean wind speeds. The weather stations are listed in descending order of their overall mean wind speeds.

Average of overall mean 30-minute wind speeds at each weather station during the daily maximum district 30-minute mean wind speeds			
North half of SD 61		South half of SD 61	
Stn. ID	Overall mean of six mean 30-min. wind speeds (m/s)	Stn. ID	Overall mean of six mean 30-min. wind speeds (m/s)
6	9.60	25	13.74
81	9.25	75	12.00
21	9.09	23	11.44
82	8.92	8	11.28
24	8.45	22	10.01
16	8.40	4	9.66
20	8.35	15	9.35
30	8.22	60	9.14
77	8.16	29	9.09
80	8.14	78	8.48
79	7.98	11	8.29
18	7.85	19	8.15
73	7.78	12	7.98
27	7.53	28	7.87
33	7.49	26	7.49
2	7.45	14	7.46
76	7.43	10	6.79
7	6.81	74	5.51
1	6.28	41	5.39
13	5.14	**Average**	**8.90**
5	4.07		
3	3.70		
9	2.65		
17	2.02		
Average	**7.11**		

Table 4.16: Percentage and mean wind speed of each wind direction in SD 61 as a whole and an area including Oakland Elementary School (Stn. ID 4), Victoria High School (Stn. ID 8), South Park Elementary School (Stn. ID 23), Lansdowne Middle School (Stn. ID 25) and Central Middle School (Stn. ID 75) during the six 30-minute periods which recorded the daily maximum district overall mean 30-minute wind speed during the selected days (Figures 4.15, 4.18, 4.21, 4.24, 4.27 and 4.30). The units of missing data in the parenthesis are minutes. MWS is mean wind speed.

Wind direction	SD 61		Oakland (Stn. 4), Victoria (Stn. 8), South Park (Stn. 23), Lansdowne (Stn. 25), Central (Stn. 75)	
	%	MWS (m/s)	%	MWS (m/s)
NNE	0.17	2.12	0.00	-
ENE	0.04	2.64	0.00	-
ESE	0.04	2.38	0.00	-
SSE	0.43	4.36	0.89	9.47
SSW	15.12	7.12	10.11	10.39
WSW	71.49	8.36	85.67	11.84
WNW	12.20	7.20	3.33	10.51
NNW	0.50	2.77	0.00	-
Note	Missing data: Stn. 3 (30), 9 (60), 11 (22), 13 (16), 16 (30), 73 (30), 79 (30).		Missing data: 0.	

Figure 4.42: Weather stations with high wind speeds in SD 61. The values of latitude, longitude and elevation in the bottom of the image are not any of the weather stations' (Google Earth 2011b). The information regarding the weather stations was added by the author of this study.

Figure 4.43: Topographic map of southeastern SD 61. The middle part of the map is the high wind speed area. Map Scale 1: 50,000 (Natural Resources Canada, 2010b). The names of the weather stations were added by the author of this study.

Figure 4.44: Lansdowne Middle School and its vicinity. The orange pin indicates the anemometer location. The values of latitude, longitude and elevation in the bottom of the image are not the weather station's (Google Earth 2011c). The information regarding the weather station was added by the author of this study.

Willows Elementary School (Stn. ID 14) is located at the north end of a south corridor parallel to the high wind speed area mentioned above (Figure 1.1). However, the average of overall mean 30-minute wind speed at the weather station is much lower than that at the weather stations in the high wind speed area (Table 4.15). It is considered that tall trees just southwest of the anemometer mitigated wind speed.

In terms of the secondary high wind speed areas in SD 61, such as north and south of the Gorge Waterway and the north and northeast of the school district, there is difference in elevation within each area (Figure 1.1). Most of the weather stations in these areas are located on windward slopes relative to the dominant WSW wind. Major causes of high wind speeds in these areas were elevation above some of the upwind surface roughness and acceleration of the wind on the windward slopes.

The complex topography with great relief within SD 62 and its vicinity is sufficient enough to change the direction of the dominant WSW wind. SD 62 recorded the highest percentage occurrence of strong WNW and NNW winds among the school districts during the six 30-minute periods which recorded the daily maximum district overall mean 30-minute wind speed during the selected days (Table 4.17). However, it was found that this tendency was not common for all weather stations in SD 62 (Table 4.18). The weather station that had this tendency most significantly was Willway Elementary School (Stn. ID 56) (Table 4.17). The percentage occurrence of WNW wind in the entire SD 62 was 15.82 % and of NNW wind was 1.77 %. Willway Elementary School had 7.00 % out of the 15.82 % of occurrence of WNW wind and 1.12 % out of the 1.77 % of occurrence of NNW wind. The weather station is located in a relatively small plane area, which is elongated in a NW-SE direction. The plane area is surrounded by relief which exceeds 300 m above sea level except for its southeast end, which meets a larger plane area. The Goldstream River running through a valley goes toward the weather station from WNW. Then the river turns north near the weather station and enters Finlayson Arm, flowing between Wolf Hill in the west and Skirt Mountain in the east. Although a well developed plane area of Langford and Colwood is located to the southeast to the weather station, the most frequent wind direction at the weather station was overwhelmingly WNW followed by NNW. It indicates that the valley where the

Goldstream River runs channeled winds into the WNW and NNW directions recorded at the weather station (Figures 4.45 and 4.46).

Table 4.17: Percentage and mean wind speed of each wind direction at Willway Elementary School in SD 62 during the six 30-minute periods which recorded the daily maximum district overall mean 30-minute wind speed during the selected days (Figures 4.15, 4.18, 4.21, 4.24, 4.27 and 4.30). The units of missing data are minutes. MWS is mean wind speed.

Wind direction	SD 62		Willway (Stn. 56)	
	%	MWS (m/s)	%	MWS (m/s)
NNE	0.30	2.42	0.56	5.81
ENE	0.30	1.34	0.00	-
ESE	1.06	1.96	0.00	-
SSE	4.41	3.01	0.00	-
SSW	27.08	5.54	0.00	-
WSW	49.24	5.51	10.56	4.46
WNW	15.82	5.02	76.67	5.16
NNW	1.77	3.74	12.22	4.20
Note	Missing data: Stn. 31 (32), 35 (120), 36 (35), 38 (60), 39 (30), 58 (61) 71 (30).		Missing data: 0.	

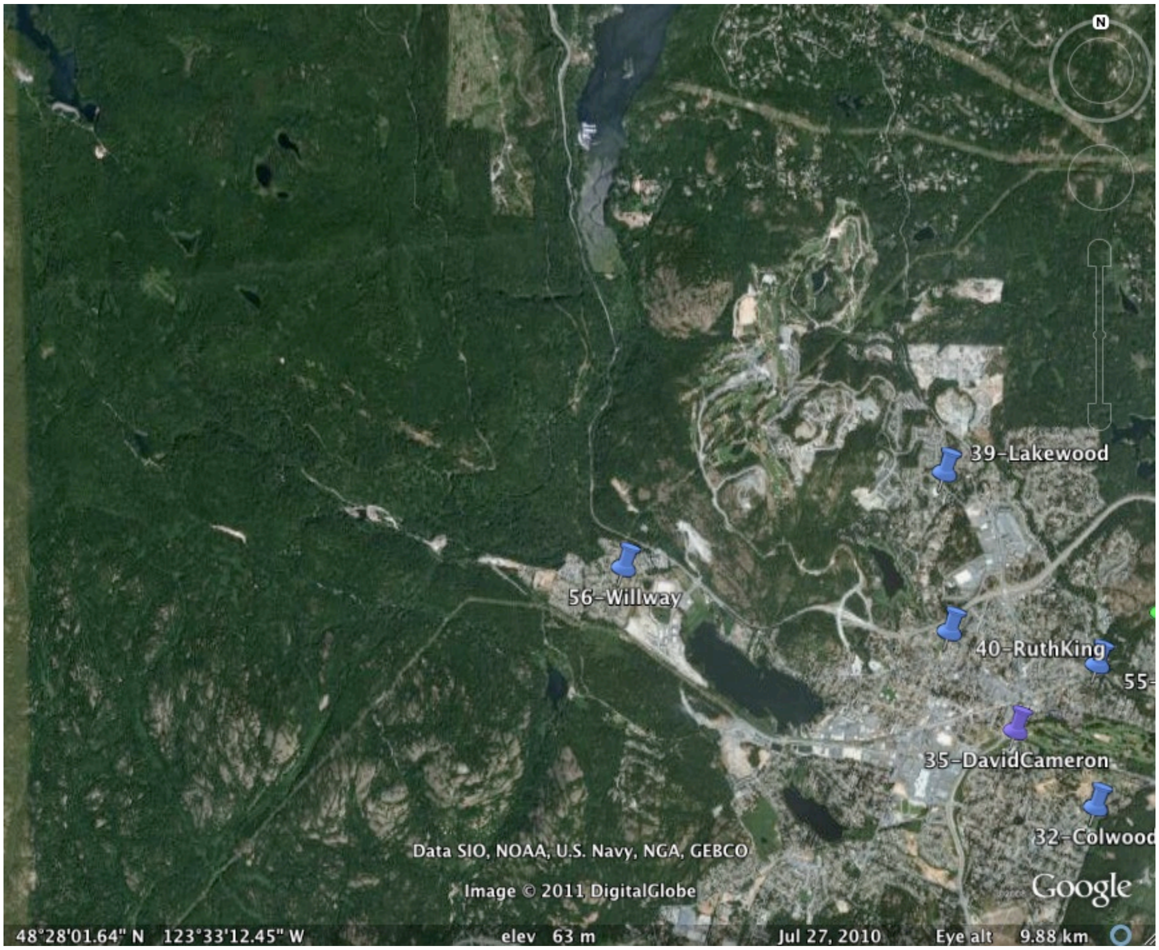

Figure 4.45: Willway Elemenatry School and its vicinity. The values of latitude, longitude and elevation in the bottom of the image are not the weather station's (Google Earth 2011d). The information regarding the weather stations was added by the author of this study.

Figure 4.46: Topographic map of Willway Elemenatry School and its vicinity. The name of the river under the north arrow is 'Goldstream River.' Map Scale 1: 45,000 (Natural Resources Canada 2010c). The names of the weather station and Skirt Mountain were added by the author of this study.

Numerous hills, mountains and wooded areas occupying most of SD 62 could make it difficult for the school district to have an area with relatively homogeneous wind speed and direction similar to the one in SD 61. Three highest and 2nd and 4th lowest overall mean 30-minute wind speeds in the entire SD 62 were found in and around the relatively plane area of Langford and Colwood in the middle east of SD 62 where most of the weather stations are located (Figure 1.1; Table 4.9). This area faces the sea in the east and southeast but is surrounded by hills in the north, west and southwest. The weather stations which recorded the three highest overall wind speeds are Dunsmuir Middle School (Stn. ID 58), Ruth King Elementary School (Stn. ID 40) and Crystal View Elementary School (Stn. ID 34). Winds at these weather stations were affected by different topographic features around them. For example, Dunsmuir Middle School in the south of the plane area had high speed winds which came exclusively from the WSW and SSW directions with the highest occurrence from the WSW in spite of the schoolyard in the ESE, the low open land in the south and the proximity of the sea to the east (Figure 4.47). Because there is no particular feature that would be able to orient winds only to the WSW and SSW directions around the immediate environment of the weather station, it is most likely that a small hill to the WSW of the weather station was related to these winds. The small hill is a part of a major relief which is situated to the southwest of the plane area. This major relief includes Braemar Heights and Triangular Hill, and the small hill located at the southeast end of the major relief (Figures 1.1 and 4.48). The east side of the small hill is approximately NE-SW oriented steep relief whose elevation exceeds the weather station's by at least 59 m (Table A1). Thus, it is considered that while air was flowing around the steep relief, it was accelerated and directed toward the weather station as WSW or SSW wind.

Table 4.18: Percentage and mean wind speed of each wind direction at Dunsmuir Middle School (Stn. ID 58), Ruth King Elementary School (Stn. ID 40) and Crystal View Elementary School (Stn. ID 34) in SD 62 during the six 30-minute periods which recorded the daily maximum district overall mean 30-minute wind speed during the selected days (Figures 4.15, 4.18, 4.21, 4.24, 4.27 and 4.30). The units of missing data are minutes. MWS is mean wind speed.

Wind direction	Dunsmuir (Stn. 58)		Ruth King (Stn. 40)		Crystal View (Stn. 34)	
	%	MWS (m/s)	%	MWS (m/s)	%	MWS (m/s)
NNE	0.00	0.00	0.00	-	0.00	-
ENE	0.00	0.00	0.00	-	0.00	-
ESE	0.00	0.00	0.00	-	0.00	-
SSE	0.00	0.00	0.00	-	0.00	-
SSW	19.33	7.67	0.56	9.39	90.00	6.94
WSW	80.67	7.16	83.33	7.04	10.00	7.00
WNW	0.00	-	16.11	7.24	0.00	-
NNW	0.00	-	0.00	-	0.00	-
Note	Missing data: 61.		Missing data: 0.		Missing data: 0.	

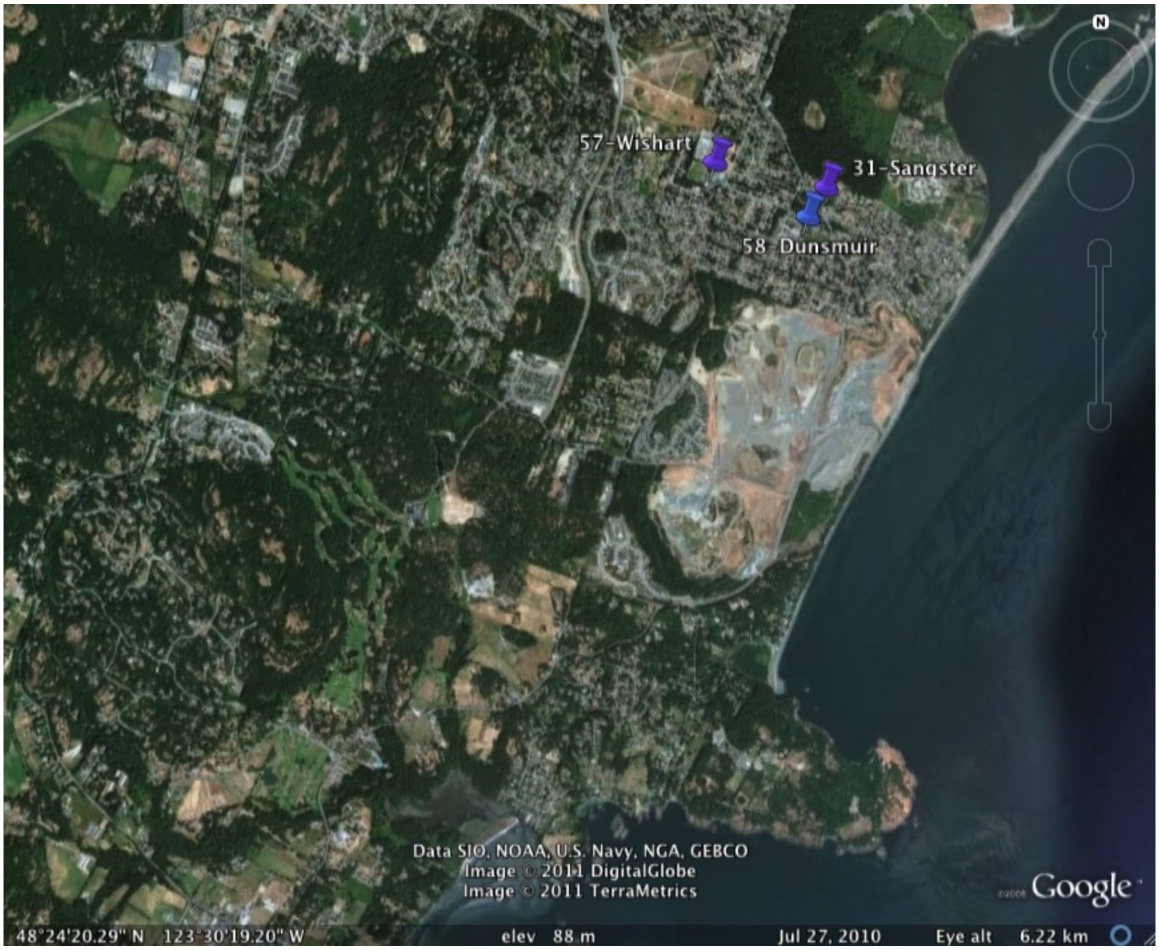

Figure 4.47: Dunsmuir Middle School, Sangster Elementary School, Wishart Elementary School and their vicinity. The values of latitude, longitude and elevation in the bottom of the image are not any of the weather stations' (Google Earth 2011e). The information regarding the weather stations was added by the author of this study.

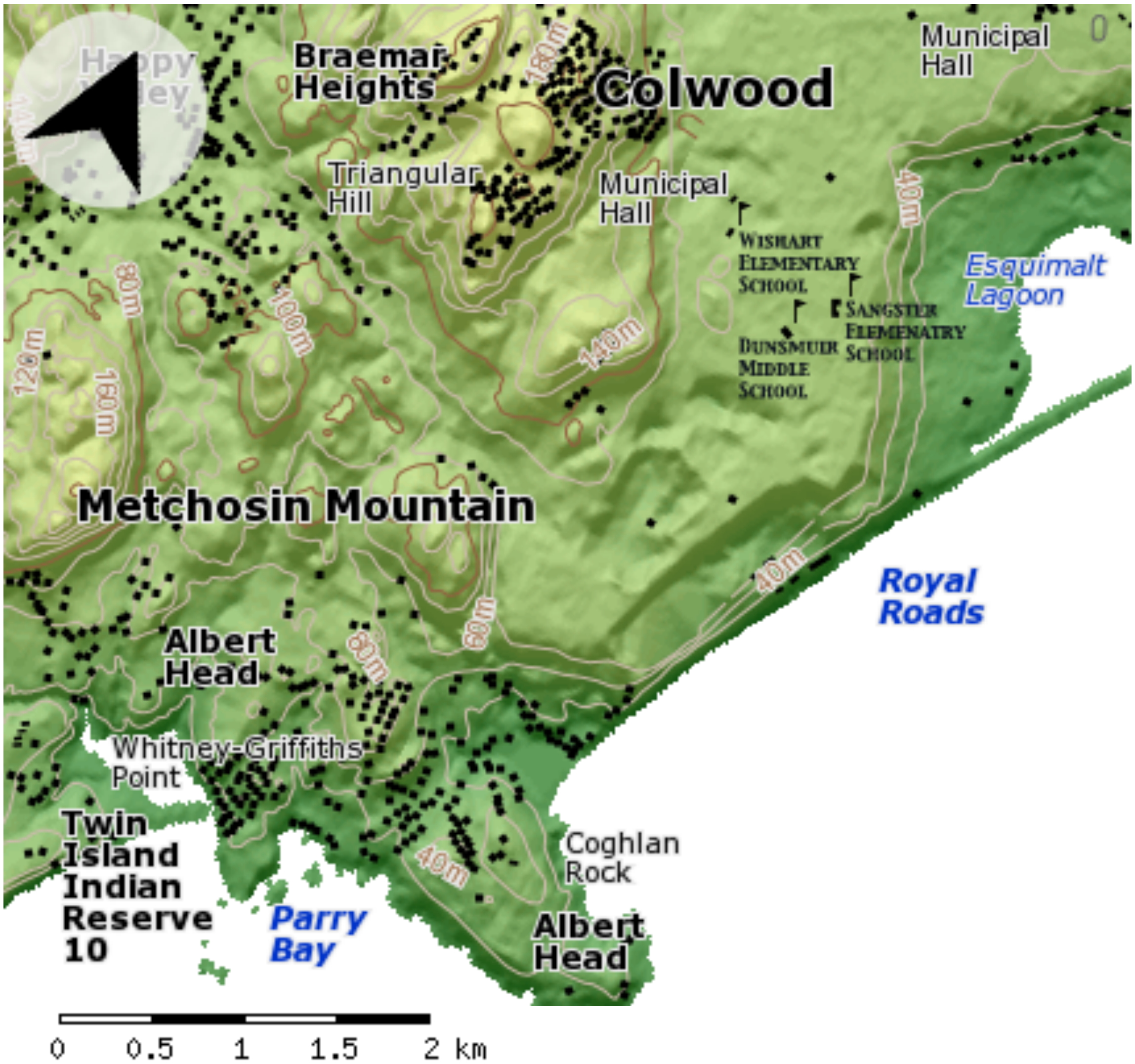

Figure 4.48: Topographic map of Dunsmuir Middle School and its vicinity. Map Scale 1: 40,000 (Natural Resources Canada, 2010d). The names of the weather stations were added by the author of this study.

A major topographic feature which contributed to high wind speeds at Ruth King Elementary School (Stn. ID 40) seems to be a constriction of hills. The weather station is located in the northwest of the plane area (Figures 1.1 and 4.49), and main wind directions found at the weather station are WSW and WNW, but the latter was much less frequent than the former (Table 4.18). There are two valleys whose exits are located to the southwest of the weather station. One between Skirt Mountain and Mount Wells has a NW-SE axis whereas the other between Mount Wells and Braemar Heights has a NE-SW axis, which is close to parallel to the dominant wind direction over the study area. The accelerated airflow through the constriction of Mount Wells and Braemar Heights spreads at the exit, and some of the spread airflow together with some other spread airflow from the constriction of Skirt Mountain and Mount Wells reached the weather station as WSW wind flowing along the relief northwest of the plane area (Figure 1.1). The less frequent WNW wind with even higher speed than WSW wind also seems to have come through a constriction of Skirt Mountain and a small hill just south of the mountain. Goldstream Avenue running toward the weather station from the WSW direction and the wide Island Highway from WNW through the constriction of Skirt Mountain and a small hill would help to maintain speed of some WSW wind before it reached the weather station, providing smoothly surfaced paths to the weather station (Figure 4.50). Some airflows passing through the weather station could enter other constrictions among hills northeast of the weather station and increase their speeds. In terms of the immediate environment around the weather station, there are a large schoolyard, which extends clockwise from the SSW through NNE directions on the west side of the school building, and relatively low density residential blocks on the west side of the schoolyard. There are no walls of tall evergreen trees or buildings to effectively screen the WSW and WNW winds. Therefore, roughness of the area around the weather station can be considered relatively low.

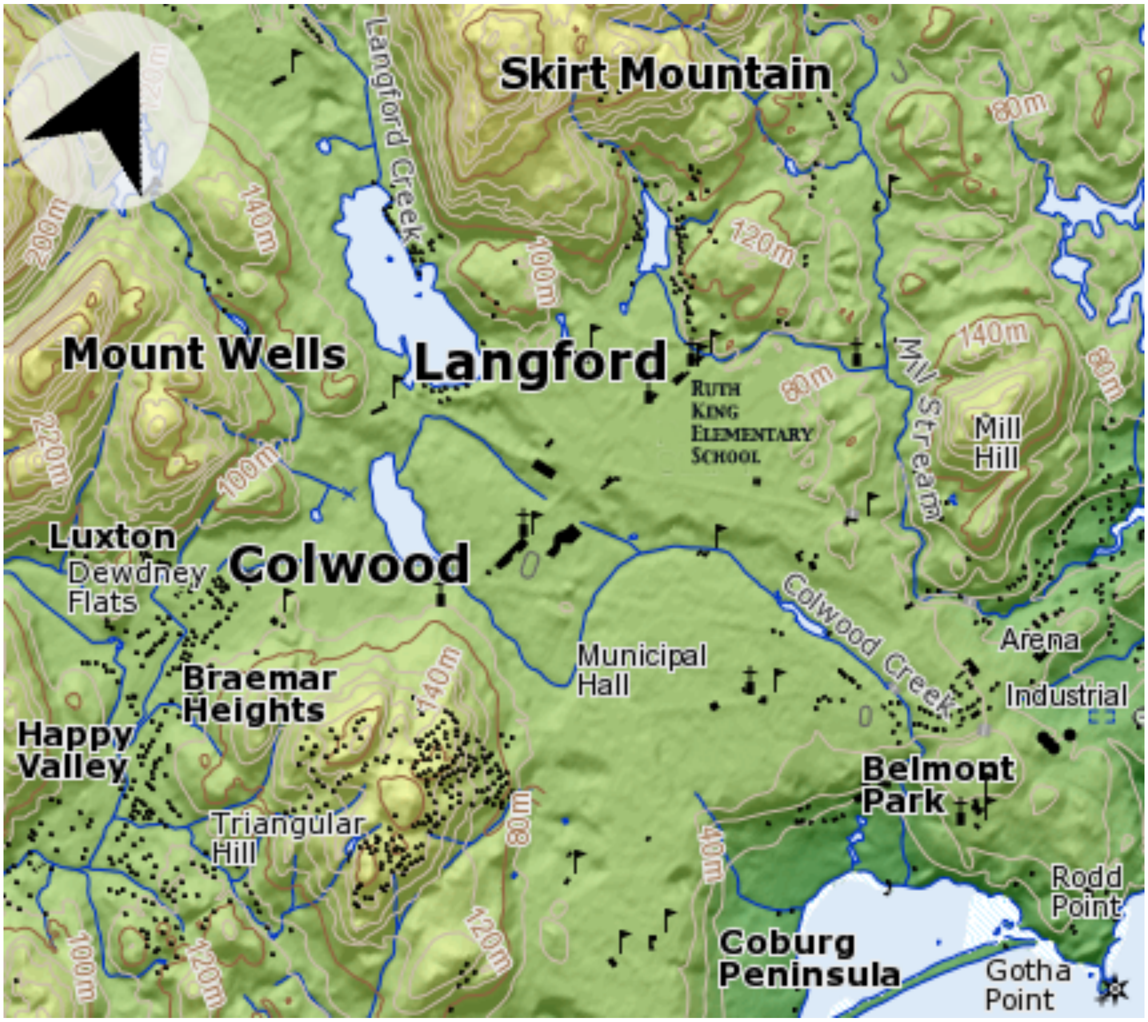

Figure 4.49: Topographic map of Ruth King Elementary School and its vicinity. Map Scale 1: 50,000 (Natural Resources Canada, 2010e). The name of the weather station was added by the author of this study.

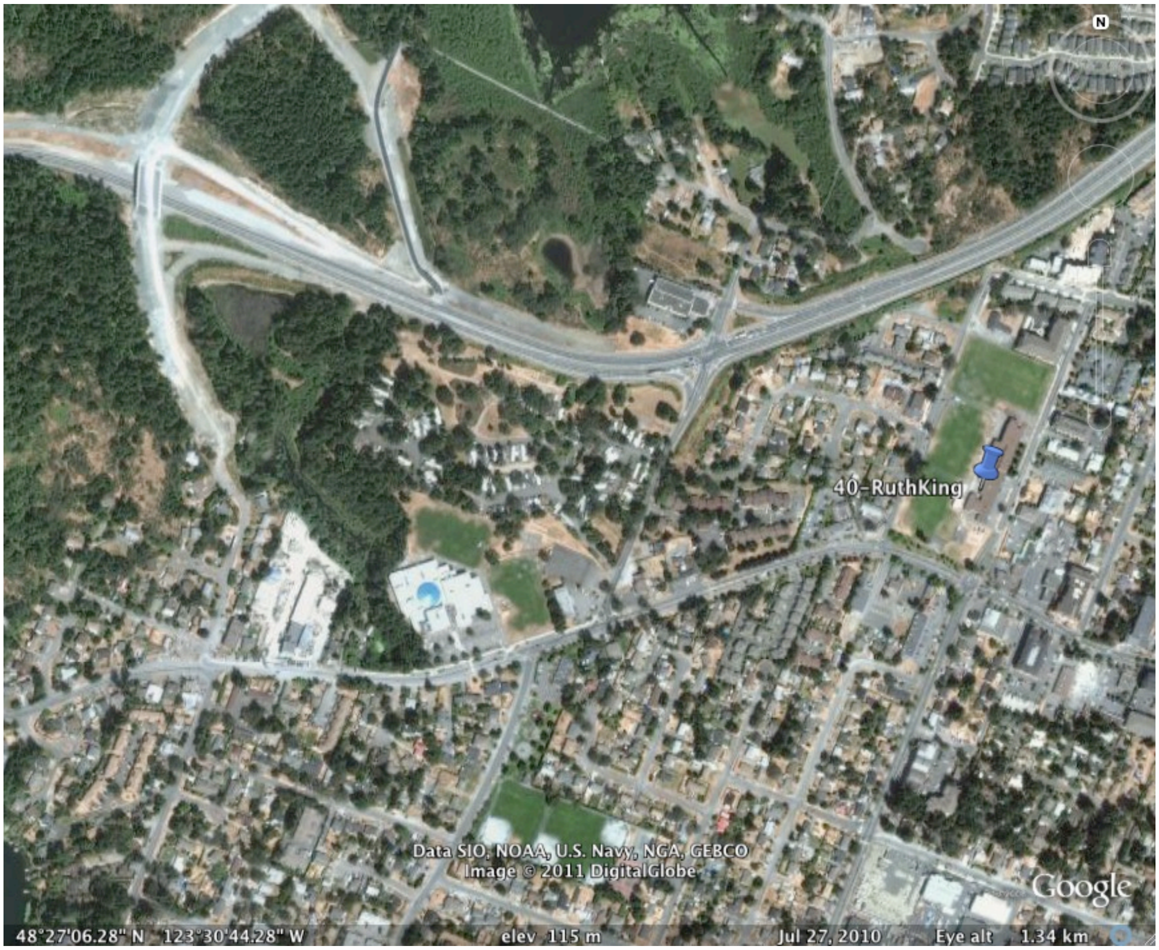

Figure 4.50: Ruth King Elementary School and its vicinity. The values of latitude, longitude and elevation in the bottom of the image are not the weather station's (Google Earth 2011f). The information regarding the weather station was added by the author of this study.

The topographic feature responsible for the high wind speed at Crystal View Elementary School (Stn. ID 34) is considered to be a windward slope location. The windward slope location outweighed high surface roughness to the WSW giving high and frequent wind speeds from the WSW and SSW (Table 4.18).

The weather stations which contributed most to SD 63's higher occurrence of the winds from the east half of the compass rose than the other school districts during six 30-minute periods when each school district recorded daily maximum overall mean 30-minute wind speed are Butchart Gardens (Stn. ID 42) near the southwest shoreline, Lochside Elementary School (Stn. ID 64) near the southeast shoreline, and Parkland Secondary School (Stn. ID 70) near the northeast shoreline (Tables 4.19 and 4.21). The occurrence of winds with east components at the first two weather stations is significant, and it was caused by local relief.

Table 4.19: Percentage and mean wind speed of each wind direction at Butchart Gardens (Stn. ID 42) and Lochside Elementary School (Stn. ID 64) in SD 63 during the six 30-minute periods which recorded the daily maximum district overall mean 30-minute wind speed during the selected days (Figures 4.15, 4.18, 4.21, 4.24, 4.27 and 4.30). The units of missing data are minutes. MWS is mean wind speed.

Wind direction	SD 63		Butchart Gardens (Stn. 42)		Lochside (Stn. 64)	
	%	MWS (m/s)	%	MWS (m/s)	%	MWS (m/s)
NNE	0.57	3.06	5.33	3.06	0.00	-
ENE	1.28	2.70	12.00	2.70	0.00	-
ESE	3.97	3.30	36.00	3.36	1.11	1.56
SSE	9.36	3.95	20.00	3.18	38.33	3.58
SSW	31.47	6.20	10.00	3.24	41.67	3.51
WSW	45.43	5.71	5.33	3.53	15.56	3.30
WNW	6.80	4.09	4.67	3.53	3.33	1.83
NNW	1.13	2.62	6.67	3.08	0.00	-
Note	Missing data: Stn. 42 (30), 61 (30), 62 (26), 65 (59), 66 (33), 70 (31).		Missing data: 30.		Missing data: 0.	

In SD 63, the area with high wind speeds was found to be the open and almost plane area between the relief created by Cloake Hill and Horth Hill at the north end of the Saanich Peninsula and Mt. Newton a little northwest of the centre of the school district. The area is a mixture of agricultural, residential and industrial land use, and Victoria International Airport occupies a large part of the middle south of this area. Sidney Elementary School (Stn. ID 67), Parkland Secondary School (Stn. ID 70) and Deep Cove Elementary School (Stn. ID 62) are located in the east and north of this area (Figures 4.51 and 4.52). The observed wind distribution in this high wind speed area features a high percentage occurrence of SSW wind (Table 4.20). However, if the winds are analyzed at each weather station, it is clear that the winds in this area are not homogeneous (Table 4.21). The dominance of SSW wind in both percentage occurrence and speed was greatest at Sidney Elementary School (Stn. ID 67) in the east of this area. At Parkland Secondary School (Stn. ID 70) north-northwest of Sidney Elementary School, the impact of dominant SSW wind was less because of its slightly lower mean speed than that at Sidney Elementary School and more inflow of winds from other directions. The dominance of SSW wind disappeared at Deep Cove Elementary School (Stn. ID 62) in the northwest. On the other hand, the percentage occurrence and speed of WSW wind increased from Sidney Elementary School to Parkland Secondary School to Deep Cove Elementary School where WSW wind became dominant. However, the mean speed of WSW wind at Deep Cove Elementary School was lower than that of SSW wind at Sidney Elementary School and Parkland Secondary School. The relative location of Mt. Newton to Sidney Elementary School and Parkland Secondary School and its shape (Figure 1.1) suggest that the winds flowing around Mt. Newton reached these schools as SSW wind. An isolated hill such as Mt. Newton could increase speed of airflow not only on its windward slope, but also around its sides (Oke 1987). In addition, very smooth surface of the sea on the west side and smooth surface of agricultural areas on the east side of Mt. Newton could facilitate the acceleration. The higher occurrence and wind speed of SSW wind at Sidney Elementary School than these at Parkland Secondary School can be attributed to its shorter distance from Mt. Newton, less obstacles on the wind's path to Sidney Elementary School (Figure 4.51), slightly higher elevation (Table A1) and greater anemometer height. Furthermore, air flowing up Haro Strait from the south may have contributed to the more southerly wind direction at Sidney Elementary School and Parkland Secondary School. The relatively strong WSW wind at Deep Cove Elementary School is most likely to have come from Saanich Inlet because of the weather station's proximity to the sea in the west. It is considered that the winds from Saanich Inlet increased their speed over the slope upward toward the weather station. In addition, Deep Cove Elementary School is located between small hills northwest and east of the school, so the winds could further increase their speed in the constriction between these hills. In terms of the wind direction, some southerly winds from Saanich Inlet might have become WSW while flowing around the south-facing relief of the hill immediately northwest of the school (Figures 1.1 and 4.52).

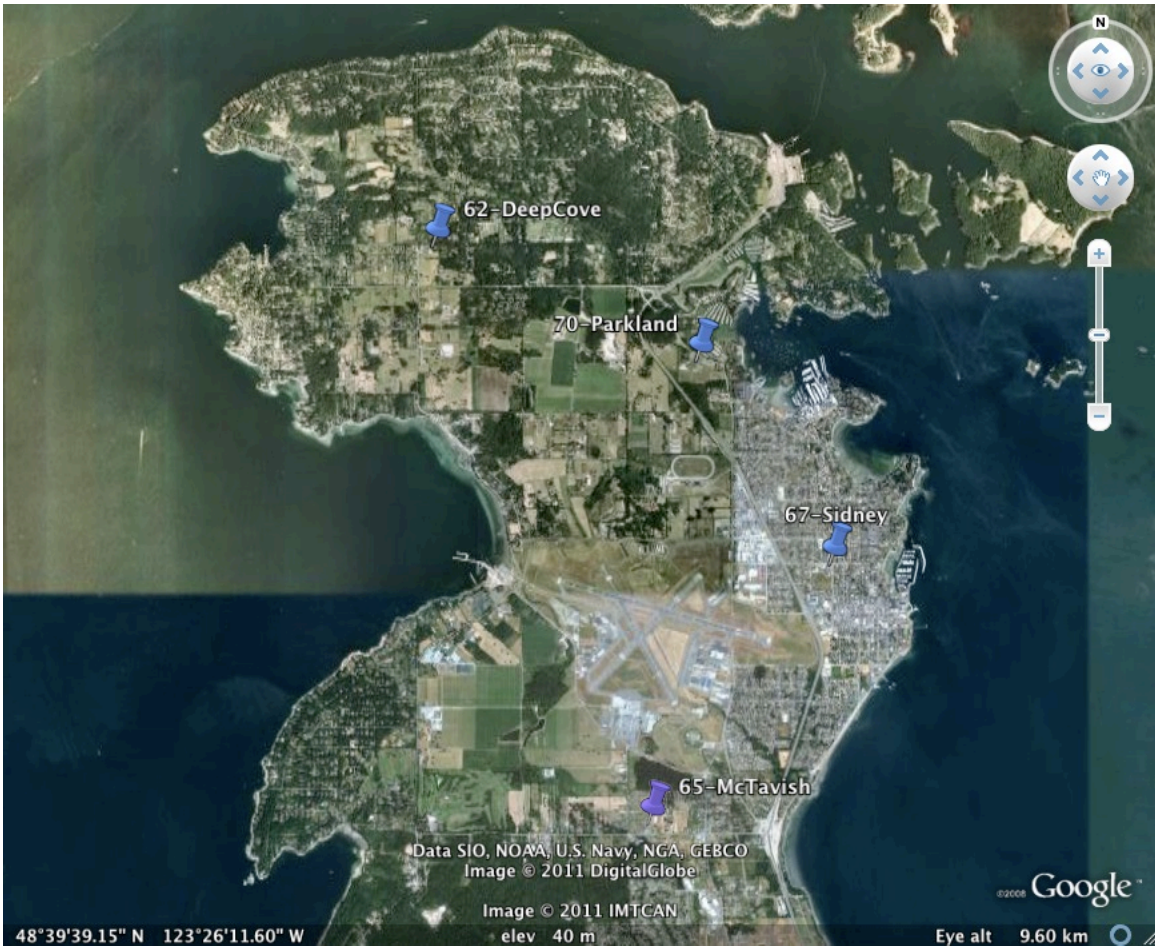

Figure 4.51: Northern part of SD 63 which includes a high wind speed area. The values of latitude, longitude and elevation in the bottom of the image are not any of the weather stations' (Google Earth 2011g). The information regarding the weather stations was added by the author of this study.

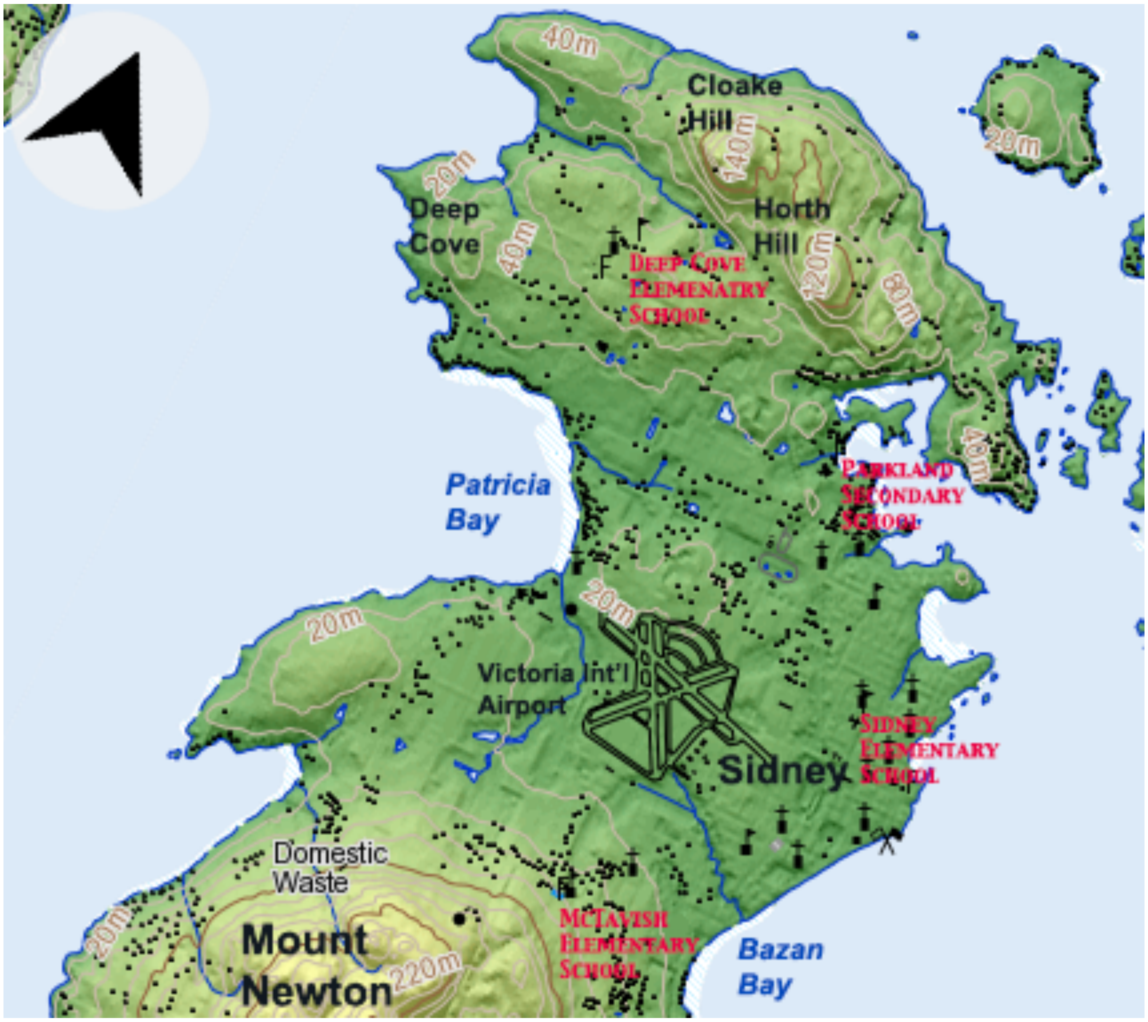

Figure 4.52: Topographic map of the northern part of SD 63 which includes a high wind speed area. Map Scale 1: 70,000 (Natural Resources Canada, 2010f). The names of the weather stations and of major topographic features were added by the author of this study.

Table 4.20: Percentage and mean wind speed of each wind direction in an area including Deep Cove Elementary School (Stn. ID 62), Sidney Elementary School (Stn. ID 67) and Parkland Secondary School (Stn. ID 70) during the six 30-minute periods which recorded the daily maximum district overall mean 30-minute wind speed during the selected days (Figures 4.15, 4.18, 4.21, 4.24, 4.27 and 4.30). The units of missing data are minutes. MWS is mean wind speed.

Wind direction	Deep Cove (Stn. 62), Sidney (Stn. 67) and Parkland (Stn. 70)	
	%	MWS (m/s)
NNE	0.00	-
ENE	0.00	-
ESE	0.00	-
SSE	5.80	5.96
SSW	51.35	7.77
WSW	39.54	6.16
WNW	3.11	4.76
NNW	0.21	1.12
Note	Missing data: Stn. 62 (26), 70 (31).	

Table 4.21: Percentage and mean wind speed of each wind direction at Deep Cove Elementary School (Stn. ID 62), Sidney Elementary School (Stn. ID 67) and Parkland Secondary School (Stn. ID 70) during the six 30-minute periods which recorded the daily maximum district overall mean 30-minute wind speed during the selected days (Figures 4.15, 4.18, 4.21, 4.24, 4.27 and 4.30). The units of missing data are minutes. MWS is mean wind speed.

Wind direction	Deep Cove (Stn. 62)		Sidney (Stn. 67)		Parkland (Stn. 70)	
	%	MWS (m/s)	%	MWS (m/s)	%	MWS (m/s)
NNE	0.00	-	0.00	-	0.00	-
ENE	0.00	-	0.00	-	0.00	-
ESE	0.00	-	0.00	-	0.00	-
SSE	0.00	-	1.67	7.06	16.78	5.82
SSW	4.55	6.29	82.78	8.07	61.74	7.40
WSW	87.01	6.66	15.56	4.72	19.46	5.25
WNW	7.79	4.94	0.00	-	2.01	4.06
NNW	0.65	1.12	0.00	-	0.00	-
Note	Missing data: 26		Missing data: 0.		Missing data: 31.	

4.9 Summary of wind characteristics of each school district and influence of topography during the daily maximum district overall mean 30-minute wind speed

The generalized regional high wind speed distribution among the school districts and the generalized high wind speed distribution within each school district were described in light of the local topography. The observed temporal difference in the significant increase in district mean 30-minute wind speed on the arrival of WSW wind among the school districts was connected to relative location of the school districts within the study area. In addition, difference in the magnitude of increase in district mean 30-minute wind speed on the arrival of WSW wind and of its subsequent daily maximum among the school districts were generally consistent with the difference in distance from the south-facing shoreline to the weather stations and a degree of relief and surface roughness in the WSW wind's paths to each school district and within each school district. All of the high wind speed areas in the school districts had topographic features that could accelerate winds around the weather stations, such as a windward slope relative to southwesterly winds, a constriction of hills, steep relief and an isolated hill. In addition, smooth surface and great height of anemometer also seemed to contribute to the high wind speeds. The high occurrence of WNW and NNW winds in SD 62 and of winds with an east component in SD 63 resulted from deviation of winds caused by local topography around a few weather stations and not the general tendency of the other weather stations in these school districts. A caution is that the multitude of differences in the local environment of the anemometers on and around the schools means the spatial variations of wind speed are valid only for the particular schools and particular wind direction and not the entire area around the school and all wind directions.

Chapter 5

Discussion

This chapter presents some key points of this study and their practical implications. Most wind damage studies don't have as high spatial and temporal resolutions as does the School-Based Weather Station Network. Therefore, there are few studies which are similar to this preliminary study, and most of the new information on wind characteristics of the Greater Victoria area provided in this study is attributed to the resolution of the Network.

5.1 Effects of topography on wind speed and direction

Important contributions of this study are the presentation of temporal and spatial distributions of high speed winds and their possible causes. Topography of the Greater Victoria area is rich in variation, including sea, lakes, hills and various land use, such as residential, commercial, forest and agricultural. Moore (1958) and Stamp (1966) indicate that topography in its original and comprehensive meaning includes not only relief but also all the natural and human produced features on the surface. Therefore, it is quite insufficient to understand wind characteristics of the whole area relying just on the data from a few weather stations. The Network provided 65 stations located in different topography. Because of the uncontrolled environment, the Network data might be influenced by many things. However, the wind distribution of the Greater Victoria area made it possible to see some influence of certain topographic features around the weather stations on local winds with observed numerical values. The effects of these features are basically well known (Nägeli 1946 in Oke 1987; Davidson *et al*. 1964; van Eimern *et al.* 1964; Geiger 1965; Watts 1965; Munn 1970; Page 1976; Landsberg 1981; WMO 1981; Taylor and Lee 1984; Hosker 1985; Oke 1987; ASHRAE 1989; Geiger *et al.* 1995; Wieringa *et al.* 2001; Walker and Nickling 2002; Mertens 2003; Walker and Hesp 2013). This study showed that the weather stations with high wind speeds in the Greater Victoria area can be explained by the effects of these topographic features around them. In addition, although Chilton's study (1973) on air pollution potential estimated directions of very light winds within the Greater Victoria area based on relief and presented them with arrows, the Network's observed numerical values of wind direction at 65 sites helped to find wind directions significantly different from the regional wind direction at a few weather stations near steep relief (Tables 4.17 and 4.19; Figure 4.46). Therefore, the assumption that the spatial wind distribution is affected by local topographic features including weather station conditions was proved to be true. Observed numerical differences between highest and lowest wind speeds within the Greater Victoria area are also new and useful information to estimate the approximate range of wind speed within the Greater Victoria area under the influence of the same mid-latitude cyclones (Table 4.9). Although there are numerous studies which show effects of relatively large scale topographic features on regional winds (Colle and Mass 1998; Saaroni *et al*. 1998; Klink 1999; Colle and Mass 2000; Zhong *et al*. 2008), this study is rather unique because of its attempt to explain spatial variation in regional high wind speed distributions associated with mid-latitude cyclones over a relatively small area based on various local topographic features around the weather stations.

One of the practical implications of the findings of this study is that it alerts people to look at the topography around them and its relation with winds more closely. Knowing what topographic features are around, from which direction wind might come and how much wind speed could increase under the influence of mid-latitude cyclones would make it easier for residents to prepare for the windstorms and minimize damage. Municipality and utility staff would also benefit from the findings because they could focus on the most vulnerable areas. BC Hydro, the telephone company and cable company are also vulnerable and would benefit from this knowledge. In order to protect the community, there are many things they can do with the new knowledge. For example, they can prioritize the areas which need special attention regarding wind damage and trim or remove trees (EmergeX Planning 2006) and repair facilities that were already damaged. The knowledge of potential for high wind speeds and their direction also aids planning, building design and evaluation of land use change.

5.2 Diurnal mean wind speed, daily maximum gust wind speed and air density

The diurnal pattern of school district mean wind speeds had multiple peaks before or after the primary peak (Figures 4.15, 4.18, 4.21, 4.24, 4.27 and 4.30). Although there are not many wind studies which analyze change in wind speed during a day under the influence of mid-latitude cyclones, the similar multiple peaks were found in Poland during a period between 2002 and 2007 (Wieclaw-Michniewska and Piotrowicz 2011). This finding has an important implication in wind damage perspective. The decrease in wind speed before or after the primary peak does not guarantee that wind speed keeps on decreasing. There is a possibility that wind regains its speed to reach similar or greater magnitude to damage an object already weakened by the wind during the previous or primary peak.

The observed values and temporal distribution of gust wind speed demonstrated in this study are not only new, but also important knowledge especially when wind damage is concerned (Figures 4.32 through 4.37). Hofherr and Kunz (2010) stated that gust wind plays a decisive role in damaging vulnerable structures, such as buildings and forest stands. Penwarden (1973) suggested that when wind speed reached 17.2 m s^{-1} to 20.7 m s^{-1}, pedestrians start feeling great difficulty with balance in gusts. Lopes *et al.* (2008) also reported that the timing of peak occurrences of tree fall agreed with that of maximum gust. This study showed that the daily maximum gust wind speed at a weather station could occur before or after the daily maximum 30-minute mean wind speed in the area around the weather station (Figures 4.32 through 4.37; Table 4.10).

The implication of this finding is similar to the case of multiple diurnal wind speed peaks, but the maximum gust might be more strongly related to wind damage. This knowledge would help people including repair and cleanup personnel reconsider the safe time to go outside. Despite the importance of gusts on wind damage, Hofherr and Kunz (2010) also admitted mesoscale numerical models' inability to produce realistic gust wind speed near the surface. If relative magnitude of gust wind speeds and their spatial distribution in the Greater Victoria area are the same as that of overall mean wind speeds and their distribution, the overall mean wind speeds could give a good indication for gust wind speeds. However, Figures 4.31, 4.38 and 4.39 showed that it might not be the case. Pashardes and Christofides (1995) found that spatial distributions of the highest mean hourly wind speed and the highest gust wind speed with a period of 2 seconds were similar but not the same in Cyprus. Thus, having gust wind speed is another benefit of the Network data. If more gust wind data are collected in the Network, the observed data and their distribution will allow better assessment of the impact of windstorms, determination of gust wind factors (the ratio of the maximum gust wind speed to the mean wind speed over a particular time period), gust wind speed for certain return periods and the development of numerical models (Goyette *et al.* 2003; Campbell 2005; Hofherr and Kunz 2010).

Air density is rarely discussed in wind damage studies. Although air density is included in the equation of wind pressure (Equation 13) and wind power, its actual values are frequently neglected (Golding 1955; Johnson 1985; Ahmed Shata and Hanitsch 2006; Belu and Koracin 2009; Keyhani *et al*. 2010). It is a minor control of wind pressure, and variation in air density at each weather station is much smaller than that of winds (Table 4.12). For example, the highest and lowest air densities in the Greater Victoria area during the selected days are 1.275 kg m^{-3} at Cal Revelle Nature Sanctuary (Stn. ID 71) on Feb. 5, 2008 and 1.211 kg m^{-3} at Parkland Secondary School (Stn. ID 70) on Nov. 15, 2006, respectively. The difference between them is only 0.064 kg m^{-3}. On the other hand, the highest and lowest daily maximum gust wind speeds are 30.85 m s^{-1} at Lansdowne Middle School (Stn. ID 25) on Dec. 15, 2006 and 9.83 m s^{-1} at Butchart Gardens (Stn. ID 42) on Feb. 5, 2008, respectively. Therefore, the difference in their squares for wind pressure calculation becomes 855.1 m^2 s^{-2}. These actually observed data confirm that the assumption of studies that do not incorporate time and space variations in air density is justifiable. However, a precise value of wind pressure requires a good reliable value of air density for quantitative studies. In addition, the knowledge of air density distribution would contribute to in-depth understanding of wind pressure characteristics in an area. Although air density does not vary much within a small area, the difference among areas could be noticeable (Table 4.11). Differences could also be greater among seasons or regions of a country (Belu and Koracin 2009). The Network gives data of gust wind speed, air temperature, air pressure and humidity, which allows relatively easy calculation of air density and wind pressure at the time when those data were recorded. These data can become a database for the wind pressure in complex terrain.

5.3 Synoptic and mesoscale atmospheric conditions and near surface winds

The storms observed during the selected days acted like those given in general textbooks (Ahrens 1988; Lutgens and Tarbuck 1989; Moran and Morgan 1994; Aguado and Burt 2004; Mass 2008). Forecasts have been getting better in predicting a high wind speed event, even though they might error on the actual magnitude. What is needed now is how wind speed and direction vary within a region with complex topography. This study presented valuable spatial variation in Greater Victoria for six winter storms. It provided data for mesoscale and smaller area models to be tested and improved.

5.4 Missing data

Missing data were a problem. Although the Davis system lists an upper limit of 67 m s^{-1} for the anemometer (Table 3.1), some of the systems cut out at speeds that were likely well below this. The problem could be in the sensors or data transmission systems and could be a result of wind, rain, or other causes. Thus, very robust equipment needs to be selected for projects investigating severe windstorms.

Chapter 6

Conclusion

The purpose of this study was to investigate the spatial and time patterns of wind speed, wind direction, wind pressure, and air density and its variables in the Greater Victoria area associated with winter mid-latitude cyclones based on climate data from the School-Based Weather Station Network during a total of 6 selected days in the winters of 2006, 2007 and 2008.

i. Brief analysis of upper air conditions conformed with accepted theory. The storms had regions of pronounced upper air divergence allowing large pressure gradients and high wind speeds at the surface.

ii. Sudden increase in wind speed and change in wind direction to WSW accompanied by the passage of a cold or an occluded front were observed. Multiple wind speed peaks before or after the primary wind speed peak and daily maximum gust wind speeds before or after the primary peak were found.

iii. The effects of spatial variation in air density and its controls within the Greater Victoria area was determined to be negligible in the variations of wind pressure and hence in general assessments of the spatial variation in wind damage potential in the local area.

iv. The highest wind speed and wind pressure area, therefore, the most susceptible area for windthrow was identified as the area surrounding the downtown on its east side and extending to Lansdowne Middle School (Stn. ID 25) where multiple topographic features favourable to high wind speed exist, such as close proximity to the south facing shoreline, gentle relief, large open space and great anemometer height.

Besides the results stated above, the following findings were made. The regional winds over the Greater Victoria area on the case study days were determined by two major mesoscale factors. One is the air circulation around the cyclone centre, and the other is the Strait of Juan de Fuca. When the mid-latitude cyclones pass north to the Greater Victoria area, the air circulation over the Greater Victoria mainly became southerly. Even if it was northwesterly, the Strait of Juan de Fuca channeled northwesterly winds entering the strait into southerly or southwesterly winds. These southerly winds, especially WSW wind, caused by air circulation around the cyclone centre and topographic forcing turned out to have greater speeds than the winds from any other directions. The effects of local topography on wind direction and speed were also observed. More deviation of wind direction from dominant WSW wind was found in SD 62 and SD 63 than in SD 61 presumably due to the effects of local relief on winds around a few weather stations in SD 62 and SD 63. In addition, SD 61, which is in close proximity to the south-facing shoreline, recorded higher district mean wind speed than the other school districts most of the time. Thus, although forecasting of severe storms is generally good, this study showed that actual resulting wind speeds and directions could vary greatly with local topography.

Although the spatial resolution of the Network was exceptionally high, it did not cover all areas with potentially high wind speeds and damage potential. For example, a relatively open and plane area between Keating Elementary School (Stn. ID 63) and Mt. Newton seems to be a potentially high wind speed area because of the fairly high wind speeds at Keating Elementary School and windward slopes and constriction of hills in the middle of this area and around the south half of Mt. Newton. Wind speeds in this area are considered to be similar to or even higher than those in the high wind speed area in the north (Table 6.1).

Table 6.1: Percentage and mean wind speed of each wind direction in an area including Deep Cove Elementary School (Stn. 62), Sidney Elementary School (Stn. 67) and Parkland Secondary School (Stn. 70) and at Keating Elementary School (Stn. 63) in SD 63 during the six 30-minute periods which recorded the daily maximum district overall mean 30-minute wind speed during the selected wind days (Figures 4.15, 4.18, 4.21, 4.24, 4.27 and 4.30). The units of missing data are minutes. MWS is mean wind speed.

Wind direction	SD 63		Deep Cove (Stn. 62), Sidney (Stn. 67) and Parkland (Stn. 70)		Keating (Stn. 63)	
	%	MWS (m/s)	%	MWS (m/s)	%	MWS (m/s)
NNE	0.57	3.06	0.00	-	0.00	-
ENE	1.28	2.70	0.00	-	0.00	-
ESE	3.97	3.30	0.00	-	0.00	-
SSE	9.36	3.95	5.80	5.96	0.00	-
SSW	31.47	6.20	51.35	7.77	7.78	5.68
WSW	45.43	5.71	39.54	6.16	90.56	7.03
WNW	6.80	4.09	3.11	4.76	1.67	7.33
NNW	1.13	2.62	0.21	1.12	0.00	-
Note	Missing data: Stn. 42 (30), 61 (30), 62 (26), 65 (59), 66 (33), 70 (31).		Missing data: Stn. 62 (26), 70 (31).		Missing data: 0.	

The Network data used in this study produced credible results, which were consistent with the change in mesoscale atmospheric conditions and exhibited the influence of weather stations' site location conditions. Thanks to the ever-expanding

Network and its accumulating climate data, numerous research opportunities are provided. In terms of the research opportunities associated with the topic of this study, more accurate and general distribution of strong winds during the winter storms can be studied utilizing the spatially and temporally greater number of samples. Other areas with potentially high wind speeds can be investigated. A gust factor can be calculated. Following Mass and Ferber (1990) and Ferber and Mass (1990), close examination of air pressure data during winter wind storms might reveal general or various patterns of pressure perturbation by the interaction between the surface low pressure systems and regional topography of the Greater Victoria area, which in turn would give more insight into the distributions of strong winds. Storms that go south of Victoria and the influence of change in configuration of mesoscale surface pressure systems on winds over the Greater Victoria area can also be investigated.

As with other climate variables, winds can be both a resource and force of destruction. Therefore, it is important to know their origin, relation with local topography, and influence on people's lives. It is hoped that this study becomes the beginning of many fruitful studies on winds over Greater Victoria.

References

Aguado, E and J. E. Burt. 2004. *Understanding Weather and Climate*, 3rd ed. Pearson: New Jersey, 560 pp.

Ahmed Shata, A. S. and R. Hanitsch. 2006. Evaluation of wind energy potential and electricity generation on the coast of Mediterranean Sea in Egypt. *Renewable Energy*, 31, 1183-1202.

Ahrens, C. D. 1988. *Meteorology Today: An Introduction to Weather, Climate, and the Environment*, 3rd ed. WEST: San Francisco, 582 pp.

ASHRAE (American Society of Heating Refrigerating and Air-Conditioning Engineers). 1989. Airflow Around Buildings. In 1989 *ASHRAE handbook: fundamentals*. American Society of Heating Refrigerating and Air-Conditioning Engineers, Inc.: Atlanta.

BC Hydro. 2007. BC Hydro winter storm report, October 2006-January 2007. BC Hydro and BCUC (B.C. Utilities Commission), Technology Report, 2007. [Online]. Available: http://www.bchydro.com/etc/medialib/internet/documents/info/pdf/news_winter_storm_report_october_2006_january_2007.Par.0001.File.news_winter_storm_report_october_2006_january_2007.pdf

Belu, R. and D. Koracin. 2009. Wind characteristics and wind energy potential in western Nevada. *Renewable Energy*, 34, 2246-2251.

Brasseur, O. 2001. Development and application of a physical approach to estimating wind gusts. *Monthly Weather Review*, 129, 5-25.

Brendle-Moczuk, D. "Study area and weather stations" [map]. 1:170000. 092B [raster digital data]. Dataset: 1.1 Metadata: 2. Sherbrooke, Quebec, Canada: Government of Canada, Natural Resources Canada, Centre for Topographic Information, 1999-04-28. Using: ESRI. ArcMap 10.0 [GIS software]. 10.0. Redlands, CA: ESRI. 2010. Modified by M. Matsuda. Using Adobe® Photoshop® CS6 EXTENDED [PSD software]. 13.0 x64. San Jose, CA: Adobe Systems Incorporated. 1990-2012.

Campbell, S. 2005. *The History of wind damage in Hong Kong*. Wind Engineering Research Centre, Graduate School of Engineering, Tokyo Polytechnic University: Japan, 37 pp.

Chien, F.-C., C. F. Mass, and P. J. Neiman. 2001. An observational and numerical study of an intense landfalling cold front along the northwest coast of the United States during COAST IOP 2. *Monthly Weather Review*, 129, 934-955.

Chilton, R. R. 1973. Climate summary for Greater Victoria region. In Stanley-jones, C. V. and Benson, W. A., editors, *An Inventory of Land Resources and Resource Potentials in the Capital Regional District*, British Columbia Land Inventory, Pacific Forestry Research Centre, Canadian Forestry Service Soil Survey Section and Canada Department of Agriculture: Victoria, British Columbia, 5-21.

Colle, B. A. and C. F. Mass. 1996. An observational and modeling study of the interaction of low-level southwesterly flow with the Olympic Mountains during COAST IOP 4. *Monthly Weather Review*, 124, 2152-2175.

Colle, B. A. and C. F. Mass. 1998. Windstorms along the western side of the Washington Cascade Mountains. Part I: A high-resolution observational and modeling study of the 12 February 1995 Event. *Monthly Weather Review*, 126, 28-52.

Colle, B. A. and C. F. Mass. 2000. High-resolution observations and numerical simulations of easterly gap flow through the Strait of Juan de Fuca on 9-10 December 1995. *Monthly Weather Review*, 128, 2398-2422.

Colle, B. A., C. F. Mass, and B. F. Smull. 1999. An observational and numerical study of a cold front interacting with the Olympic Mountains during COAST IOP5. *Monthly Weather Review*, 127, 1310-1333.

Davidson, B., N. Gerbier, S. D. Papagianakis and P. J. Rijkoort. 1964. Sites for wind-power installations. WMO Technical Note No. 63, WMO - No. 156. TP. 76.

Davis, R. S. 1992. Equation for the determination of the density of moist air (1981/91). *Metrologia,* 29, 67-70.

Davis Instruments. Wireless Vantage Pro2™ & Vantage Pro2™ Plus Stations, including Fan-Aspirated Models. http://www.davisnet.com/product_documents/weather/spec_sheets/6152_62_53_63_SS.pdf Last accessed, January 12, 2012.

Doyle, J. D. and N. A. Bond. 2001. Research aircraft observations and numerical simulations of a warm front approaching Vancouver Island. *Monthly Weather Review*, 129, 978-998.

EmergeX Planning Inc. 2006. *Hazard risk and vulnerability assessment city of Victoria final report March 2006.* EmergeX Planning Inc.: Vancouver.

Environment Canada. 2007. http://www.ec.gc.ca/default.asp?lang=En&n=FD9B0E51-1 Last accessed, 2007.

Environment Canada. 2011a. National climate data and information archive. Station results. http://climate.weatheroffice.gc.ca/advanceSearch/searchHistoricDataStations_e.html?searchType=stnProx&timeframe=1&txtRadius=50&optProxType=city&selCity=48%7C25%7C123%7C22&selPark=&txtCentralLatDeg=&txtCentralLatMin=&txtCentralLatSec=&txtCentralLongDeg=&txtCentralLongMin=&txtCentralLongSec=&optLimit=yearRange&StartYear=1840&EndYear=2012&Month=1&Day=15&Year=2012&selRowPerPage=25&cmdProxSubmit=Search Last Accessed, January 16, 2012.

Environment Canada. 2011b. Weather and meteorology – Glossary. http://www.ec.gc.ca/meteo-weather/default.asp?lang=En&n=B8CD636F-1&def=hide16E8FB9DE#wsDTB1A0A996 Last accessed, January 16, 2012.

ESRL (Earth System Research Laboratory). 2012. Physical Science Division, Monthly/Seasonal Climate Composite, http://www.esrl.noaa.gov/psd/cgi-bin/data/composites/printpage.pl Last accessed, Feb. 14, 2012.

Ferber, G. K. and C. F. Mass. 1990. Surface pressure perturbations produced by an isolated mesoscale topographic barrier. Part II: Influence on regional circulations. *Monthly Weather Review*, 118, 2597-2606.

Gardiner, B. A. and C. P. Quine. 2000. Management of forests to reduce the risk of abiotic damage — a review with particular reference to the effects of strong winds. *Forest Ecology and Management*, 135, 261-277.

Geiger, R. 1965. *The climate near the ground*. Harvard University: Cambridge, 625 pp.

Geiger, R., R. H. Aron and P. Todhunter. 1995. *The climate near the ground*, 5th edition. Vieweg: Braunschweig, Germany, 528 pp.

Giacomo P. 1982. Equation for the determination of the density of moist air (1981). *Metrologia,* 18, 33-40.

Golding, E. W. 1955. *The generation of electricity by wind power*. E.&F. N. Spon: London.

Google Earth. 2011a. "Locations of the low pressure centres at 500 hPa around the time of daily maximum overall mean 30-minute wind speeds" [satellite image]. *Google Earth* [computer satellite image]. 4.3.7204.0836 (beta). Mountain View, CA:

TerraMetrics Inc. 2011 and Cnes/Spot Image Inc. 2011. Modified by M. Matsuda. 2012. Using the information from NCEP (The National Centers for Environmental Prediction). 2012. SRRS Analysis and Forecast Charts, http://nomads.ncdc.noaa.gov/ncep/NCEP

Google Earth. 2011b. “Weather stations with high wind speeds in SD 61” [satellite image]. *Google Earth* [computer satellite image]. 4.3.7204.0836 (beta). Mountain View, CA: DigitalGlobe Inc. 2011. Modified by M. Matsuda. 2011.

Google Earth. 2011c. “Lansdowne Middle School and its vicinity” [satellite image]. *Google Earth* [computer satellite image]. 4.3.7204.0836 (beta). Mountain View, CA: DigitalGlobe Inc. 2011. Modified by M. Matsuda. 2011.

Google Earth. 2011d. “Willway Elemenatry School and its vicinity” [satellite image]. 4.3.7204.0836 (beta). Mountain View, CA: DigitalGlobe Inc. 2011. Modified by M. Matsuda. 2011.

Google Earth. 2011e. “Dunsmuir Middle School, Sangster Elementary School, Wishart Elementary School and their vicinity” [satellite image]. *Google Earth* [computer satellite image]. 4.3.7204.0836 (beta). Mountain View, CA: DigitalGlobe Inc. 2011 and TerraMetrics Inc. 2011. Modified by M. Matsuda. 2011.

Google Earth. 2011f. “Ruth King Elementary School and its vicinity” [satellite image]. *Google Earth* [computer satellite image]. 4.3.7204.0836 (beta). Mountain View, CA: DigitalGlobe Inc. 2011. Modified by M. Matsuda. 2011.

Google Earth. 2011g. “Northern part of SD 63 which includes a high wind speed area” [satellite image]. *Google Earth* [computer satellite image]. 4.3.7204.0836 (beta). Mountain View, CA: DigitalGlobe Inc. 2011 and IMTCAN Inc. 2011. Modified by M. Matsuda. 2011.

Google Maps. 2014a. “A weather station mounted on the roof of Central Middle School (Stn. ID 75)” [street map]. Retrieved on Feb. 3, 2014 from https://maps.google.ca

Google Maps. 2014b. “Central Middle School indicated by “A” is located near Victoria’s urban core” [satellite image]. Cnes/Spot Image, DigitalGlobe, Landsat and USDA Farm Service Agency. 2014. Retrieved on Feb. 3, 2014 from https://maps.google.ca

Google Maps. 2014c. “A weather station mounted on the roof of Sangster Elementary School (Stn. ID 31)” [street map]. Retrieved on Feb. 3, 2014 from https://maps.google.ca

Google Maps. 2014d. “Sangster Elementary School indicated by “A” is located in a residential area” [satellite image]. Cnes/Spot Image, DigitalGlobe and USDA Farm Service Agency. 2014. Retrieved on Feb. 3, 2014 from https://maps.google.ca

Google Maps. 2014e. “A weather station mounted on the roof of Deep Cove Elementary School (Stn. ID 62)” [street map]. Retrieved on Feb. 3, 2014 from https://maps.google.ca

Google Maps. 2014f. “Deep Cove Elementary School indicated by “A” is located in a rural area” [satellite image]. Cnes/Spot Image, DigitalGlobe, IMTCAN and USDA Farm Service Agency. 2014. Retrieved on Feb. 3, 2014 from https://maps.google.ca

Government of Canada, Natural Resources Canada, Centre for Topographic Information. 1999. 092B [raster digital data] Dataset: 1.1 Metadata: 2. “Weather station elevation.” [table]. Generated by D. Brendle-Moczuk. Using: ESRI. ArcMap 10.0 [GIS software]. 10.0. Redlands, CA: ESRI. 2010. (May 2010).

Goyette, S., O. Brasseur and M. Beniston. 2003. Application of a new wind gust parameterisation; multi-scale case studies performed with the Canadian RCM. Journal of Geophysical Research, 108, 4371–4389.

Hofherr, T. and M. Kunz. 2010. Extreme wind climatology of winter storms in Germany. *Climate Research*, 41, 105-123.

Hosker, R. P. Jr. 1985. Flow around isolated structures and building clusters: A review, *ASHRAE Trans.*, 91 (2B), 1671-1692.Mardia, K. V. 1972. *Statistics of Directional Data.* Academic Press: New York, 357 pp.

Johnson, G. L. 1985. *Wind energy systems*. Prentice-Hall: Englewood Cliffs, NJ.

Keyhani, A., M. Ghasemi-Varnamkhasti, M. Khanali and R. Abbaszadeh. 2010. An assessment of wind energy potential as a power generation source in the capital of Iran, Tehran. *Energy*, 35, 188-201.

Klink, K. 1999. Climatological mean and interannual variance of United States surface wind speed, direction and velocity. *International Journal of Climatology*, 19, 471-488.

Landsberg, H. E. 1981. *The UrbanClimate*. AcademicPress: San Francisco, 285 pp.

Laporte, D. J. 2010. A surface roughness parameterization study near two proposed windfarm locations in Southern Ontario (Master's thesis). University of Victoria, B.C., Canada.

Lopes, A., S. Oliveira, M. Fragoso, J. Andrade and P. Pedro. 2008. Wind risk assessment in urban environments: the case of falling trees during windstorm events in Lisbon. In: K. Strelcová *et al*. (Eds.). *Bioclimatology and Natural Hazards*. Springer: Dordrecht, 55-74.

Lutgens, F. K. and E. J. Tarbuck. 1989. *The Atmosphere: An Introduction to Meteorology*, 4th ed. Prentice Hall: Eaglewood Cliffs, 491 pp.

Mardia, K. V. 1972. *Statistics of Directional Data.* Academic Press: New York, 357 pp.

Mass, C. 2008. *The Weather of the Pacific Northwest*. University of Washington Press, 281 pp.

Mass, C. F. and G. K. Ferber. 1990. Surface pressure perturbations produced by an isolated mesoscale topographic barrier. Part I: General characteristics and dynamics. *Monthly Weather Review*, 118, 2579-2596.

Mass, C. and B. Dotson. 2010. Major extratropical cyclones of the northwest United States: Historical review, climatology, and synoptic environment. *Monthly Weather Review*, 138, 2499-2527.

Mass, C. F., S. Businger, M. D. Albright, and Z. A. Tucker. 1995. A windstorm in the lee of a gap in a coastal mountain barrier. *Monthly Weather Review*, 123, 315-331.

Massen, F. 2003. A short calibration study of the Vantage Pro Plus weathestation. meteoLCD. http://meteo.lcd.lu/papers/comparison_vantage/vantage_calibration.html Lkd. at "About the School-Based Weather Station Network." http://www.victoriaweather.ca/about.php Last accessed, January 11, 2012.

McIntyre, D. P. 1952. A technique for wind analysis and forecasting as applied to Victoria, British Columbia. *Quarterly Journal of the Royal Meteorological Society*, 78 (336), 247-254.

Mertens, S. 2003. The energy yield of roof mounted wind turbines. *Wind Engineering*, 27 (6), 507–18.

Moore, W. G. 1958. *A dictionary of geography*. Penguin Books: Middlesex, England, 191 pp.

Moran, J. M. and M. D. Morgan. 1994. *Meteorology: The Atmosphere and the Science of Weather*, 4th ed. Maxwell Macmillan Canada: Toronto, 517 pp.

MSC (Meteorological Service of Canada). 2001. Meteorological Service of Canada MSC STDS 2 – 2001 Version 2.4, 11 pp.

Munn, R. E. 1970. Airflow in urban areas. In: Urban climates. WMO Technical Note No. 108, WMO - No. 254. TP. 141.

Nägeli, W. 1946. Weitere Untersuchungen uber die Windverhaltnisse im Bereich von Windschutzanlagen. *Mitteil. Schweiz. Anstalt Forstl. Versuchswesen*, Zurich, 24, 659-737.

Natural Resources Canada. 2010a. The Atlas of Canada, http://atlas.nrcan.gc.ca/site/english/maps/topo/map Last accessed, Oct. 4, 2012.

Natural Resources Canada. 2010b. "Topographic map of southeastern SD 61" [map]. 1: 50000. Natural Resources Canada, The Atlas of Canada. http://atlas.nrcan.gc.ca/site/english/maps/topo/map Last accessed, Mar. 4, 2012. Modified by M. Matsuda. Using Adobe® Photoshop® CS6 EXTENDED [PSD software]. 13.0 x64. San Jose, CA: Adobe Systems Incorporated. 1990-2012. Sep. 2012.

Natural Resources Canada. 2010c. "Topographic map of Willway Elemenatry School and its vicinity" [map]. 1: 45000. Natural Resources Canada, The Atlas of Canada. http://atlas.nrcan.gc.ca/site/english/maps/topo/map Last accessed, Mar. 4, 2012. Modified by M. Matsuda. Using Adobe® Photoshop® CS6 EXTENDED [PSD software]. 13.0 x64. San Jose, CA: Adobe Systems Incorporated. 1990-2012. Sep. 2012.

Natural Resources Canada. 2010d. "Topographic map of Dunsmuir Middle School and its vicinity" [map]. 1: 40000. Natural Resources Canada, The Atlas of Canada. http://atlas.nrcan.gc.ca/site/english/maps/topo/map Last accessed, Mar. 4, 2012. Modified by M. Matsuda. Using Adobe® Photoshop® CS6 EXTENDED [PSD software]. 13.0 x64. San Jose, CA: Adobe Systems Incorporated. 1990-2012. Sep. 2012.

Natural Resources Canada. 2010e. "Topographic map of Ruth King Elementary School and its vicinity" [map]. 1: 50,000. Natural Resources Canada, The Atlas of Canada. http://atlas.nrcan.gc.ca/site/english/maps/topo/map Last accessed, Mar. 4, 2012. Modified by M. Matsuda. Using Adobe® Photoshop® CS6 EXTENDED [PSD software]. 13.0 x64. San Jose, CA: Adobe Systems Incorporated. 1990-2012. Sep. 2012.

Natural Resources Canada. 2010f. "Topographic map of the northern part of SD 63 which includes a high wind speed area" [map]. 1: 70,000. Natural Resources Canada, The Atlas of Canada. http://atlas.nrcan.gc.ca/site/english/maps/topo/map Last accessed, Mar. 4, 2012. Modified by M. Matsuda. Using Adobe® Photoshop® CS6 EXTENDED [PSD software]. 13.0 x64. San Jose, CA: Adobe Systems Incorporated. 1990-2012. Sep. 2012.

NCEP (The National Centers for Environmental Prediction). 2012. SRRS Analysis and Forecast Charts, http://nomads.ncdc.noaa.gov/ncep/NCEP Last accessed, Feb. 14, 2012.

Oke, T. R. 1987. *Boundary Layer Climates*, 2nd edition. Methuen: London, 435 pp.

Overland, J. E. and B. A. Walter Jr. 1981. Gap winds in the Strait of Juan de Fuca. *Monthly Weather Review,* 109, 2221-2233.

Overland, J. E. and N. A. Bond. 1995. Observation and scale analysis of coastal wind jets. *Monthly Weather Review,* 123, 2934-2941.

Page, J. K. 1976. Application of building climatology to the problems of housing and building for human steelements. WMO Technical Note No. 150, WMO - No. 441.

Pasharde, S. and C. Christofides. 1995. Statistical Analysis of Wind Speed and Direction in Cyprus. *Solar Energy*, 55 (5), 405-414.

Penwarden, A. D. 1973. Acceptable wind speeds in towns, *Building Science*, 8, 259-267.

Picard, A., and H. Fang. 2003. Methods to determine the density of moist air. *IEEE Transactions on Instrumentation and Measurement,* 52, 504-507.

Picard, A., H. Fang, and M. Gläser. 2004. Discrepancies in air density determination between the thermodynamic formula and a gravimetric method: Evidence for a new value of the mole fraction of argon in air. *Metrologia*, 41, 396-400.

Picard, A., R. S. Davis, M. Gläser, and K. Fujii. 2008. Revised formula for the density of moist air (CIPM-2007). *Metrologia*, 45, 149-155.

Reyes, A. and M. Tutsch. 1999. An Investigation of Wind Interaction with Two Conifer Species, Victoria, British Columbia. Term paper, University of Victoria, Victoria.

Saaroni, H., B. Ziv, A. Bitan and P. Alpert. 1998. Easterly wind storms over Israel. *Theoretical and Applied Climatology*, 59, 61-77.

Saenko, A. V. 2008. Assessment of Wind Energy Resources for Residential Use in Victoria, BC, Canada (Master's thesis). University of Victoria, B. C., Canada.

School-Based Weather Station Network, 2011a. How we installed the weather stations. http://www.victoriaweather.ca/installphotos.php Last Accessed, January 16, 2012.

School-Based Weather Station Network. 2011b. The weather variables we measure and store. http://www.victoriaweather.ca/information.php. Last Accessed, January 27, 2012.

School-Based Weather Station Network. 2012a. About the School-Based Weather Station Network. http://www.victoriaweather.ca/about.php Last Accessed, January 16, 2012.

School-Based Weather Station Network. 2012b. School-Based Weather Station Network. http://www.victoriaweather.ca/ Last Accessed, October 10, 2012.

School-Based Weather Station Network. Anatomy of the weather station. http://www.victoriaweather.ca/anatomy.php Last Accessed, January 16, 2012.

Sellers, W.D. 1965. *Physical Climatology*. University of Chicago Press: Chicago, 272 pp.

Stamp, L. D. Ed. 1966. *A glossary of geographical terms*, 2nd edition. Wiley: New York, 539 pp.

Steenburgh, W. J. and C. F. Mass. 1996. Interaction of an intense extratropical cyclone with coastal orography. *Monthly Weather Review*, 124, 1329-1352.

Taylor, P. A. and R. J. Lee. 1984. Simple guidelines for estimating wind speed variations due to small-scale topographic features. *Climatological Bulletin*, 18, 3-32.

Tuller, S. E. 1974. Microclimatic variations in a downtown urban environment. *Geografiska Annaler,* 54A 3-4, 123-135.

Tuller, S.E. 1995. Onshore flow in an urban area: Microclimatic effects. *International Journal of Climatology,* 15, 1387-1398.

Tuller, S.E. 2004. Measured wind speed trends on the west coast of Canada. *International Journal of Climatology,* 24, 1359-1374.

van Eimern, J., R. Karschon, L. A. Razumova and G. W. Robertson. 1964. Windbreaks and shelterbelts. WMO Technical Note No. 59, WMO - No. 147. TP. 70.

Walker, I. J. and W. G. Nickling. 2002. Dynamics of secondary airflow and sediment transport over and in the lee of transverse dues. *Progress in Physical Geography,* 26, 47-75.

Walker, I. J. and P. A. Hesp. 2013. Fundamentals of Aeolian Sediment Transport: Airflow Over Dunes. In: John F. Shroder (Editor-in-chief), N. Lancaster, D. J. Sherman, and A. C. W. Baas (Volume Editors). *Treatise on Geomorphology*, Vol 11, Aeolian Geomorphology. Academic Press: San Diego, 109-133 pp.

Watts, A. 1965. Wind and Sailing Boats. Quadrangle Books: Chicago, 224 pp.

Weaver, A. J. 2006. High density weather station network. Application for NSERC Research Tools and Instruments – Category 1. School of Earth and Ocean Sciences, University of Victoria, PO Box 3055, Victoria, B.C., V8W 2Y2.

Weaver, A. J. and Wiebe, E. C. 2006. Micro meteorological network in Greater Victoria schools. www.victoriaweather.ca *CMOS Bulletin, 34* (4), 184-190.

Wieclaw-Michniewska, J. and K. Piotrowicz. 2011. Seasonal and annual variability of days with strong winds and wind damage in Krakow (Poland) during the period 2000–2007. *Natural Hazards*, 59, 949-965.

Wieringa, J., Davenport, A., Grimmond, C.S.B., and Oke, T.R. 2001. New revision of Davenport roughness classification. In: Proceedings of the Third European and African Conference on Wind Engineering, Eindhoven, Netherlands.

WMO. 1981. Meteorological aspects of the utilization of wind as an energy source. WMO Technical Note No. 175, WMO - No. 575.

Yu, C.-K. and N. A. Bond. 2002. Airborne Doppler observations of a cold front in the vicinity of Vancouver Island. *Monthly Weather Review*, 130, 2692-2708.

Zhong, S., J. Li, C. D. Whiteman, X. Bian and W. Yao. 2008. Climatology of high wind events in the Owens Valley, California. *Monthly Weather Review*, 136, 3536–3552.

Appendix

Table A1: School district; station ID, name, latitude, longitude and elevation of each weather station in the study area (Government of Canada, Natural Resources Canada, Centre for Topographic Information. 1999; School-Based Weather Station Network 2012b).

School District	Stn. ID	Name	Latitude	Longitude	Elevation (m)
61	1	Ian Stewart Complex/Mt. Douglas High School	48.4699	-123.319	56
	2	Swan Lake Nature Sanctuary	48.4632	-123.378	22
	3	Strawberry Vale Elementary School	48.4776	-123.417	45
	4	Oaklands Elementary School	48.4408	-123.339	30
	5	Cedar Hill Middle School	48.466	-123.337	50
	6	Marigold Elementary School/Spectrum High School	48.4616	-123.408	31
	7	Campus View Elementary	48.465	-123.321	53
	8	Victoria High School	48.4293	-123.347	36
	9	Frank Hobbs Elementary School	48.4651	-123.3	30
	10	MacAulay Elementary School	48.4253	-123.405	25
	11	James Bay Elementary School	48.4169	-123.38	8
	12	Victoria West Elementary School	48.4346	-123.388	25
	13	Shoreline Middle School	48.4533	-123.426	16
	14	Willows Elementary School	48.4359	-123.311	21
	15	Sir James Douglas Elementary School	48.4153	-123.348	20
	16	Tillicum Elementary School	48.4519	-123.393	22
	17	Eagle View Elementary School	48.4663	-123.442	31
	18	Torquay Elementary School	48.4865	-123.324	61
	19	Monterey Elementary School	48.4182	-123.314	13
	20	Lake Hill Elementary School	48.4788	-123.365	37
	21	Rogers Elementary School	48.4744	-123.381	46
	22	Cloverdale Elementary School	48.4534	-123.359	46
	23	South Park Elementary School	48.4178	-123.367	15
	24	Hillcrest Elementary School	48.4849	-123.314	70
	25	Lansdowne Middle School	48.4451	-123.328	32
	26	Doncaster Elementary School	48.4562	-123.338	52
	27	Glanford Middle School	48.4769	-123.391	26
	28	Sundance Elementary School	48.4275	-123.328	29
	29	George Jay Elementary School	48.4329	-123.351	26
	30	Northridge Elementary School	48.4806	-123.4	22
	33	Reynolds High School	48.4683	-123.359	35
	41	The AChannel Studio	48.4281	-123.366	17
	60	Esquimalt High School	48.4382	-123.396	15
	73	Craigflower Elementary School	48.4537	-123.421	18
	74	Quadra Elementary School	48.4456	-123.361	34
	75	Central Middle School	48.4235	-123.347	43

	76	Lambrick Park High School	48.4792	-123.331	46
	77	McKenzie Elementary School	48.4669	-123.392	29
	78	SJ Willis Alternative School	48.4408	-123.363	29
	79	Arbutus Middle School	48.4713	-123.307	60
	80	Gordon Head Middle School	48.4821	-123.33	45
	81	Braefoot Elementary School	48.4697	-123.345	44
	82	Colquitz Middle School	48.4608	-123.393	19
62	31	Sangster Elementary School	48.4205	-123.486	82
	32	Colwood Elementary School	48.4356	-123.486	72
	34	Crystal View Elementary School	48.4529	-123.477	101
	35	David Cameron Elementary School	48.4428	-123.496	70
	36	Hans Helgesen Elementary School	48.364	-123.554	103
	38	John Stubbs Elementary School	48.436	-123.463	59
	39	Lakewood Elementary School	48.4655	-123.506	90
	40	Ruth King Elementary School	48.451	-123.505	83
	55	Savory Elementary School	48.4488	-123.486	80
	56	Willway Elementary School	48.4572	-123.549	74
	57	Wishart Elementary School	48.4218	-123.495	82
	58	Dunsmuir Middle School	48.4191	-123.488	81
	71	Cal Revelle Nature Sanctuary	48.5376	-123.501	225
63	42	Butchart Gardens	48.5621	-123.466	30
	61	Cordova Bay Elementary School	48.5273	-123.37	30
	62	Deep Cove Elementary School	48.6804	-123.457	53
	63	Keating Elementary School	48.5677	-123.403	71
	64	Lochside Elementary School	48.5014	-123.361	42
	65	McTavish Elementary School	48.6307	-123.428	45
	66	Prospect Lake Elementary School	48.5234	-123.433	61
	67	Sidney Elementary School	48.6529	-123.404	16
	70	Parkland Secondary School	48.6701	-123.421	14

Table A2: Time periods of missing wind speed data at each weather station in the study area during the selected days. 'All' means that all data were missed whereas '0' means that no datum was missed during a day. The time within the parentheses is all inclusive.

School District	Stn. ID	15-Nov	13-Dec	15-Dec	9-Jan	5-Feb	7-Feb
61	1	0	0	(02:36-11:24)	(15:53-16:12)	(13:08-14:14)	0
	2	0	0	0	0	(00:01) (01:01) (03:01) (06:01) (10:01) (11:01) (13:01) (14:01) (15:01) (16:01) (18:01) (22:01)	(01:01) (02:01) (02:26-02:32) (04:01) (09:01) (11:01) (15:01) (16:01) (17:01) (19:01) (20:01) (22:01)

3	0	0	(03:10-04:42)	(08:47-14:50)	0	0
4	0	0	0	0	0	0
5	0	0	0	(16:06)	0	0
6	0	0	(03:24-09:40)	0	0	0
7	0	0	0	0	0	0
8	0	0	0	0	0	0
9	0	(00:00-15:04)	(01:08-02:01) (08:19-23:59)	0	0	0
10	0	0	0	0	0	0
11	0	0	(01:38-03:09)	0	0	0
12	0	0	0	0	0	0
13	0	0	0	0	(10:09-10:42) (13:37-14:26) (16:15-16:30)	(01:22-01:37) (03:13-03:45) (19:34-19:48)
14	0	0	(02:36-23:59)	0	0	0
15	0	0	0	0	0	0
16	0	0	0	0	(00:00-08:55) (22:06-23:59)	(00:00-08:58) (19:39-23:59)
17	0	0	(03:06-09:18)	0	0	0
18	0	0	0	0	0	0
19	0	0	0	(09:30)	0	0
20	0	0	0	0	0	0
21	0	0	0	0	(04:04)	0
22	(22:51-23:06)	0	0	0	(13:29-13:48) (14:32-14:33) (14:40)	0
23	0	0	0	0	0	0
24	0	(06:53-06:54)	(02:47-09:51)	0	0	0
25	0	0	0	0	0	0
26	0	(09:55-23:59)	0	(16:05-16:06)	(00:00-12:16) (13:31-23:59)	(00:00-15:02) (16:58-23:59)
27	0	(07:22)	0	0	0	0
28	0	0	0	0	0	0
29	0	0	0	0	0	0
30	0	(07:39-09:33) (13:05-13:06)	(03:22-08:48)	0	0	0
33	0	0	0	0	0	0
41	(13:03-13:08)	0	0	0	0	(17:29-17:59)
60	0	0	0	0	0	0
73	0	0	0	(00:00-14:53) (16:52)	0	(00:00-01:19) (22:16-22:30)
74	0	(09:55-10:55)	0	0	0	0
75	(23:08-23:59)	0	0	0	0	0
76	0	0	0	0	0	0
77	0	0	0	0	0	0
78	0	0	0	0	0	0
79	0	0	(02:36-11:22)	0	(13:08-16:41) (16:43)	0
80	0	0	0	0	0	0
81	0	0	0	0	0	0
82	0	0	0	0	0	0

62	31	(00:13-01:01)	(00:13-01:01) (03:39-04:54) (17:17-17:27)	(00:13-01:01) (01:08-13:33)	(00:13-01:01)	(16:22-17:23)	(12:00-12:01)
	32	0	(00:00-01:02)	(03:06-03:08)	0	0	0
	34	0	0	(01:42-21:46)	0	0	0
	35	(23:43-23:59)	(03:47-13:22)	All	All	(07:54-20:36)	(00:00-12:55)
	36	(19:33-22:54)	All	(01:25-23:59)	0	0	0
	38	0	0	(03:06-23:59)	0	All	All
	39	0	0	0	0	All	(00:00-11:23)
	40	0	0	(01:42-13:53) (19:02-19:04)	0	0	0
	55	0	0	(01:42-19:56)	0	0	0
	56	(17:49-17:50)	0	(01:49-17:39)	0	0	0
	57	0	0	(01:52-01:54) (01:59-02:01) (02:17-14:52)	0	0	(08:19-09:09) (09:11)
	58	0	(03:39-04:53) (17:17-17:27)	(01:08-13:32) (13:34-15:52)	(00:00-00:36) (00:56-19:53)	(16:21-17:22)	(11:59-12:00) (21:40-21:50)
	71	All	0	(02:46-07:07) (07:31-08:18) (09:56-13:13) (14:54-16:04)	0	0	0
63	42	0	(09:08-11:59) (12:02-12:09) (12:27-12:28) (13:06-15:10)	(03:15-11:41)	0	0	0
	61	0	(06:57-08:13)	(03:01-23:59)	(14:06-15:08)	0	0
	62	0	(08:15-08:16) (08:58) (09:55-09:57) (10:37-16:38)	(02:31-02:32) (02:59-03:00) (03:06-03:08) (03:11-17:24) (17:38-20:55)	(00:00-09:05)	0	0
	63	0	0	0	0	0	0
	64	0	0	0	(12:40-12:43)	(14:50-14:53) (15:35-16:59)	0
	65	0	(08:15-12:40)	(02:31-20:35)	0	0	0
	66	(13:15-13:27) (18:44-21:49)	(00:00-01:23) (07:44-08:44) (10:44-10:46) (11:35-11:37) (12:29-12:31)	(03:36-11:54)	0	0	0
	67	0	0	(03:06-03:07)	0	0	0
	70	0	(08:15) (09:55-13:20)	(02:59) (03:11) (03:37-15:01)	0	0	0

Table A3: Time periods of missing wind direction data at each weather station in the study area during the selected days. 'All' means that all data were missed whereas '0' means that no datum was missed during a day. The time within the parentheses is all inclusive.

School District	Stn. ID	15-Nov	13-Dec	15-Dec	9-Jan	5-Feb	7-Feb
61	1	0	0	(02:36-11:24) (11:53-12:10) (13:28-13:45) (15:16-18:23) (18:28-19:38) (19:59-21:07) (21:37-23:57)	0	(13:08-14:14)	0
	2	0	0	0	0	(00:01) (01:01) (03:01) (06:01) (10:01) (11:01) (13:01) (14:01) (15:01) (16:01) (18:01) (22:01)	(01:01) (02:01) (02:26-02:32) (04:01) (09:01) (11:01) (15:01) (16:01) (17:01) (19:01) (20:01) (22:01)
	3	0	0	(03:10-04:42)	(08:47-14:50)	0	0
	4	0	0	0	0	0	0
	5	0	0	0	(16:06)	0	0
	6	0	0	(03:24-09:40)	0	0	0
	7	0	0	0	0	0	0
	8	0	0	0	0	0	0
	9	0	(00:00-15:04)	(01:08-02:01) (08:19-23:59)	0	0	0
	10	0	0	0	0	0	0
	11	0	0	(01:38-03:09)	0	0	0
	12	0	0	0	0	0	0
	13	0	0	0	0	(10:09-10:42) (13:37-14:26) (16:15-16:30)	(01:22-01:37) (03:13-03:45) (19:34-19:48)
	14	0	0	(02:36-23:59)	0	0	0
	15	0	0	0	0	0	0
	16	0	0	0	0	(00:00-08:55) (22:06-23:59)	(00:00-08:58) (19:39-23:59)
	17	0	0	(03:06-09:18)	0	0	0
	18	0	0	0	0	0	0
	19	0	0	0	(09:30)	0	0
	20	0	0	0	0	0	0
	21	0	0	0	0	(04:04)	0
	22	0	0	0	0	(13:29-13:48) (14:32-14:33) (14:40)	0
	23	0	0	0	0	0	0
	24	0	(06:53-06:54)	(02:47-09:51)	0	0	0
	25	0	0	0	0	0	0
	26	0	(09:55-23:59)	0	0	(00:00-12:16) (13:31-23:59)	(00:00-15:02) (16:58-23:59)
	27	0	(07:22)	(10:47-10:53)	0	0	0

	28	0	0	0	0	0	0
	29	0	0	0	0	0	0
	30	0	(07:39-09:33) (13:05-13:06)	(03:22-08:48)	0	0	0
	33	0	0	0	0	0	0
	41	(13:03-13:08)	0	0	0	0	(17:29-17:59)
	60	0	0	0	0	0	0
	73	0	0	0	(00:00-14:53) (16:52)	0	(00:00-01:19) (22:16-22:30)
	74	0	(09:55-10:55)	0	0	0	0
	75	(23:08-23:59)	0	0	0	0	0
	76	0	0	0	0	0	0
	77	0	0	0	0	0	0
	78	0	0	0	0	0	0
	79	0	0	(02:36-11:22)	0	(13:08-16:41) (16:43)	0
	80	0	0	0	0	0	0
	81	0	0	0	0	0	0
	82	0	0	0	0	0	0
62	31	(00:13-01:01)	(00:13-01:01) (03:39-04:54) (17:17-17:27)	(00:13-01:01) (01:08-13:33)	0	(16:22-17:23)	(12:00-12:01)
	32	0	(00:00-01:02)	(03:06-03:08)	0	0	0
	34	0	0	(01:42-21:46)	0	0	0
	35	(23:43-23:59)	(03:47-13:22)	All	All	(07:54-20:36)	(00:00-12:55)
	36	(19:33-22:54)	All	(01:25-23:59)	0	0	0
	38	0	0	All	0	All	All
	39	0	0	0	0	All	(00:00-11:23)
	40	0	0	(01:42-13:53) (19:02-19:04)	0	0	0
	55	0	0	(01:42-19:56)	0	0	0
	56	(17:49-17:50)	0	(01:49-17:39)	0	0	0
	57	0	0	(01:52-01:54) (01:59-02:01) (02:17-14:52)	0	0	(08:19-09:09) (09:11)
	58	0	(03:39-04:53) (17:17-17:27)	(01:08-13:32) (13:34-15:52)	(00:00-00:36) (00:56-19:53)	(16:21-17:22)	(11:59-12:00) (21:40-21:50)
	71	All	0	(02:46-07:07) (07:31-08:18) (09:56-13:13) (14:54-16:04)	0	0	0
63	42	0	(09:08-11:59) (12:02-12:09) (12:27-12:28) (13:06-15:10)	(03:15-11:41)	0	0	0
	61	0	(06:57-08:13)	(03:01-23:59)	(14:06-15:08)	0	0
	62	0	(08:15-08:16) (08:58) (09:55-09:57) (10:37-16:38)	(02:31-02:32) (02:59-03:00) (03:06-03:08) (03:11-17:24)	(00:00-09:05)	0	0
	63	0	0	0	0	0	0
	64	0	0	0	(12:40-12:43)	(14:50-14:53) (15:35-16:59)	0
	65	0	(08:15-12:40)	(02:31-20:35)	0	0	0

	66	(13:15-13:27) (18:44-21:49)	(00:00-01:23) (07:44-08:44) (10:44-10:46) (11:35-11:37) (12:29-12:31)	(03:36-11:54)	0	0	0
	67	0	0	(03:06-03:07)	0	0	0
	70	0	(08:15) (09:55-13:20)	(02:59) (03:11) (03:37-15:01)	0	0	0

Table A4: Time periods of missing gust wind speed data at each weather station in the study area during the selected days. 'All' means that all data were missed whereas '0' means that no datum was missed during a day. The time within the parentheses is all inclusive.

School District	Stn. ID	Nov. 15	Dec. 13	Dec. 15	Jan. 9	Feb. 5	Feb. 7
61	1	0	0	(02:36-11:25)	(15:53-16:12)	(13:08-14:14)	0
	2	0	0	0	0	(00:01) (01:01) (03:01) (06:01-06:05) (10:01) (11:01) (13:01) (14:01) (15:01) (16:01) (18:01) (22:01)	(01:01) (02:01) (02:26-02:31) (04:01) (09:01) (11:01) (15:01) (16:01) (17:01) (19:01) (20:01) (22:01)
	3	0	0	(03:10-04:42)	(08:47-14:50)	0	0
	4	0	0	0	0	0	0
	5	0	0	0	(16:06)	0	0
	6	0	0	(03:24-09:40)	0	0	0
	7	0	0	0	0	0	0
	8	0	0	0	0	0	0
	9	0	(00:00-15:04)	(01:08-02:01) (08:19-23:59)	0	0	0
	10	0	0	0	0	0	0
	11	0	0	(01:38-03:09)	0	0	0
	12	0	0	0	0	0	0
	13	0	0	0	0	0	0
	14	0	0	(02:36-23:59)	0	0	0
	15	0	0	0	0	0	0
	16	0	0	0	0	0	(08:08-08:58)
	17	0	0	(03:06-09:18)	0	0	0
	18	0	0	0	0	0	0
	19	0	0	0	(09:30-09:31)	0	0
	20	0	0	0	0	0	0
	21	0	0	0	0	(04:04)	0
	22	0	0	0	0	(13:29-13:48) (14:32-14:33) (14:40)	0

	23	0	0	0	0	0	0
	24	0	(06:53-06:54)	(02:47-09:51)	0	0	0
	25	0	0	0	0	0	0
	26	0	0	0	(16:05-16:06)	(10:14-12:16)	(08:06-15:02)
	27	0	(07:22)	0	0	0	0
	28	0	0	0	0	0	0
	29	0	0	0	0	0	0
	30	0	(07:37-09:33) (13:05-13:06)	(03:22-08:48)	0	0	0
	33	0	0	0	0	0	0
	41	(13:03-13:08)	0	0	0	0	0
	60	0	0	0	0	0	0
	73	0	0	0	(00:00-14:53) (16:52)	0	0
	74	0	(09:55-10:55)	0	0	0	0
	75	0	0	0	0	0	0
	76	0	0	0	0	0	0
	77	0	0	0	0	0	0
	78	0	0	0	0	0	0
	79	0	0	(02:36-11:22)	0	(13:08-16:41) (16:43)	0
	80	0	0	0	0	0	0
	81	0	0	0	0	0	0
	82	0	0	0	0	0	0
62	31	(00:13-01:01)	(00:03-01:01) (03:39-04:54) (17:17-17:27)	(00:13-01:01) (01:08-13:33)	(00:13-01:01)	(16:22-17:23)	(12:00-12:01)
	32	0	(00:00-01:02)	(03:06-03:08)	0	0	0
	34	0	0	(01:42-21:46)	0	0	0
	35	0	0	All	All	0	(02:31-12:55)
	36	(19:33-22:54)	All	(01:25-23:59)	0	0	0
	38	0	0	(03:06-23:59)	0	All	All
	39	0	0	0	0	All	(00:00-11:23)
	40	0	0	(01:42-13:53) (19:02-19:04)	0	0	0
	55	0	0	(01:41-19:56)	0	0	0
	56	(17:49-17:50)	0	(01:49-17:43)	0	0	0
	57	0	0	(01:52-01:54) (01:59-02:01) (02:17-14:54)	0	0	(08:19-09:09) (09:11)
	58	0	(03:39-04:53) (17:17-17:27)	(01:08-13:32) (13:34-16:02)	0	(16:21-17:22)	(11:59-12:00) (21:40-21:50)
	71	(15:58-23:59)	0	(02:46-07:07) (07:31-08:18) (09:56-13:13) (14:54-16:04)	0	0	0
63	42	0	(09:08-11:59) (12:02-12:09) (12:27-12:28) (13:06-15:10)	(03:15-11:41)	0	0	0
	61	0	(06:57-08:13)	(03:01-23:59)	(14:06-15:08)	0	0
	62	0	(08:15-08:16) (08:58) (09:55-09:57) (10:37-16:38)	(02:31-02:32) (02:59-03:00) (03:06-03:08) (03:11-17:26) (17:38-20:57)	(00:00-09:05)	0	0

	63	0	0	0	0	0	0
	64	0	0	0	(12:39-12:43)	(14:50-14:53) (15:35-17:00)	0
	65	0	(08:15-12:40)	(02:31-20:35)	0	0	0
	66	(13:15-13:27) (18:44-21:49)	(00:00-01:23) (07:44-08:44) (10:44-10:46) (11:35-11:37) (12:29-12:31)	(03:36-11:54)	0	0	0
	67	0	0	(03:06-03:07)	0	0	0
	70	0	(08:15) (09:55-13:20)	(02:59) (03:11) (03:37-15:01)	0	0	0

Table A5: The missing data regarding the variables of air density (AT-air temperature, RH-relative humidity and AP-air pressure) at the time of daily maximum gust wind speed on the selected days.

School District	Stn. ID	Nov. 15	Dec. 13	Dec. 15	Jan. 9	Feb. 5	Feb. 7
61	1	0	0	0	0	0	0
	2	0	0	0	0	0	0
	3	0	0	0	0	0	0
	4	0	0	0	0	0	0
	5	0	0	0	0	0	0
	6	0	0	0	0	RH, AP	RH, AP
	7	0	0	0	0	0	0
	8	0	0	0	0	0	0
	9	0	0	0	0	0	0
	10	0	0	0	0	RH, AP	RH, AP
	11	0	0	0	0	0	0
	12	0	0	0	0	0	0
	13	0	0	0	0	0	0
	14	0	0	0	0	0	0
	15	0	0	0	0	0	0
	16	0	0	0	0	0	0
	17	0	0	0	0	0	0
	18	0	0	0	0	0	0
	19	0	0	0	AT, RH, AP	0	0
	20	0	0	0	0	0	0
	21	0	0	0	0	0	0
	22	0	0	0	0	0	0
	23	0	0	0	0	0	0
	24	0	0	0	0	0	0
	25	0	0	0	0	0	0
	26	0	0	0	0	0	0
	27	0	0	0	0	0	0
	28	0	0	0	0	0	0

	29	0	0	0	0	0	0
	30	0	0	0	0	0	0
	33	0	0	0	0	0	0
	41	0	0	0	0	0	0
	60	0	0	0	0	0	0
	73	0	0	0	0	0	0
	74	0	0	0	0	0	0
	75	0	0	0	0	0	0
	76	0	0	0	0	0	0
	77	0	0	0	0	0	0
	78	0	0	0	0	0	0
	79	0	0	0	0	0	0
	80	0	0	0	0	0	0
	81	0	0	0	0	0	0
	82	0	0	0	0	0	0
	31	0	0	0	0	0	0
	32	0	0	0	0	0	0
	34	0	0	0	0	0	0
	35	0	0	-	-	0	0
	36	0	-	0	0	0	0
	38	0	0	0	0	-	-
62	39	0	0	0	0	-	0
	40	0	0	0	0	0	0
	55	0	0	0	0	0	0
	56	0	0	0	0	0	0
	57	0	0	0	0	0	0
	58	0	0	0	0	0	0
	71	AT, RH, AP	0	0	0	0	0
	42	0	0	0	0	0	0
	61	0	0	0	0	0	0
	62	0	0	0	0	0	0
	63	0	0	0	0	0	0
63	64	0	0	0	0	0	0
	65	0	0	0	0	0	0
	66	0	0	0	0	0	0
	67	0	0	0	0	0	0
	70	0	0	0	0	0	0